1. Report No. FHWA/TX-87/78+401-8F	2. Government Accession No.	3. Recipient's Catalog No.	
4. Title and Subtitle PRESTRESSED CONCRETE PAVEMENT DESIGN—DESIGN AND CONSTRUCTION OF OVERLAY APPLICATIONS		5. Report Date November 1986	
		6. Performing Organization Code	
7. Author's) B. Frank McCullough and Ned H. Burns		8. Performing Organization Report No. Research Report 401-8F	
9. Performing Organization Name and Address Center for Transportation Research The University of Texas at Austin Austin, Texas 78712-1075		10. Work Unit No.	
		11. Contract or Grant No. Research Study 3-8-84-401	
12. Sponsoring Agency Name and Address Texas State Department of Highways and Public Transportation; Transportation Planning Division P. O. Box 5051 Austin, Texas 78763-5051		13. Type of Report and Period Covered Final	
		14. Sponsoring Agency Code	

15. Supplementary Notes

Study conducted in cooperation with the U. S. Department of Transportation, Federal Highway Administration. Research Study Title: "Prestressed Concrete Pavement Design—Design and Construction of Overlay Applications"

16. Abstract

This report covers a detailed characterization of the performance of prestressed concrete pavement, in terms of failures, joint movement, steel stresses, and prestressed concrete pavement stresses, that has been derived from information collected in previous general and specific studies in connection with this project. This project has contributed information in connection with strand placement, anchorage, early stressing, subbase friction, and fatigue test. Using this information, a detailed design procedure has been developed that considers the interaction of thickness, joint spacing, and post tensioning range and level to cover a wide range of input variables for a specific location. In addition, the report also presents information collected in connection with the design, construction, and performance monitoring of a one-mile project on IH-35 in McLennan County, Texas. In addition, the report presents new concepts that may be used in the design and construction of prestressed concrete pavement to expedite the operations and possible improve performance that will net a more efficient expenditure of public funds.

17. Key Words performance, concrete pavement, prestressed, failures, joint movement, steel stresses, design procedure	18. Distribution Statement No restrictions. This document is available to the public through the National Technical Information Service, Springfield, Virginia 22161.		
19. Security Classif. (of this report) Unclassified	20. Security Classif. (of this page) Unclassified	21. No. of Pages 156	22. Price

Form DOT F 1700.7 (8-69)

PRESTRESSED CONCRETE PAVEMENT DESIGN –
DESIGN AND CONSTRUCTION OF OVERLAY APPLICATIONS

by

B. Frank McCullough
Ned H. Burns

Research Report 401-8F

Prestressed Concrete Pavement Design--
Design and Construction of Overlay Applications
Research Project 3-8-84-401

conducted for

Texas State Department of Highways
and Public Transportation

in cooperation with the
U.S. Department of Transportation
Federal Highway Administration

by the

Center for Transportation Research
Bureau of Engineering Research
The University of Texas at Austin

November 1986

PREFACE

This study has been a most rewarding activity for the principal investigators and CTR staff and other individuals involved. The project took place over a three year period and has resulted in numerous reports, including those that cover numerous significant additions to the state-of-the-art, the last being a very encompassing design procedure that permits a more reliable design of PCP. Although it is not possible to adequately recognize the contributions of Neil Cable, Alberto Mendoza, Joe Maffei, Brian Dunn, Way Chia, and Scott O'Brien, these individuals represent four Master's theses and one Ph.D. dissertation that were developed in connection with this project. We feel these results validate the use of fresh, young minds together with individuals with experience, to broaden the state of knowledge and provide for a better use of tax payers' money in the design, construction, and operation of pavements. The project also demonstrates how successful interaction with other projects and numerous phases of one project can be used to pull together one complete design procedure.

We also wish to express our appreciation to James L. Brown, Jerry Daleiden, Frank Craig, and Bill Wiese of the Texas State Department of Highways and Public Transportation, who have patiently contributed many ideas and recommendations to the study. Finally, we also wish to recognize the CTR staff of James Long, Leon Snider, Carl Bertran, Rachel Hinshaw, Lyn Gabbert, and Sue Tarpley who have contributed to the success of this project.

B. Frank McCullough
Ned H. Burns

Blank Page

LIST OF REPORTS

Report No. 401-1, "Very Early Post-tensioning of Prestressed Concrete Pavements," by J. Scott O'Brien, Ned H. Burns, and B. Frank McCullough, presents the results of tests performed to determine the very early post-tensioning capacity of prestressed concrete pavement slabs, and gives recommendations for a post-tensioning schedule within the first 24 hours after casting.

Report No. 401-2, "New Concepts in Prestressed Concrete Pavement," by Neil D. Cable, Ned H. Burns, and B. Frank McCullough, presents the following: (a) a review of the available literature to ascertain the current state of the art of prestressed concrete pavement; (b) a critical evaluation of the design, construction, and performance of several FHWA sponsored prestressed concrete pavement projects which were constructed during the 1970s; and (c) several new prestressed concrete pavement concepts which were developed based on (a) and (b).

Report No. 401-3, "Behavior of Long Prestressed Pavement Slabs and Design Methodology," by Alberto Mendoza-Diaz, N. H. Burns, and B. Frank McCullough, presents the development of a model to predict the behavior of long prestressed concrete pavement slabs and incorporate the predictions from the model into a design procedure.

Report No. 401-4, "Instrumentation and Behavior of Prestressed Concrete Pavements," by Joseph R. Maffei, Ned H. Burns, and B. Frank McCullough, describes the development and implementation of an instrumentation program used to monitor the behavior of a one-mile-long experimental prestressed concrete pavement and presents the results of measurements of ambient and concrete temperatures, horizontal slab movement, slab curling, concrete strain, very early concrete strength, concrete modulus of elasticity, and slab cracking.

Report No. 401-5, "Field Evaluation of Subbase Friction Characteristics," by Way Seng Chia, Ned H. Burns, and B. Frank McCullough, presents the results of push-off tests performed on four experimental test slabs at Valley View, Texas, to determine the maximum coefficient of friction of several friction reducing mediums for future implementation in the prestressed pavement projects in Cooke and McLennan Counties.

Research Report No. 401-6, "Friction Losses in Unbonded Post-Tensioning Tendons," by Brian W. Dunn, Ned H. Burns, and B. Frank McCullough, presents results from experimental tests at Valley View, Texas, to determine friction losses in post-tensioning tendons to be used in the prestressed concrete pavement project in McLennan County, Texas. Data collected from the pavement project are also presented.

Research Report No. 401-7, "Effect of Prestress on the Fatigue Life of Concrete," by Way Seng Chia, Ned H. Burns, and B. Frank McCullough, presents results from fatigue tests on prestressed concrete beams conducted at the Portland Cement Association and The University of Texas at Austin to determine the effects of prestressing on the fatigue life of concrete.

Research Report No. 401-8F, "Prestressed Concrete Pavement Design -- Design and Construction of Overlay Applications," by B. Frank McCullough and Ned H. Burns, presents a detailed characterization of the performance of prestressed concrete pavement, in terms of failures, joint movement, steel stresses, and PCC stresses, that has been derived from information collected from previous general and specific studies in connection with this project. In this report a detailed design procedure has been developed that considers the interaction of thickness, joint spacing, and post tensioning range and level to cover a wide range of input variables for a specific location. In addition, the report presents new concepts that may be used in the design and construction of PCP to expedite the operations and possibly improve performance that will net a more efficient expenditure of public funds.

ABSTRACT

This report covers a detailed characterization of the performance of prestressed concrete pavement, in terms of failures, joint movement, steel stresses, and prestressed concrete pavement stresses, that has been derived from information collected in previous general and specific studies in connection with this project. This project has contributed information in connection with strand placement, anchorage, early stressing, subbase friction, and fatigue test. Using this information, a detailed design procedure has been developed that considers the interaction of thickness, joint spacing, and post tensioning range and level to cover a wide range of input variables for a specific location. In addition, the report also presents information collected in connection with the design, construction, and performance monitoring of a one-mile project on IH–35 in McLennan County, Texas. In addition, the report presents new concepts that may be used in the design and construction of prestressed concrete pavement to expedite the operations and possibly improve performance that will net a more efficient expenditure of public funds.

Blank Page

SUMMARY

In order to investigate the potential use of prestressed concrete pavements (PCP) for highway roads, particularly for overlay applications, the Texas State Department of Highways and Public Transportation and the Federal Highway Administration sponsored a study on the design and construction of two one-mile prestressed overlay projects on Interstate Highway 35 in Cooke and McLennan Counties, Texas. The study was conducted by the Center for Transportation Research at The University of Texas at Austin.

The design phase of the work plan for the project consisted of three distinct aspects: (a) a thorough review of the available literature on design of PCP to determine the variables that are relevant to the design of slab length, joint details, thickness, and prestress level in the longitudinal and transverse directions, (b) development of models and procedures for accurately predicting the effect of these variables on the elements of the PCP structure, and (c) development of a PCP design based on (a) and (b) for implementation in both projects. The design of the PCP slabs was also to include recommendations with regard to adequate time of slab placement and application of prestress forces.

The McLennan County Project, located 15 miles north of Waco, Texas, was constructed between September and November 1985. Eighteen 240-foot and fourteen 440-foot PCP slabs were cast on the two southbound lanes of IH-35. The construction of the Cooke County Project was cancelled due to cost, considering that it might not provide additional valuable information, given its similarity to the McLennan County Project.

The completion of the three aspects of the McLennan County Project design led to the study of the effect of environmental factors on PCP slabs.

Of the variables affecting PCP behavior, frictional resistance was found to be one of the most influential. The contraction and expansion movements of PCP slabs during daily temperature cycles are restrained by the subbase frictional resistance. The length of the PCP slabs commonly ranges from 200 to 600 feet. As the length increases, the magnitude of the concrete friction restraint stresses becomes more important.

Blank Page

IMPLEMENTATION STATEMENT

The design procedure developed in connection with this study may be used on a PCP for new construction or as an overlay of an existing pavement. The design procedure will permit the engineer to select the optimum pavement thickness, joint spacing, and post tension level for a specific set of conditions considering a wide range of input variables. This procedure may be reliably applied to any project, since it has been developed on the basis of extensive performance data.

In addition, construction procedures may be studied in more detail for possibly expediting construction and, thus, lowering cost and also improving performance. For example, the most effective looping pattern and stress pockets may be developed as well as criteria for early stressing to prevent premature cracking.

Finally, the new concepts presented in Chapter 6 should be incorporated into an experimental project to evaluate their capability and adaptability in field situations. It is quite possible these steps will expedite the time of construction, thus lowering the cost and permitting a more extensive use of this pavement type.

Blank Page

TABLE OF CONTENTS

CHAPTER 1. INTRODUCTION

This report presents the findings of Research Project 4-8-84-401, entitled "Prestressed Concrete Pavement Design -- Design and Construction of Overlay Applications," that was conducted by the Center for Transportation Research for the Texas State Department of Highways and Public Transportation (SDHPT) in cooperation with the Federal Highway Administration (FHWA). This chapter covers the background and objectives of the study and the scope of the report.

BACKGROUND

After Word War II and during the 1950's, numerous prestressed concrete pavements for airports and highways were constructed in Europe. During the same period, several PCP airport pavements were constructed in the United States. By the 1960's the construction of prestressed concrete had subsided. Most of these projects had been designed on an empirical basis, and, since performance data were not collected, the basic state-of-the-art for design experienced only limited improvement.

In the 1970's the FHWA explored the development of prestressed concrete pavements as one of its primary research and implementation activities. They awarded a research project with the objective of considering past experience, conducting laboratory testing, and developing a design procedure. During this same time period, the FHWA worked closely with four states to construct PCP on inservice roadways. Projects of varying lengths were constructed in Virginia, Pennsylvania, Mississippi, and Arizona. These projects covered a wide range of environmental regions, from wet and cold to dry and hot. As a result of the general interest in this topic, substantial performance data were collected from these projects, though no activity has been instigated to review this information together and revise the design procedure as needed. The thickness of all pavements was set at 6 inches with excellent subbases, but there was variation in joint spacing and stressing level for the various projects.

As a result of these activities in other states and the need for rehabilitation of many existing pavements, the Texas SDHPT contracted with the FHWA to design, construct, and monitor PCP overlays in Texas. It was decided to investigate projects for two different

locations using the Center for Transportation Research to conduct the basic study with supervision from the Texas SDHPT. Thus, Projects 1-3D-84-555 and 1-9D-84-556 were initiated with the CTR in 1984. As a part of this project, the CTR was responsible for recommending the location for construction of two projects on IH-35 In Cooke and McLennan Counties. Each project was to be approximately one mile in length in one direction. The CTR was also responsible for the design of, recommendations for, and monitoring of the construction and performance of the projects. Although both projects were designed, only the McLennan County project was constructed, due to cost factors. Although these projects are separate from the specific topic of this report, and the results have been presented elsewhere, the studies are highly dependent on and provide supplemental material for this project.

In order to extend the state of knowledge, the Texas SDHPT and the FHWA sponsored a three year project with the CTR to develop an improved design procedure based on past experience. The principal investigators for the project were Drs. Ned H. Burns and B. Frank McCullough, with James L. Brown of the Texas SDHPT to provide overall guidance.

OBJECTIVES

The objective of this report is to provide an overview of the findings developed in connection with the various phases of the project. The detailed findings may be found in the seven other reports on various phases, as outlined in the list of reports.

The specific objectives of the study may be summarized as follows:

(1) Characterize the performance of PCP in the field in terms of joint movements, slab stresses, wheel load repetitions, support conditions, subbase friction characteristics, environmental history, and construction techniques.

(2) From models characterizing the PCP performance as outlined in Item 1 develop a design procedure that considers the interaction of thickness, joint spacing, and post tensioning to develop a pavement structure for the design life.

(3) Assist in the design of inservice pavements, and then monitor the construction and performance.

(4) Explore new concepts that may be used in the design and construction of PCP that will make it more cost competitive with other pavement types with the same performance characteristics.

SCOPE

Figure 1.1 is flow diagram illustrating the development of this final report. In moving from top to bottom the activities may be considered in terms of time. The interaction of the various phases is shown by the arrows that illustrate the flow of information to the next phase. The Projects 555/556 report is included in this diagram, since its activities were instrumental in developing the findings for this particular study. Therefore, its relative position in the development process is shown. The solid lines indicate a direct flow and dependency of information. The dashed lines show an interaction between activities.

Chapter 2 presents a summary of the pilot subbase friction study. Chapter 3 presents the tendon looping and stress pocket study that was conducted on slabs near Greenville, Texas. Chapter 4 summarizes the findings of an end-anchorage study and the criteria that permit early stressing of the pavement to prevent cracking during the first day. These studies are basically concentrated in the first 24 hours of pavement life. Chapter 5 covers the pavement instrumentation and observations made in connection with the experimental project constructed on IH-35 in McLennan County. Chapter 6 covers the PCP fatigue test results on a laboratory fatigue test. This study was conducted to provide supplemental fatigue information to validate assumptions made relative to fatigue performance of PCP. Chapter 7 presents the basic concepts used in a design method that permits the balancing of pavement thickness, joint spacing, and prestress level to account for stresses developed by the input variables. Chapter 8 provides an overview of new concepts that may be used in the construction of PCP to lower costs and improve performance. The final chapter covers the conclusions and recommendations of this study.
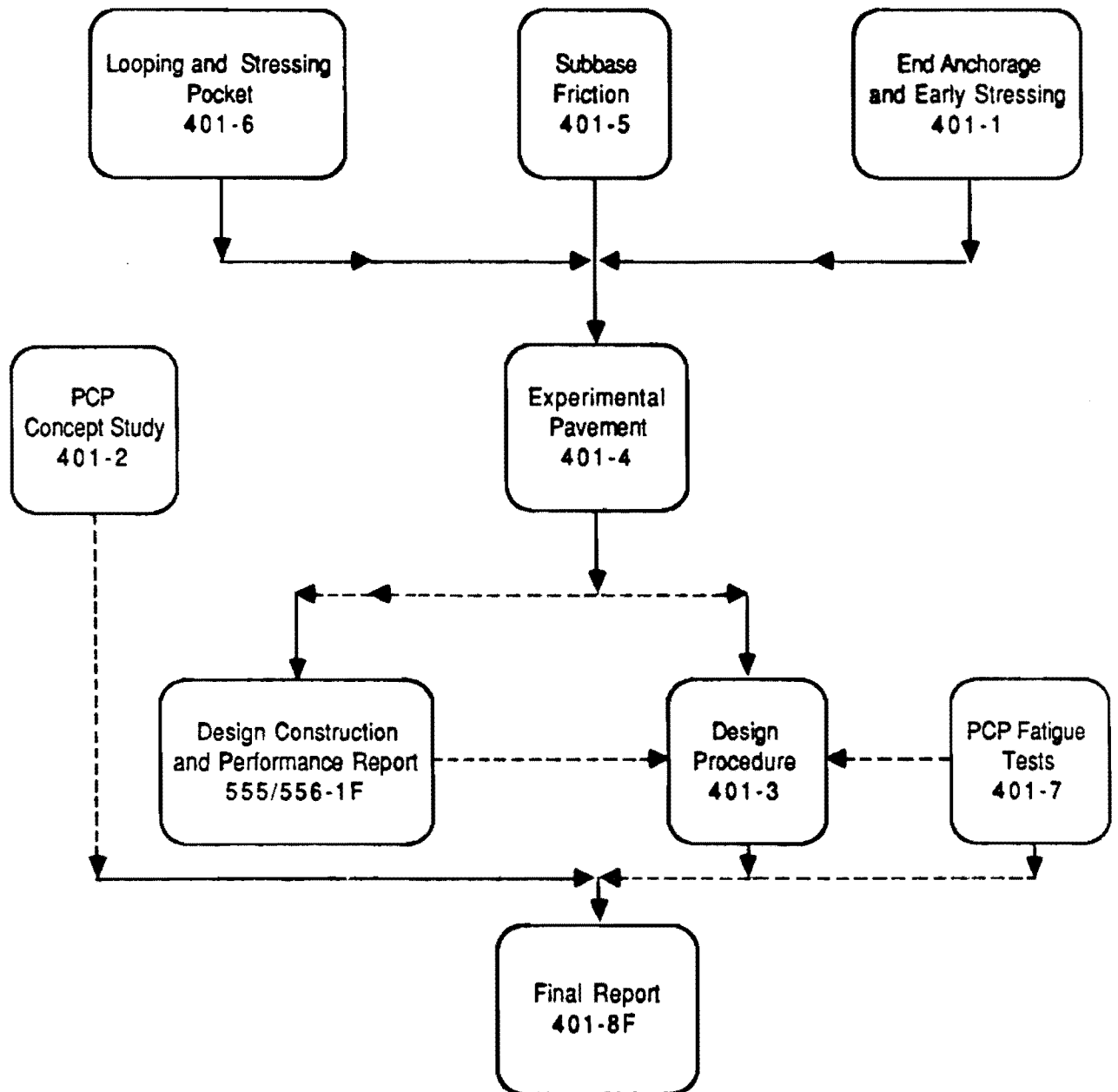
Fig 1.1. Flow diagram illustrating the development of this final report.

CHAPTER 2. FIELD EVALUATION OF SUBBASE FRICTION CHARACTERISTICS

In the design phase of any prestressed concrete pavement, an important factor to be considered is the friction characteristics of the slab-support interface.

Frictional forces develop when the prestressed slab contracts as a result of a drop in temperature, moisture reduction, concrete shrinkage, and/or creep. As the slab contracts, the movement is resisted by the friction at the interface. The resistance to movement produces a direct tensile stress in the concrete. The local movement of the slab increases from zero at the center to a maximum at the edges. The tensile stresses produced in the slab by the restraint decrease from a maximum at the geometric center to zero at the free edges, since the frictional resistance to the movement builds from the slab ends. The higher the restraint, the higher will be the tensile stresses generated along the slab length. This situation is graphically presented in Fig 2.1.

Resistance to movement is where the friction reducing medium comes into play. The role of the friction reducing medium is to reduce the tensile stresses by reducing the frictional restraint between the slab and the underlying surface.

Also, with less frictional restraint the post-tensioning will work more effectively. Higher compressive prestress can be reached at every point along the slab for a given post-tensioning force, since loss due to restraint of the force applied at the ends through the tendon anchorages will be reduced. This situation is shown in Fig 2.2

From a practical standpoint, it is not possible to completely eliminate the frictional restraint, and, in fact, it is not desirable to totally eliminate it. Reducing the frictional restraint too much would result in excessive widening of the pavement joints, thereby increasing the potential for deterioration of the slab around the joints. Moreover, working and doing construction on a slippery material may be difficult and even hazardous. Therefore, a compromise should be sought between all these factors when selecting a friction reducing medium.
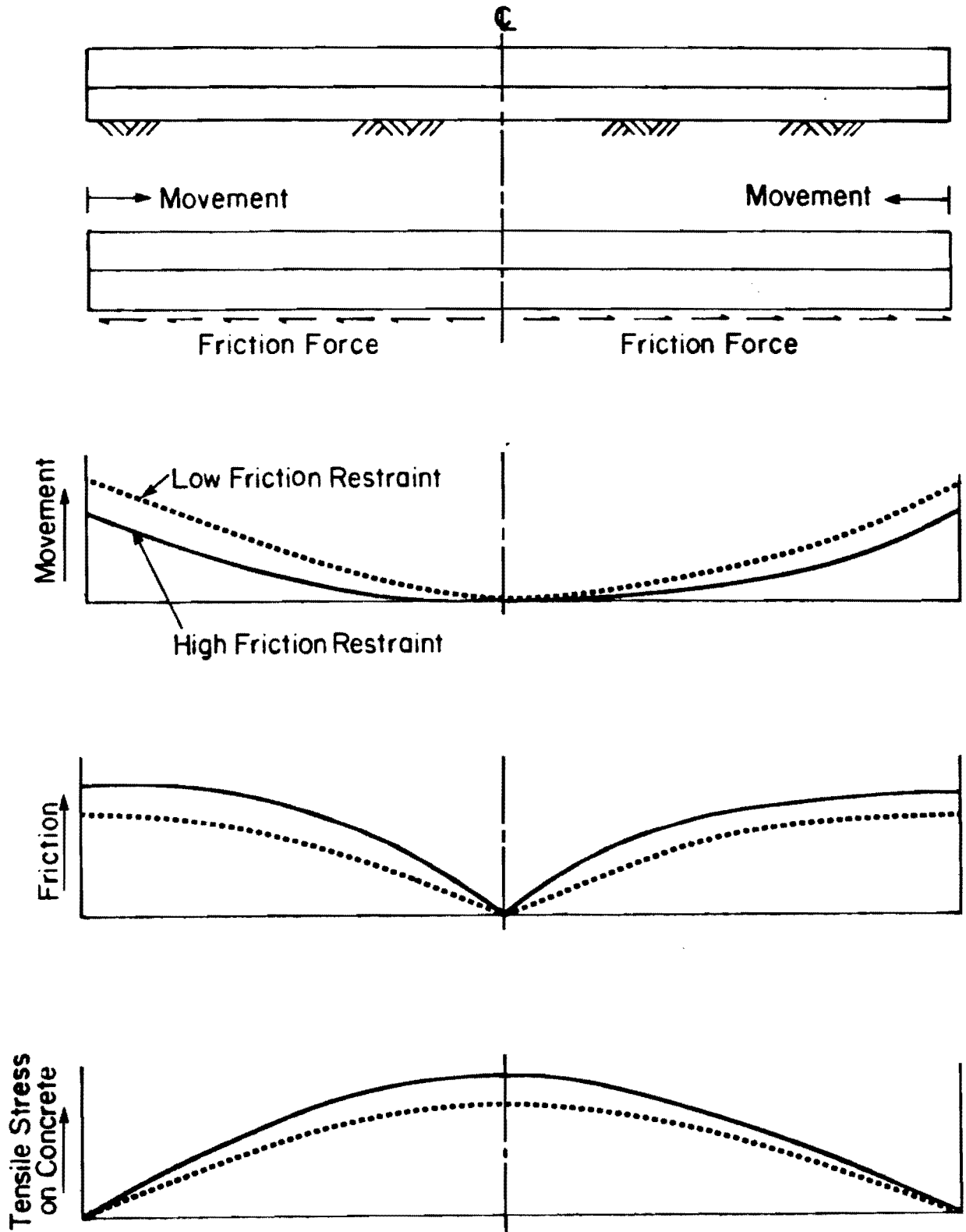
Fig 2.1. Effect of the restraint provided by the support on a concrete slab.
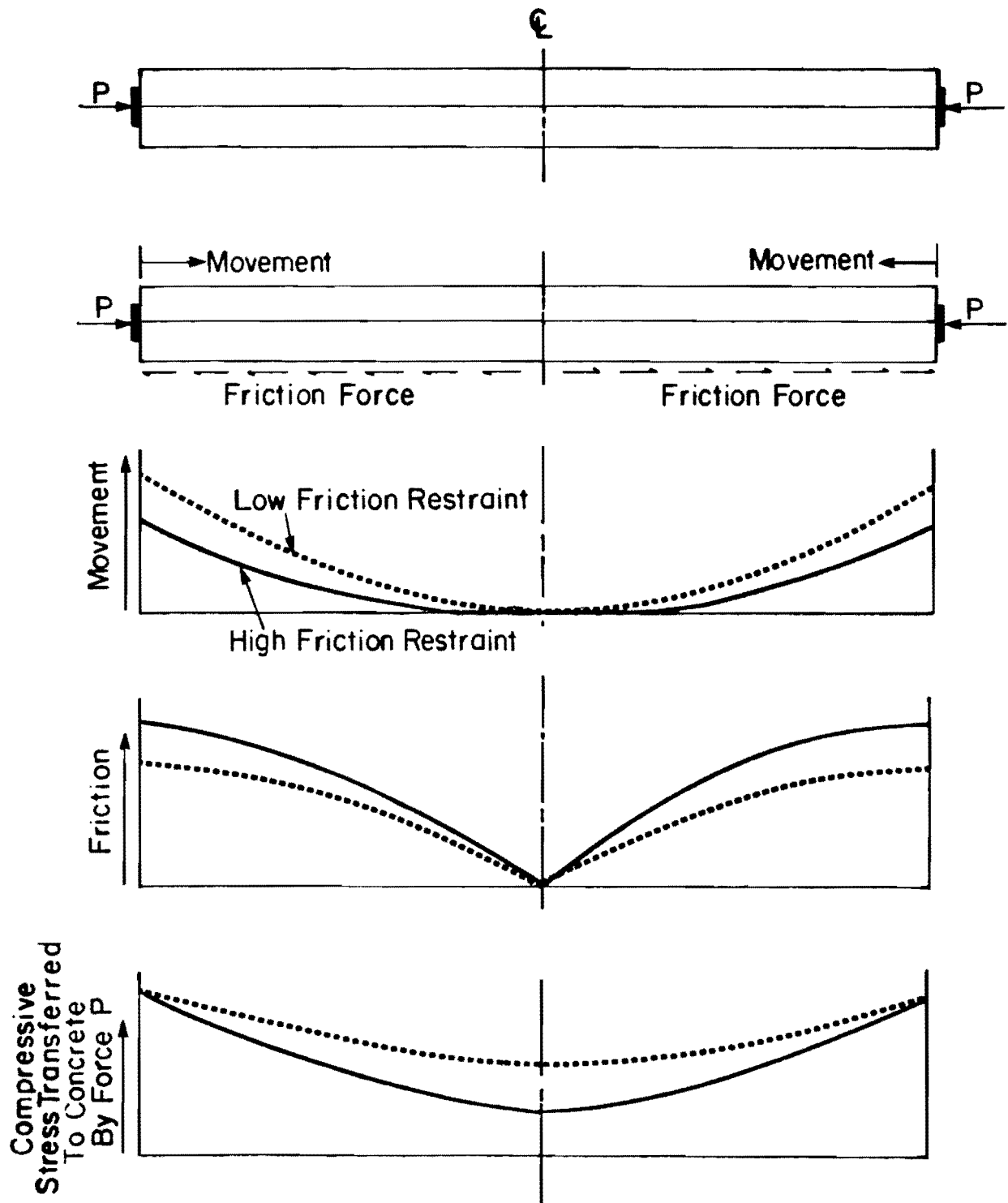
Fig 2.2. Effect of friction restrain on the compressive stress transferred to the concrete by the post-tensioning force P.

8

FIELD TESTS

Three friction-reducing mediums were investigated using push-off tests conducted on four experimental slabs.

(1)   Test Slab No. 1: a 10 x 12 x 0.5–foot rectangular slab on a double layer of 6-mil polyethylene sheeting.

(2)   Test Slab No. 2: a 10 x 12 x 0.5–foot rectangular slab cast on a spray applied concrete curing compound to serve as a debonding material.

(3)   Test Slab No. 3: a 10 x 10 x 0.5–foot square slab on a single layer of 6-mil polyethylene sheeting.

(4)   Test Slab No. 4: a 10 x 20 x 0.5–foot rectangular slab on a single layer of 6-mil polyethylene sheeting.

To fully utilize the slabs, three separate sets of push-off tests were conducted over a period of one year. The first test was conducted on May 31 and June 1, 1984, the second test on August 22, 1984, and the third test on April 23, 1985.

EXPERIMENTAL TESTING PROCEDURES

For the push-off tests, a D9 dozer was used as a dead weight to react against. The load was applied in increments of approximately 0.5 kip with a 60-kip Enerpac center hole stressing ram reacting against the dozer blade and the test slab, as shown in Fig 2.3. The applied load was determined from the readings of a 100-kip load cell and checked against the stressing ram dial gage. Four 0.5-inch travel dial gages were used on each slab to measure the movements obtained with every load increment. Three dial gages were installed against the slab face being loaded and a fourth gage was placed on the opposite face to detect any possible differential movement.

The testing procedures for the third series of tests, which were conducted on April 23, 1985, were slightly different from the first two series. Details of the three series of tests are presented in another report (Ref 1).
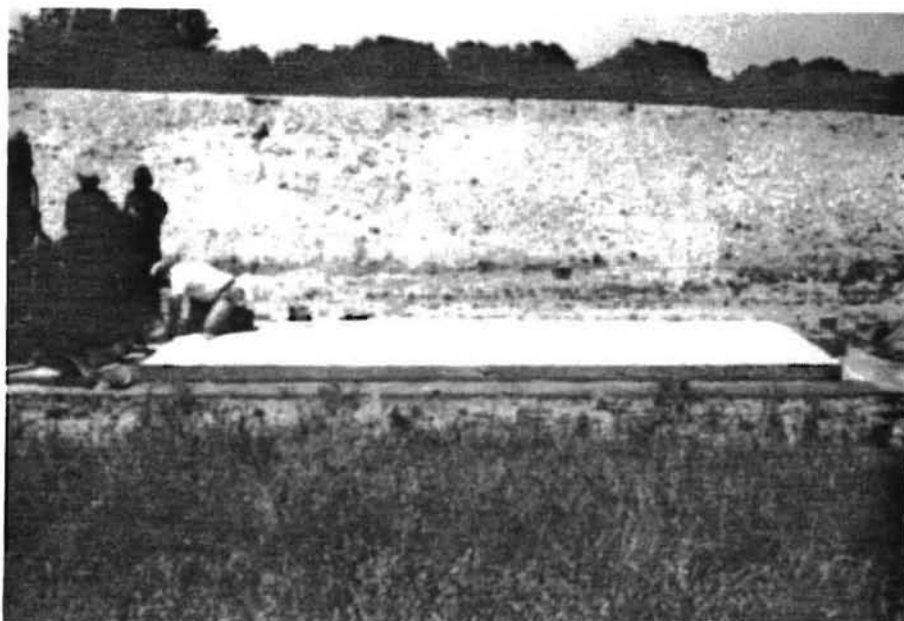
Fig 2.3. Stressing ram reacting against dozer blade and test slab.

COMPARISON OF TEST RESULTS

A summary of test results from the three series of tests is presented in Table 2.1. The most important parameter for comparison is the maximum coefficient of friction. For Slabs 3 and 4, respectively, the maximum coefficient of friction found in the third series of tests were 16 and 38 percent lower than those found in the first series of tests and 23 and 33 percent lower than those found in the second series of tests. Two possible explanations are given below.

(1) The effect of weather or temperature changes in the seven month period between the second and third series of tests may have caused movement of the slabs, which loosened the single layer of polyethylene.

(2) Since the personnel conducting the first and second series of tests were not present at the third series of tests, differences in testing technique may have caused some discrepancy. It was noted that the rate of loading affected the peak load obtained. Differences in testing technique could not, however, be responsible for the entire discrepancy between the third series of tests and the first and second series of tests.

For Slab 1, the value of the maximum coefficient of friction for the third series of tests was 13 percent higher than that for the first series of tests and 24 percent lower than that for the second series of tests. This is the only slab for which there had been any large variance between the results of the first and second series of tests. This increase in maximum coefficient of friction was attributed to a bonding of the two layers of polyethylene. The ensuing decrease in coefficient of friction recorded in the third series of test is not, however, due to a subsequent debonding of the two layers of polyethylene. This conclusion is based on the visual inspection of the double layer membrane, which was conducted after completion of the third test. When Slab 1 was picked up, the double layers were found to have adhered to the concrete. Although the two layers were not strongly fused together and could easily be pulled apart, it was clear that during the push-off tests the two layers of polyethylene moved as one. Also, a decrease in maximum coefficient of friction was recorded for Slabs 3 and 4, which had only a single layer of polyethylene.

TABLE 2.1. SUMMARY OF MAXIMUM COEFFICIENTS OF FRICTION AND MOVEMENTS AT SLIDING FROM PUSH-OFF TESTS

Test Slab Number	Friction Relieving Material	Test Performed on June 2, 1984		Test Performed on September 22, 1984		Test Performed on April 23, 1985	
		Maximum Coefficient of Friction	Movement at Sliding (in.)	Maximum Coefficient of Friction	Movement at Sliding (in.)	Maximum Coefficient of Friction	Movement at Sliding (in.)
1	Double Layer of Polyethylene File	0.47	0.004	0.70	0.006	0.53	0.007
2	Spray-Applied Bond Breaker	>3.19	0.03	>3.19	0.003	>0.68	0.001
3	Single Layer of Polyethylene Film	0.82	0.001	0.90	0.009	0.69	0.007
4	Single Layer of Polyethylene Film	0.92	0.02	0.85	0.02	0.57	0.005

SUMMARY

(1) Based on the three series of tests, the best friction reducing medium is the double layer polyethylene sheeting. Its maximum coefficients of friction range from 0.47 to 0.70.

(2) The maximum coefficients of friction of the single layer polyethylene sheeting range from 0.57 and 0.92.

(3) The physical dimensions of the test slabs also seem to affect the maximum coefficient of friction. The results from the rectangular test slab produce lower coefficients of friction in two of the three series of tests when compared to those from the square specimen.

(4) Both the single layer and double layer polyethylene sheeting were observed to move along with the concrete slab during displacement. This indicates that the friction measured occurred between the bottom surface of the polyethylene sheeting and the asphalt surface.

(5) The large variances in the maximum coefficient of friction between the three series of tests indicate that the weather and temperature may have some influence on the performance of the friction reducing medium.

(6) The spray-applied bond breaker consisting of white machine oil cut with 1/3 gasoline does not work.

RR401-8F/02

CHAPTER 3. TENDON LOOPING AND STRESS POCKET STUDY

EXPERIMENTAL SLABS - WOBBLE AND FRICTION COEFFICIENT

Prior to construction of the prestressed concrete pavement overlay in McLennan County, a series of experimental tests were performed to provide information about the type and arrangement of post-tensioning tendons to be used in the overlay. The test provided information about loss of prestress due to friction, methods of stressing the tendons, and the feasibility of certain tendon layouts. This information was helpful in making recommendations for the construction of the overlay. All of the experimental tests were performed on the four experimental slabs described in the previous chapter.

Tests were performed on post-tensioning tendons to determine the friction losses that occur when the tendons are stressed through loops involving different angle changes. Analysis of this type of friction loss was necessary since some of the alternatives proposed for providing transverse prestress in the overlay required the looping of the tendons. Determination of the friction loss occurring in the post-tensioning tendons was also useful in predicting prestress losses in the straight tendons used in the overlay as well as the looped tendons.

The frictional losses in all post-tensioning tendons can be divided in two parts: the length effect and the curvature effect. The length effect is the amount of friction that will be encountered if the tendon is straight with only unintended curvature in the layout from construction. This frictional loss is dependent on the length of the tendon, the stress in the tendon, the method used in aligning the tendon prior to the casting of the concrete, and the coefficient of friction between the contact materials. The length effect can be substantially reduced by using tendons which are lubricated and encased in flexible thin wall plastic sheathing. The loss of prestress due to the intentional curvature effect is also dependent on the coefficient of friction between the contact materials and the pressure exerted by the tendon on the concrete as a result of the total angle change. The formula proposed by the Building Code Requirements for Reinforced Concrete (ACI 318-83) (Ref 2) to compute the frictional losses due to the length and curvature effects is

14

$$P_s = P_x e^{(kl_x + \mu\alpha)} \tag{3.1}$$

where

P_s	=	prestressing tendon force at jacking end, lb;
P_x	=	prestressing tendon force at point x, lb;
k	=	wobble friction coefficient per foot of prestressing tendon;
l_x	=	length of prestressing tendon from jacking end to any point x in feet;
μ	=	curvature friction coefficient; and
α	=	total angular change of prestressing tendon from jacking end to any point x.

In the experiments, the losses produced in loops of 180, 270, and 720° were analyzed for tendons coated in a plastic sheathing. The tendons were 0.6–inch–diameter, grade 270, seven-wire prestressing strand and were lubricated with grease and coated with a 36-mil plastic sheathing. Two of the experimental slabs had tendons with a 180°loop and the two additional slabs contained a 270° or a 720° loop.

One important aspect of the experimental tests was the investigation of methods of post-tensioning the tendons. One method consists of stressing the tendons at internal blockouts or stressing pockets which are filled with concrete after the post-tensioning force has been applied. In this method of post-tensioning, the stressing pocket is located at the centerline of the slab with the two segments of the tendon extending from the pocket to anchors set in each end of the slab. The two segments of the strand overlap in the stressing pocket and are inserted through a steel stressing sleeve known as a lock-coupler. Anchorages are installed on the protruding strand ends and the stressing ram is then attached to the end of one of the strand segments. Both segments are simultaneously stressed as the prestress force is applied. The dimensions of the stressing pockets were varied in the experiments to determine the most efficient size for the pockets.

The tests, in part, were conducted so as to quantify the amount of the friction losses generated through the lock-coupler device. This information, combined with the information

on friction losses due to the length and curvature effects, will enable the total losses due to friction to be quantified.

A second method of post-tensioning the tendons was also investigated. The two ends of the tendon to be stressed protruded from the edge of the test slabs approximately 3 feet. To stress the tendon, one end of the tendon was anchored against the slab edge while a stressing ram was placed on the other end. The stressing ram uses the edge of the slab to react against while stressing the tendon. The size of the stressing ram defines how far the end of the tendon must extend from the edge of the slab. The stressing ram used for all post-tensioning in the tests was typical of stressing rams used in the industry for stressing single-strand tendons.

As a result of the experimental tests performed on the four test slabs, several observations were made concerning friction losses, stressing methods, and tendon layouts.

Analysis of the measurements taken during post-tensioning operations resulted in values for the wobble friction coefficient, k, and the curvature friction coefficient, μ. For tendons that had no damage to the plastic sheathing, the wobble coefficient was 0.00145 and the curvature coefficient was 0.0184. The tendons with damaged plastic sheathing had values for k and μ of 0.00356 and 0.0355, respectively. These last tendons were probably damaged during transportation and handling. To reduce the values of the friction coefficients and thus the loss of prestress, it is recommended that damage to the plastic sheathing be minimized. Using high quality plastic material for the sheathing and having sufficient sheathing thickness should reduce damage during transportation and handling. The sheathing should be thick enough not to crack when the tendon is curved or looped.

The loss of prestress in the lock-coupler device was observed to vary from 2.50 kips to 4.20 kips. This loss of prestress is due to friction between the steel tendon and the steel coupling device and must be added onto the losses due to length and curvature effects.

USE OF STRESSING POCKETS

For the post-tensioning method that involves the use of stressing pockets, the size of the pocket is important. The required size of the stressing pocket is dependent on the type of stressing ram to be used and also the expected tendon elongations. The width of the pocket should be large enough to provide at least 1/4 inch of clearance on both sides of the ram. The pocket length must be long enough to accommodate the fully extended ram. Since the lock-

coupler device will change position during post-tensioning, the length of the pocket must be enough to accommodate this anticipated movement. The lock-coupler movement depends on the anticipated tendon elongation, and, therefore, on the length of the tendon and the slab.

The tests showed that stressing in properly sized pockets would be only slightly more difficult than stressing the tendons at the edge of the slab. This increase in difficulty is attributable to the more confined working space. However, on the actual pavement overlay project, a discrepancy between the anticipated and actual stressing equipment dimensions could have serious consequences. Since equipment dimensions vary, it is important for the contractor to work closely with the stressing equipment suppliers in determining required pocket sizes when paving is done.

In placing the tendons in the looped configurations, the layouts as originally designed could not be obtained exactly. The tendons were not flexible enough to allow sharp radius loops and they had to be wired in all cases to maintain the required shape. Some looped configurations may be difficult to obtain and might require that the tendon be given its shape prior to placing it inside the formwork.

McLENNAN COUNTY OVERLAY DATA - WOBBLE AND FRICTION COEFFICIENT

During construction of the prestressed concrete pavement overlay, the post-tensioning operations were monitored so that the actual amount of friction losses occurring could be determined. For each tendon, the jacking force and the resulting tendon elongation were measured. Using Eq 3.1, the wobble and curvature coefficients can be back calculated from the data obtained from the overlay. The tendons used were the same as in the experimental tests with the plastic sheathing in good condition. Analysis of the data gives wobble coefficients of 0.001 to 0.003 feet^{-1} and a curvature coefficient of 0.089 radian^{-1}.

Factors affecting the analysis of the data include the amount of friction loss through the lock-coupler and the modulus of elasticity of the tendon. The friction loss assumed was between 5 and 10 percent of the jacking. This value is an approximation based on the data obtained in the experimental tests and can vary between lock-couplers depending on the condition of the coupler (rusted or unrusted).

The modulus of elasticity was taken as 28,000 ksi, which is a value used by the manufacturer of the type of tendon used and was obtained from Ref 3. The modulus of elasticity

of steel is 29,000 ksi. However, in a 7-wire strand such as the one used in the overlay, the steel wires are wrapped around each other and can twist as the tendon is stressed. If this occurs, the tendon elongations are larger than they would be if the wires did not twist. How the tendon is stressed determines if it will twist and thus how much elongation will occur. The modulus of elasticity used should reflect how much the tendon twists and elongates.

CHAPTER 4. INITIAL STRESSING AT EARLY AGE OF CONCRETE TO PREVENT CRACKING

PROBLEM OF EARLY CRACKING

One of the attractions of prestressed concrete pavement over conventional concrete pavement is the large reduction in the number of joints. The span between joints ranged from 400 to 760 feet in the four major U.S. projects.

However, this increased length of span between joints causes a major problem. During the first night after casting, when the temperature drops, the pavement must contract. The distance from the middle of the slab to the nearest joint, where movement is possible, is so long that, as the concrete tries to move, tensile stresses build up because of the frictional resistance of the subgrade. Then, if these tensile stresses exceed the tensile strength of the concrete, a crack forms.

Cracks occurring during the first night after casting have been reported in the Mississippi, Arizona, and Virginia projects. Mississippi reported cracks in 24 of 58 slabs. Although most of the cracks were closed after post-tensioning, keeping sections uncracked is a primary reason for prestressing pavements.

OBJECTIVES AND SCOPE

This chapter concludes with recommendations for field use through the use of design aids and a reliability study. For more details than can be summarized in this chapter, the reader is referred to Research Report 401-1 (Ref 4).

This study is part of an investigation to develop a design procedure for prestressed concrete pavements and construct two demonstration projects near Waco and Gainesville, Texas. This report presents the experimental work on the strength of concrete at very early ages, the post-tensioning force that will cause cracking near the post-tension anchorage at very early ages, and the field applications of this research finding to solve the problem of temperature and shrinkage cracks.

The next section discusses the experimental program and describes the test set-up and testing technique, and includes an explanation of the experimental parameters.

THE EXPERIMENT

Purpose

An experimental program was performed to discover the earliest possible time at which concrete slabs could be post-tensioned to overcome tensile stresses due to temperature and shrinkage effects without causing an anchorage zone failure. Although data from previous tests exist, no data were available for very early post-tensioning, when concrete properties are not the same as for more mature concrete.

Description of Test

General. The test slab design simulated the materials and cross-section of two one-mile post-tensioned concrete pavement overlays which were being constructed at Waco and Gainesville, Texas in 1985. These demonstration projects are part of the experimental study at The University of Texas at Austin for the development of a design procedure for prestressed concrete pavements. The test specimens consisted of several single strand full scale concrete slabs.

The slab width was determined by the strand spacing of the actual pavement design and the length was taken as 4 feet for convenience of form work. Four feet was more than adequate to develop the anchorage zone stresses. The thickness also corresponded to the actual pavement design.

The strand used was 0.6-inch-diameter, 270 ksi, seven wire coated strand manufactured in accordance with ASTM A-416. The strand was located 1/4 inch above middepth, simulating the actual design, which called for strand placement 1/4 inch below middepth. The strand was placed above middepth rather than below so that the side with the thinner cover was visible.

To develop the bar, a closed loop (Figs 4.1 and 4.2) was used in the narrow test slabs. The design calls for continuous bars at the slab ends. The slabs were reinforced with one number 4 bar above and one below the strand just in front of the anchor.

The forms were lined with polyethylene to be consistent with the actual slabs, which were to be cast on polyethylene to reduce friction. The specimens could be easily removed
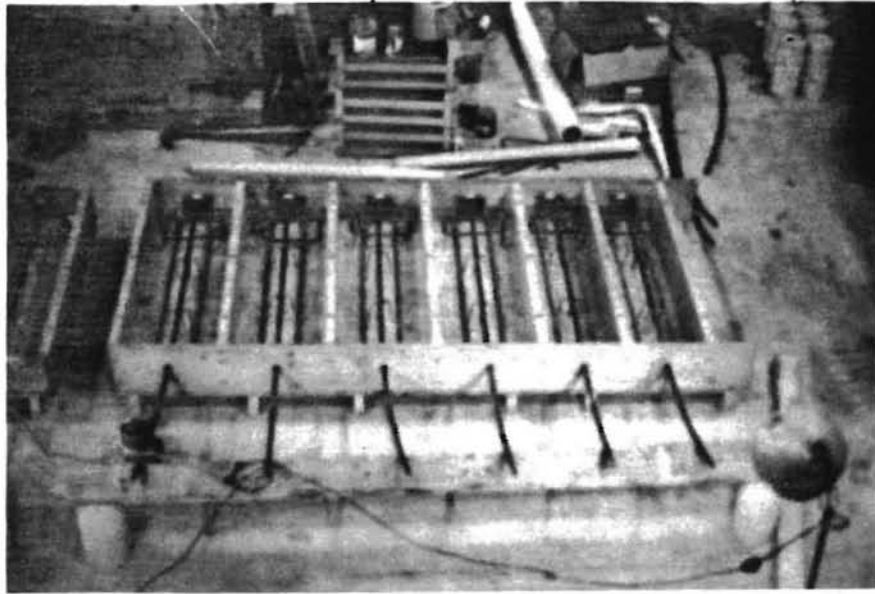
Fig 4.1. Forms for test slabs ready for concrete placement.
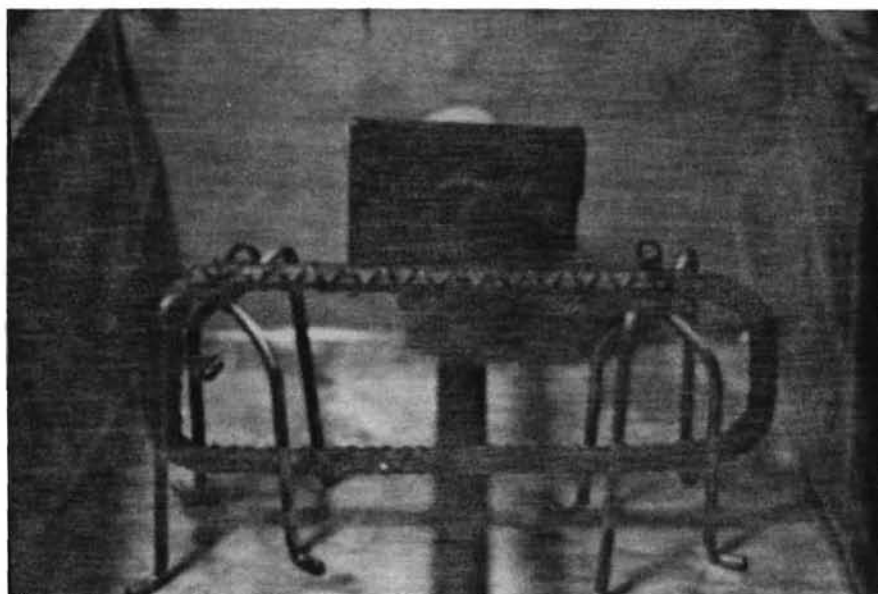
Fig 4.2. Reinforcement for test slabs.

from the forms because of this lining. A typical form for several slabs is shown in Fig 4.1. Figure 4.2 shows the anchor and reinforcing bars immediately in front of the anchor.

A readymix plant supplied the concrete mix designed in accordance with Item 360 of the Standard Texas Highway Department Specifications for slip form paving. The mix called for 5 sacks of Type I cement per cubic yard. Strength was specified as 650 psi minimum for center point load modulus of rupture tests at seven days. A more complete batch design is found in Ref 4.

Concrete was placed using an overhead crane and bucket (Fig 4.3) and was finished and covered with wet burlap and plastic. Many test beams and cylinders were cast for concrete strength measurements (see Fig 4.4).

Experimental Parameters. The variables considered in this testing program were selected to simulate the varying field conditions. Table 4.1 contains a summary of the variables for the actual pavement design.

(1)   Strand Spacing. As part of the overall investigation of prestressed concrete pavement performance, two different pavement lengths were chosen, 240 and 440 feet, to see which was more acceptable in terms of economy and pavement performance (including joints). The corresponding strand spacings to obtain the minimum prestress necessary for the 240–foot and 440–foot slabs were 24 and 16 inches, respectively, for one site and 18 and 12 inches, respectively, for the other.

According to Guyon (Ref 5) the bursting stresses in a single strand specimen with a given slab width are very similar to those of a multi-strand slab with strand spacing equal to this same width. Based on this information, strand spacings were modeled by a single strand slab with nominal widths of 12, 16, and 24 inches. Actual widths were 11, 14-1/4, and 22-1/8 inches because of limiting geometry of a 4 –foot by 8–foot sheet of plywood.

(2)   Slab Thickness. Slab thickness and prestress level depend on the supporting properties of the existing pavement structure, and loading and environmental conditions. Field conditions yielded design thicknesses of 6 and 8 inches and 65 and 100–psi effective prestress levels for the two sites. These sets of design values were determined from fatigue analysis on the two experimental sites. Thicknesses of 6 and 8 inches were chosen for the test slabs. Only the 6–inch–thick slabs at Site 1 (Fig 4.1) were actually constructed.

(3)   Anchor Size. Single strand anchor sizes range from 5-3/8 x 2-3/4 inches to 6 x 3-1/2 inches for 0.6-inch-diameter strand, depending on the manufacturer (Ref 7). Two different anchor sizes were chosen to study the bearing area effect. Anchor 1 (A1) was
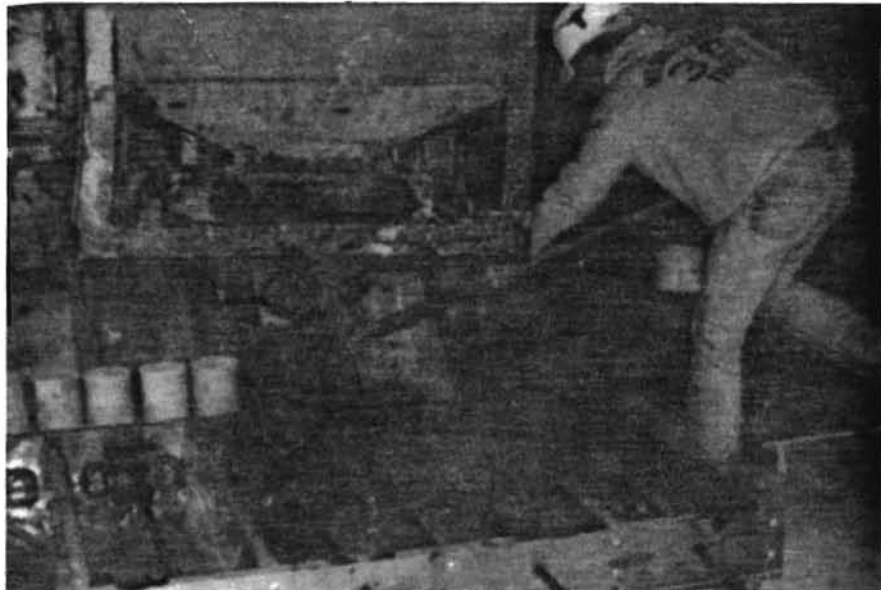
Fig 4.3. Concrete placement.

Fig 4.4. Preparing specimens for concrete strength tests.

TABLE 4.1.   SUMMARY OF SOME OF THE DESIGN PARAMETERS FOR THE TWO TEXAS
DEMONSTRATION PROJECTS

Location	Slab Length (feet)	Strand Spacing (inches)	Slab Thickness (inches)
Site 1	240	24	6
(Waco)	440	16	6
Site 2*	240	18	8
(Gainsville)	440	12	8

*Note: The design was done for the Site 2 pavement, but these
slabs with 8 inch thickness were not constructed.

4-5/8 x 3-1/2 inches and anchor 2 (A2) was 6 x 3-1/2 inches. These were in the mid to large size range. The anchors are shown in Fig 4.5.

(4)   Time. Since the objective of the testing program was to determine the earliest possible time at which post-tension force could be applied, time after casting at which the slabs were tested was a very important variable. Time since concrete batching was also used, as a more general indicator. The first crack on previous projects occurred during the first night, and, therefore, a 24-hour testing schedule was established. For the first two series testing times of 6, 12, 18, and 24 hours after casting were chosen. The times were revised to 4, 8, 12, and 16 hours for the third series.

Other Parameters Measured. Several parameters were not controlled, but were measured because they have an influence on the results of the study. These were (1) ambient temperature, (2) concrete temperature, (3) concrete maturity, and (4) concrete strength.

Concrete strength was measured using three different testing means: compressive strength, tensile strength, and flexural strength. Compressive strength was measured by testing three 6-inch-diameter by 12-inch-tall cylinders at each testing time. Tensile strength was measured using the 6-inch by 12-inch cylinders in a split cylinder test, and flexural strength was measured using the 6 x 6 x 23-inch beam in a modulus of rupture test with center point loading on an 18-inch span.

Testing Apparatus. This section describes the manner in which the slab anchorage zones were tested, including the means of load application and load measurement and the loading technique.

(1)   Load Application. For each of the test specimens the strands were stressed using a hydraulic ram with a hand pump. Load was applied slowly through a stiff spreader beam so as to distribute the load over the area of the slab end face, thus avoiding concentrated loads and possible localized failures (see Figs 4.6 and 4.7).

(2)   Load Measurement. Loads were measured using a load cell and a strain indicator which were calibrated before and after the tests. A pressure gauge for the ram was used as a backup load measuring device (see Fig 4.7).

(3)   Loading Technique. After removing the forms, loads were applied slowly at small intervals. Due to the violent nature of some of the failures, crack observation was done after each load interval rather than during loading. For this reason there is slight uncertainty
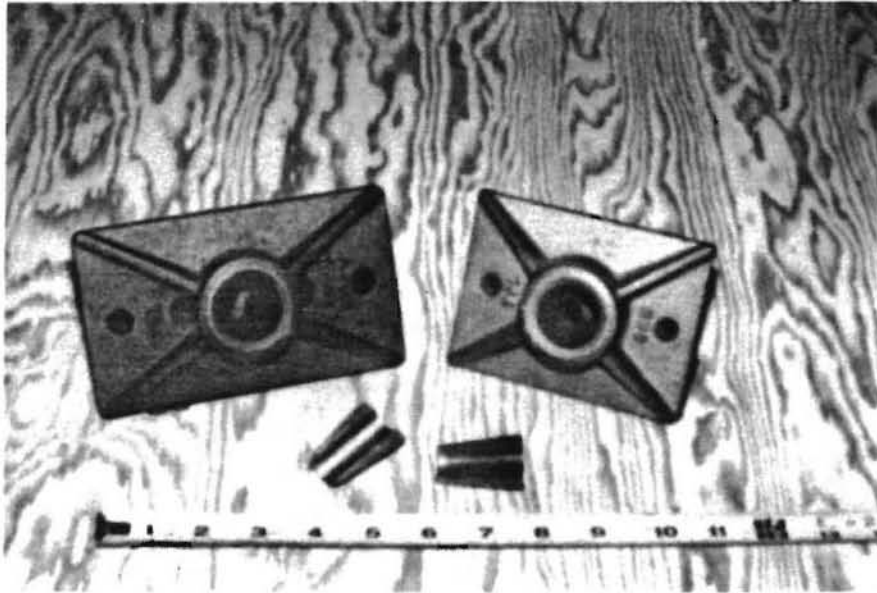
(a) Two anchors used in tests.

(b) Anchor with strand and grips in place.

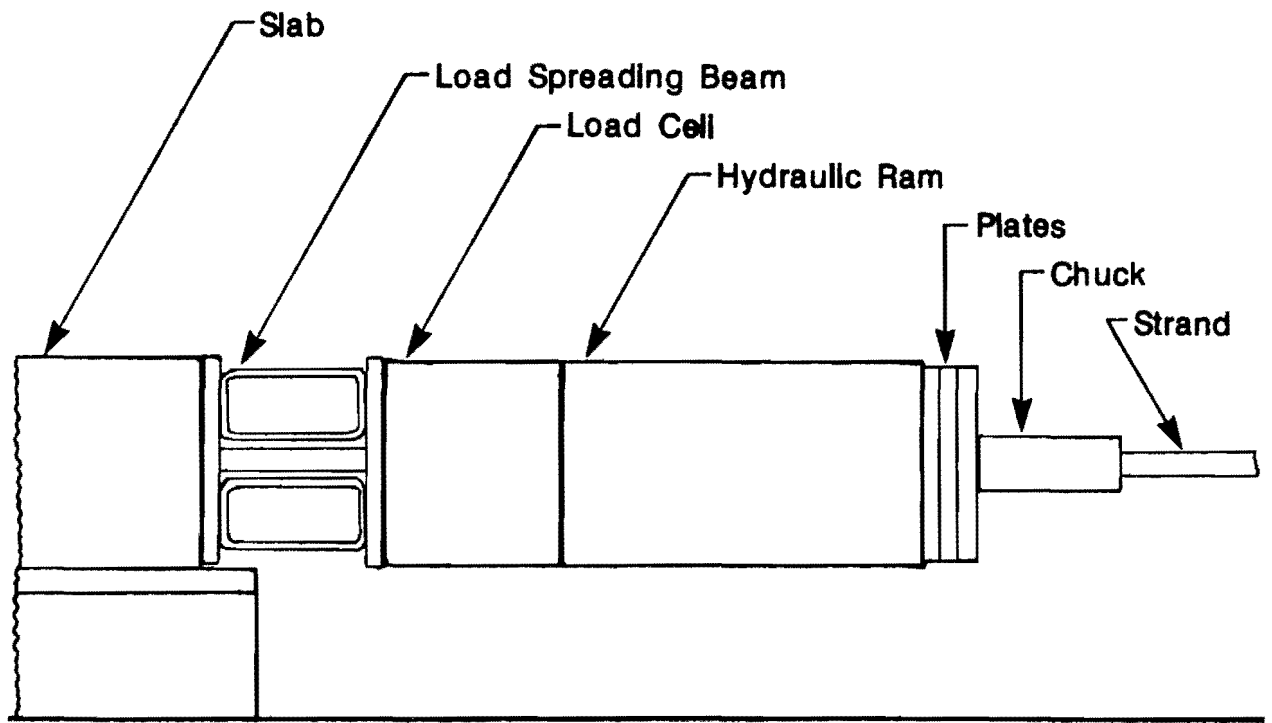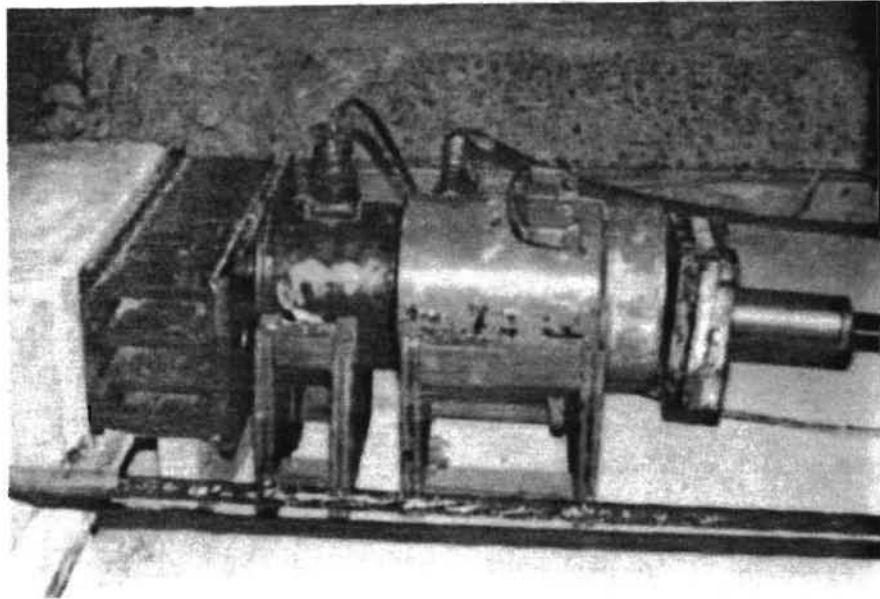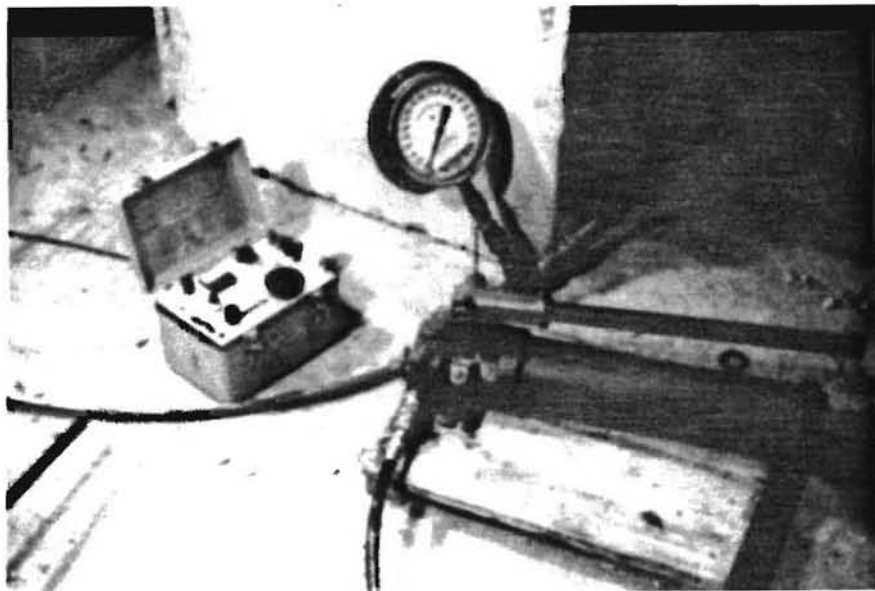Fig 4.5. Mono-strand anchorage used in tests.

Fig 4.6. Test slab loading apparatus.

(a) Load application.

(b) Strain indicator and pressure gauge for load reading.

Fig 4.7. Application of post-tensioning force to slabs.

as to the exact load at which cracking occurred, but the intervals were small enough for the recorded cracking load accuracy to be within 1 kip.

Testing Scheme

Testing was completed in three different series. Each series had a certain purpose and set-up. The following sections describe the purpose and set-up of each series.

Series I.

(1)   Purpose. The purpose of test Series I was threefold: (1) to test the loading apparatus and overall testing scheme, (2) to check for scatter in data (three identical slabs were tested each time to find out the range of cracking loads and ultimate loads), and (3) to set some preliminary data points for the study.

(2)   Set-up. The test slabs of Series I were all 6 inches thick, 16 inches wide, and contained a small anchor.

Series II.

(1)   Purpose. The purpose of Series II was to complete the testing of 6-inch-thick slabs by varying the specimen width and the anchor size. Only one slab was constructed and tested for each set of variables, because little scatter of data was observed in Series I.

(2)   Set-up. The test slabs in this series were all 6 inches thick and had widths of 16 and 24 inches. The anchor size was varied. The small anchor is designated anchor 1 (A1), and the larger anchor is designated anchor 2 (A2).

Series III.

(1)   Purpose. There were three purposes of Series III. The first was to include the variables slab thickness and strand spacing. The second was to repeat tests of Series I because of the poor quality of the concrete for the first tests. The final purpose was to test one double strand slab.

(2)   Set-up. All slabs contained the small anchor plate, because the second series of tests showed that the size of the anchor did not affect the results substantially. Five 6-inch slabs were cast. Four were 16 inches wide and one was 32 inches wide. The 32-inch slab

contained two strands which were stressed simultaneously for comparison with the single strand slabs.

Ten 8-inch-thick slabs were cast and tested. Four were 24 inches wide, four were 16 inches wide, and two were 12 inches wide. All 8-inch-slabs contained one strand each.

General

One of the major purposes of this study was to obtain practical values for cracking loads for post-tensioned slabs and to make recommendations for field use. This section contains a reliability study, some design aids, and an outline for the procedure to follow in calculating a practical allowable post-tensioning force.

Statistical Analysis and Model

A statistical computer program for stepwise multiple regression (STEP-01) was used to analyze the test data for the influence of the different variables on the cracking load. From the data, the program computes a sequence of multiple linear regression equations in a stepwise manner. Variables are added and removed from the regression equation, depending on whether or not they improve the accuracy of the equation. The calculated cracking load is compared to the actual cracking load in Fig 4.8. The regression equation is presented in the next section.

Design Aids

Three techniques for calculating the cracking load are presented below: a cracking load equation, tables of cracking loads for different variables, and a graph of cracking load versus concrete tensile strength for different variables.

Limitations

Due to their empirical nature, each of the three methods for calculating cracking load is limited to applications similar to those of this study. These are the restrictions :
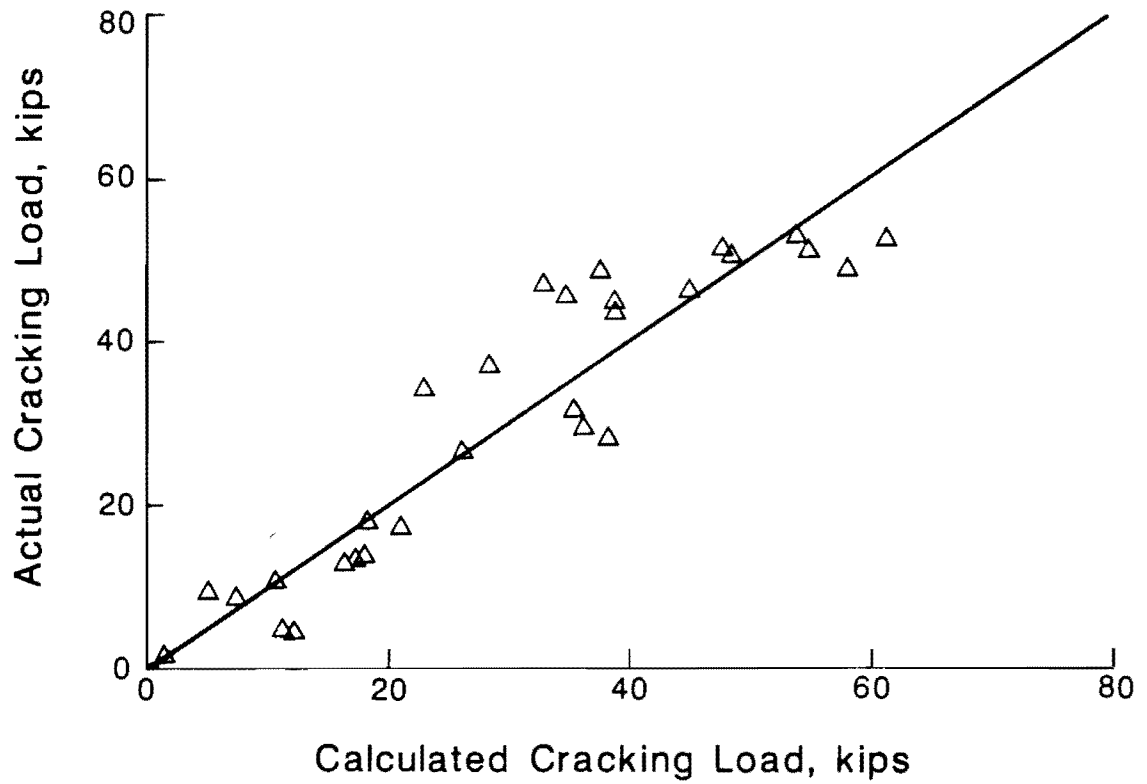
Fig 4.8. Comparison of cracking loads calculated to actual cracking loads.

(1) Concrete tensile strengths were between one and 260 psi based on split tensile tests.

(2) Slab thicknesses were 6 and 8 inches.

(3) Strand spacings were between 12 and 24 inches.

(4) Anchors were single 0.6-inch-diameter strand flat plate anchors for slabs at 16.19 and 21.00 square inches in areas.

(5) Strands were placed 1/4 inch above middepth, but eccentricity was not varied.

Equation

The data regression program yielded terms for an equation to estimate the cracking load. The equation in a slightly simplified form is

$$P_{cr} = 3.25\,t - 0.08\,(2a)\,(a") + 0.002\,f_{sp}^{\frac{1}{2}}\,t\,(2a)\,(a") \tag{4.1}$$

where

P_{cr} = cracking load, kips;

t = slab thickness, inches;

$2a$ = strand spacings, inches;

f_{sp} = concrete tensile strength, psi; and

$a"$ = anchorage area, inches^2.

The equation fits the test data well for most combinations of variables. Problems do arise when cracking loads are calculated for very low concrete strengths. For example, if a concrete tensile strength of zero psi is input, the cracking load does not come out to equal 0. For low values of thickness and high values of strand spacing and/or anchor size, the calculated cracking load is negative, which is conservative. For high values of thickness and low values of strand spacing and/or anchor size, the calculated cracking load is positive, which is unconservative.

Table. Equation 4.1 was used to generate a table of cracking loads for the slab thicknesses and strand spacings to be used in the actual design of the prestressed concrete pavement (see Table 4.2). The smaller anchor (A1) used in the test was used in the calculations.

Graphs. Equation 4.1 was used to generate Fig 4.9 for estimating cracking loads for different concrete strengths. Figure 4.9(a) is for a 6-inch-thick slab and 16 and 24-inch strand spacing. Figure 4.9(b) is for an 8-inch-thick slab and 12 and 18-inch strand spacing. Both figures are for the smaller anchor.

Reliability Study

The safety factor applied to the cracking load depends on the desired reliability. Figure 4.10 shows the safety factor for different reliabilities as developed from the cracking load predictions and the actual cracking load values.

Calculation Procedure

The procedure for determining the allowable post-tensioning force is extremely simple. The following steps give the necessary force and the allowable force required to prevent cracking.

(1) Given slab length and drop in concrete temperature, determine the tensile stress in the slab using Fig 4.11.

(2) Determine the concrete strength from the cylinder break or a previously established strength versus maturity curve.

(3) Determine the required safety factor (CSF) for the desired reliability against cracking from Fig 4.10 and calculate the allowable post-tensioning force (P_{allow}). Note: $P_{allow} \leq 0.8 f_y \times A_s$, where f_y = STRAND YIELD. $P_{allow} = P_{cr} \div SF$.

(4) Check the slab compressive stress due to P_{allow} to see if it exceeds the tensile stress due to temperature drop added to the tensile strength of the concrete. (Note: It is not necessary to overcome 100 percent of the tensile stress because the concrete has some tensile strength.)

TABLE 4.2.   PREDICTED CRACKING LOAD (KIPS) FOR DIFFERENT SLAB THICKNESSES, STRAND SPACINGS, AND CONCRETE STRENGTHS (REF 4)

Thickness (6 in.)			Thickness (8 in.)		
	Spacing (in.)			Spacing (in.)	
Tensile Strength* (psi)	16	24	Tensile Strength* (psi)	12	18
0	-1.22	-11.58	0	10.46	2.69
10	8.61	3.16	10	20.29	17.43
20	12.68	9.27	20	24.36	23.54
30	15.80	13.95	30	27.48	28.23
40	18.44	17.90	40	30.12	32.18
50	20.76	21.39	50	32.44	35.66
60	22.85	24.53	60	34.54	38.80
70	24.78	27.43	70	36.47	41.70
80	26.58	30.12	80	38.26	44.39
90	28.27	32.65	90	39.95	46.92
100	29.86	35.04	100	41.54	49.31
110	31.38	37.32	110	43.06	51.59
120	32.83	39.49	120	44.51	53.76
130	34.22	41.58	130	45.90	55.85
140	35.56	43.59	140	47.24	57.86
150	36.85	45.52	150	48.53	59.79
160	38.10	47.39	160	49.78	61.67
170	39.31	49.21	170	50.99	63.48
180	40.48	50.97	180	52.16	65.24
190	41.62	52.69	190	53.31	66.96
200	42.74	54.36	200	54.42	68.63

*Based on split tensile tests.
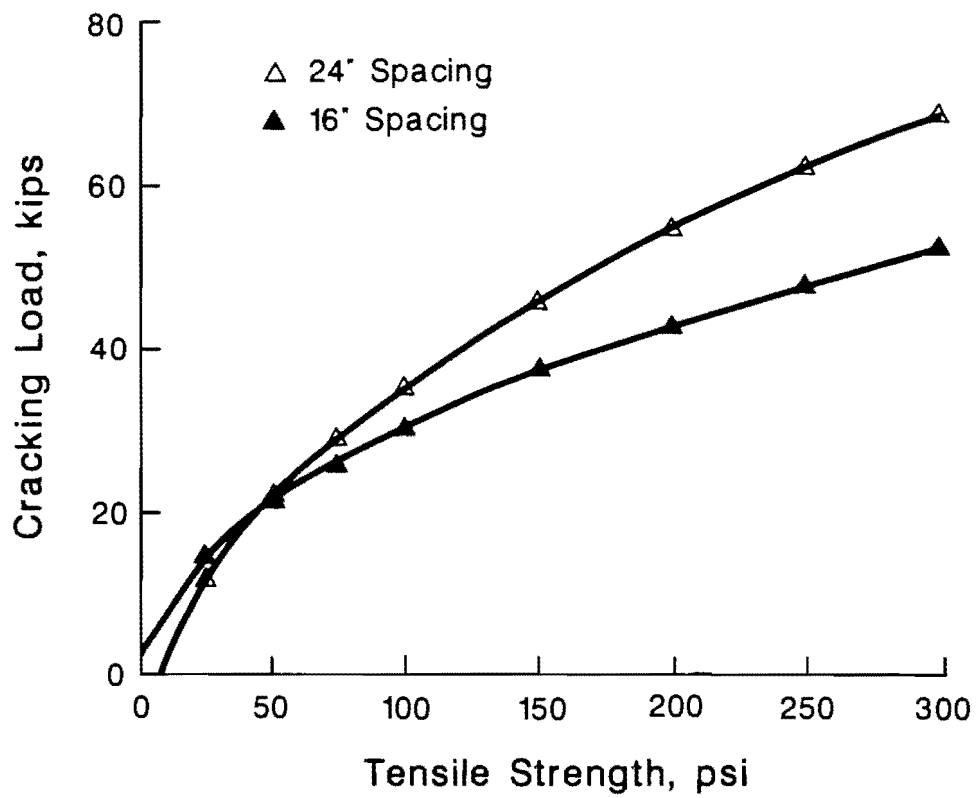
Fig 4.9(a). Predicted cracking load using Eq 4.1 (6–inch-thick slab with 16 and 24–inch strand spacings) (Ref 4).
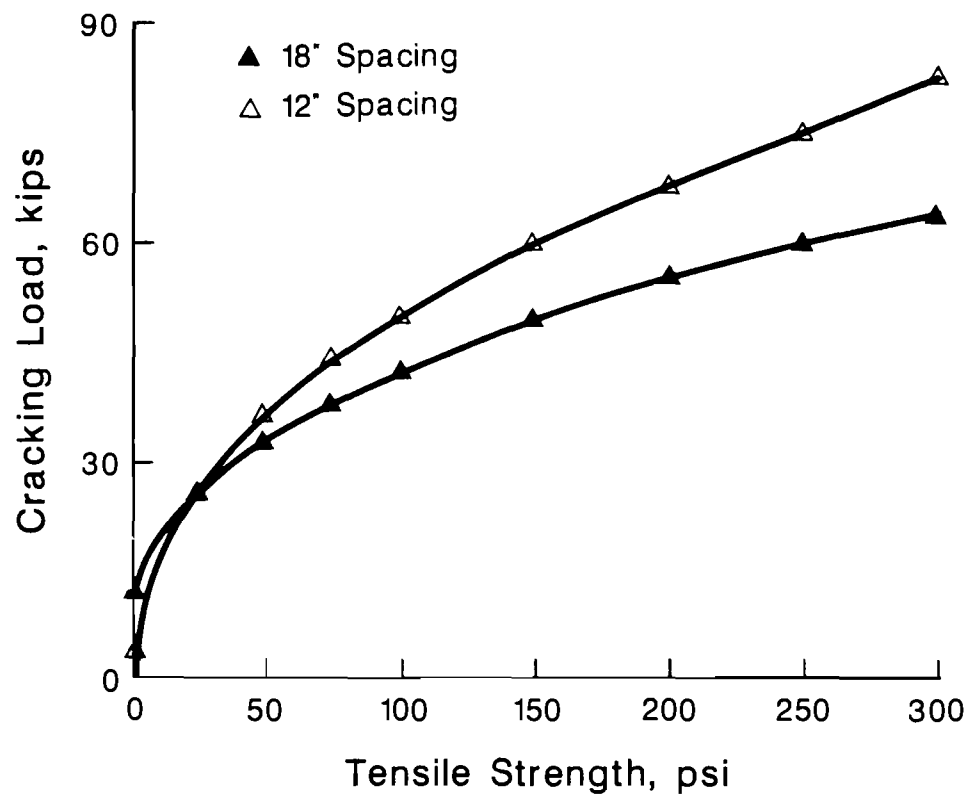
Fig 4.9(b).   Predicted cracking load using Eq 4.1 (8–inch-thick slab with 12 and 18–inch strand spacings).
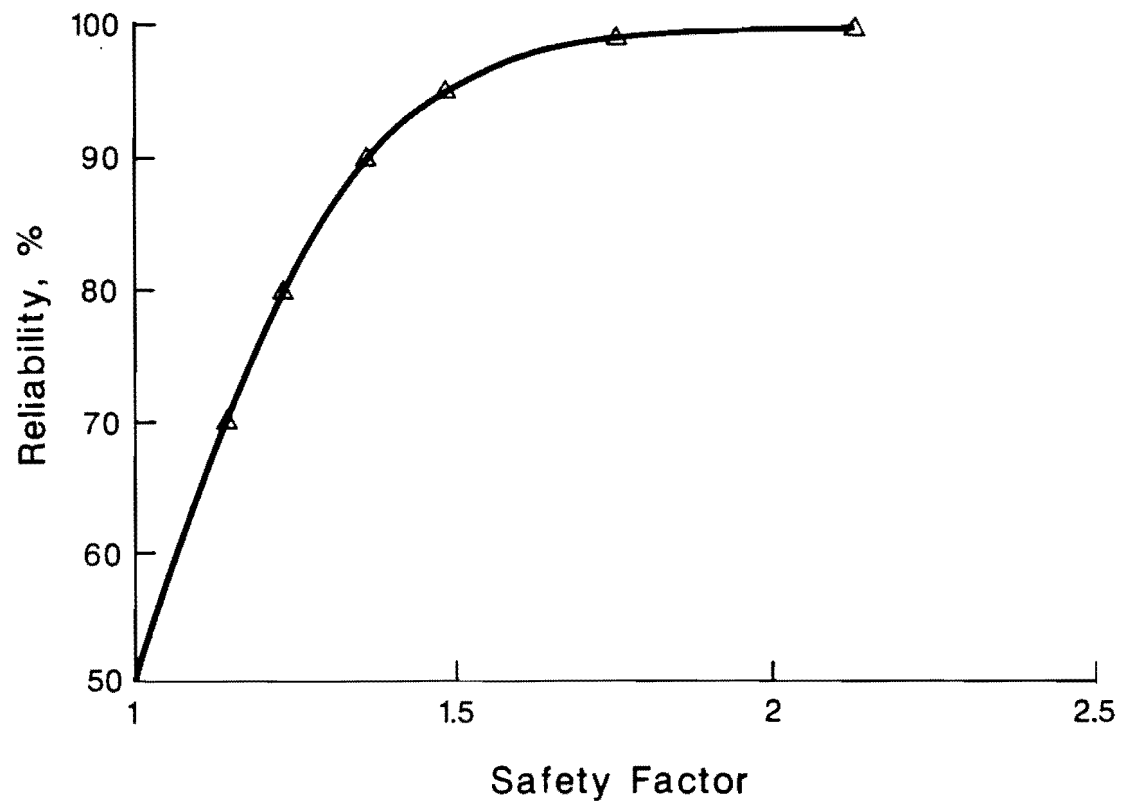
Fig 4.10.   Safety factor to be applied to cracking load prediction for various reliabilities
against cracking (Ref 4).
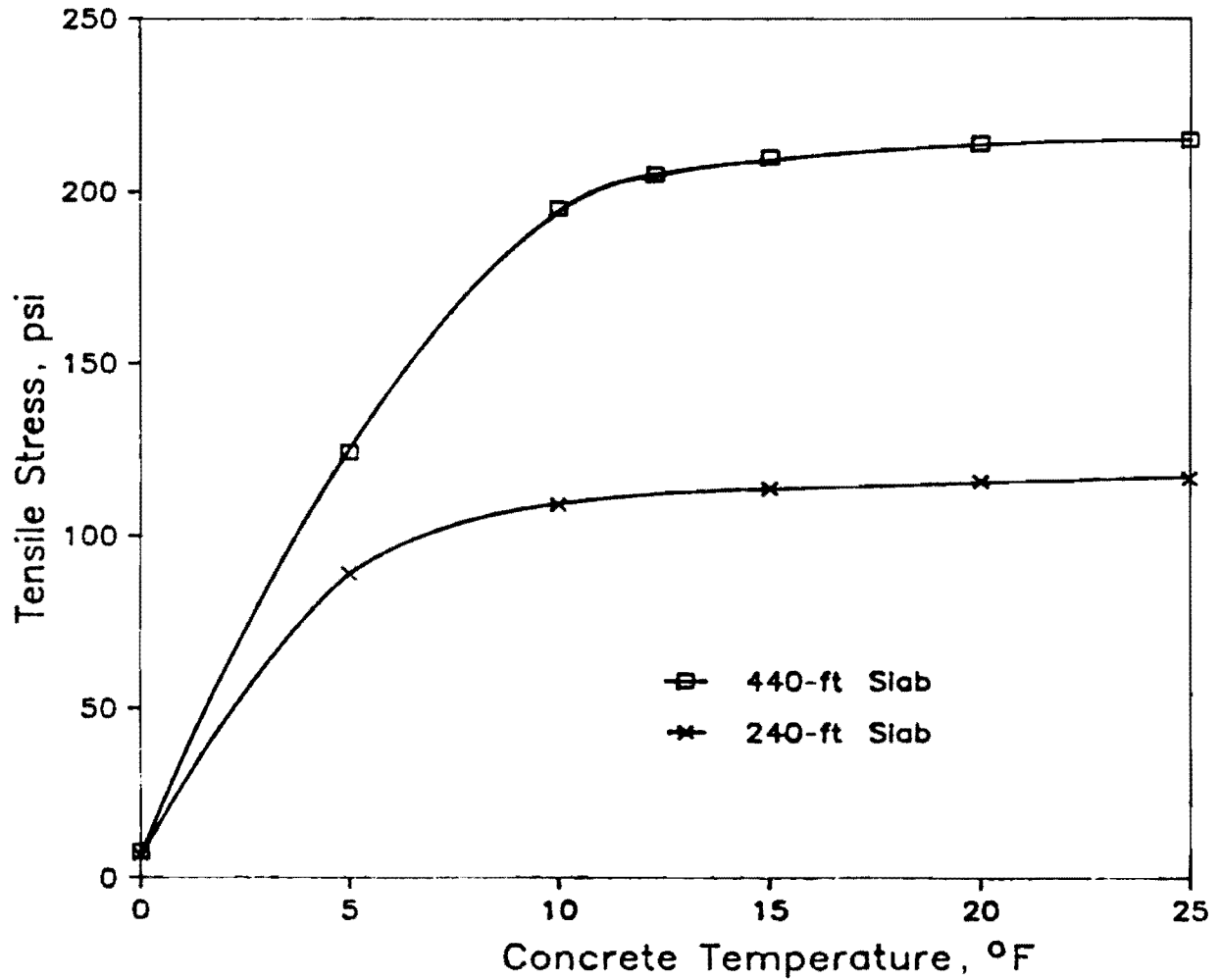
Fig 4.11.   Tensile stresses in 240 and 440–foot slabs for a drop in concrete temperature and shrinkage in the first 18 hours (Ref 4).

This procedure is illustrated in the following example.

Example

A slab is 440 feet long x 6 inches thick with strand spacing at 16 inches center to center. At 12 hours from concrete batching the concrete temperature has dropped 10°F. A split cylinder tensile test shows the concrete tensile strength to be 100 psi.

Procedure

(1)   Determine the Tensile Stress

From Fig 4.11 for L = 440 feet, T = 10°F

s_t = 200 psi

(2)   Determine P_{cr}

From Eq 4.1, Table 4.2, or Fig 4.9

P_{cr} = 29.86 kips for a concrete tensile strength of 100 psi.

(3)   Determine P_{allow}

For 95 percent reliability the safety factor equals 1.5 (Fig 4.10)

$$P_{allow} = \frac{P_{cr}}{SF} = \frac{29.86 \text{ kips}}{1.5} = 19.91 \text{ kips}$$

(4)   <u>Check</u>

The compressive stress in the slab equals

$$s_c = \frac{P_{allow}}{2at} = \frac{19.91 \text{ kips}}{(16 \text{ in.})(6 \text{ in.})} = 0.207 \text{ ksi} = 207 \text{ psi}$$

$$s_c \geq s_t - f_{sp} = 200 - 100 = 100 \text{ psi}$$

CHAPTER 5. INSTRUMENTATION AND BEHAVIOR OF THE TEXAS PRESTRESSED CONCRETE PAVEMENT

INSTRUMENTATION

This chapter describes the development and implementation of an instrumentation program used to monitor the behavior of the Texas prestressed concrete pavement. The measurements taken include continuous measurement of ambient and concrete temperature, horizontal slab movement, slab curling, and concrete strain. Other measurements include tendon elongation, very early concrete strength, concrete modulus of elasticity, and slab cracking. For a more detailed report on the instrumentation program, the reader is referred to Research Report 401-4 (Ref 6).

Instrumentation Development

This development of an instrumentation program for Texas prestressed concrete pavement is based on a review of the instrumentation of previous projects, an examination of instrumentation objectives, and the testing of instrumentation on a pavement test-slab.

Before proposing an instrumentation scheme for the Waco site, instrumentation arrangements used on similar pavement projects were reviewed. These projects include prestressed concrete pavement installations in Pennsylvania, Virginia, Mississippi, and Arizona, and slab tests conducted at Rolla, Missouri, and Slidell, Louisiana (Refs 7 through 12). Reports of these projects provided useful information on instrumentation equipment and procedures.

Before specifying an instrumentation scheme or any instrumentation equipment, the particular objectives of the instrumentation were defined. The instrumentation objectives are divided into two categories: objectives for short-term measurements and objectives for long-term measurement.

In general, short-term instrumentation was needed to verify the values of slab movement and concrete stress. This verification is important because the design of the slab lengths and the amount of prestressing are based on the critical stresses predicted analytically by the method discussed in Chapter 7. In addition, slab length design and transverse joint design are based on expected horizontal movement of the pavement slab.

The purpose of for making long-term measurements was to determine how the pavement holds up over time. Readings of transverse joint openings indicate whether or not the friction properties of the base are changing with time and show the effects of creep and shrinkage of the concrete. Load transfer measurements at the transverse joint can show if joint opening width affects load-transfer and if the effects of traffic have caused any deterioration of the joint. Measurement of the deflection characteristics of the prestressed overlay can be compared to similar measurements taken on the pavement before the overlay construction and thus indicate the increase in pavement stiffness due to the overlay. All of these measurements give an indication of the long-term performance of prestressed concrete pavements.

Before installing the instrumentation in the pavement at Waco, a pavement test-slab was built to test the functioning of the instrumentation. This slab was constructed at the Balcones Research Center at The University of Texas at Austin on an existing asphalt base. The test-slab is shown in Fig 5.1. It incorporated the following instrumentation:

Electronic Instrumentation:

      1 ambient temperature thermocouple

      6 embedded thermocouples

      10 embedment strain gages

      2 surface strain gages

      3 displacement transducers

Mechanical Instrumentation:

      3 movement dial gages

      2 sets of Demac strain reference points

The purpose of the test slab was three-fold. It provided an opportunity to (1) get familiar with the procedures for implementing the instrumentation, (2) verify that the electronic instrumentation functioned accurately, and (3) program the data acquisition system. The test slab was also used for other purposes, including testing post-tensioning anchor-zone strength and pocket stressing techniques.
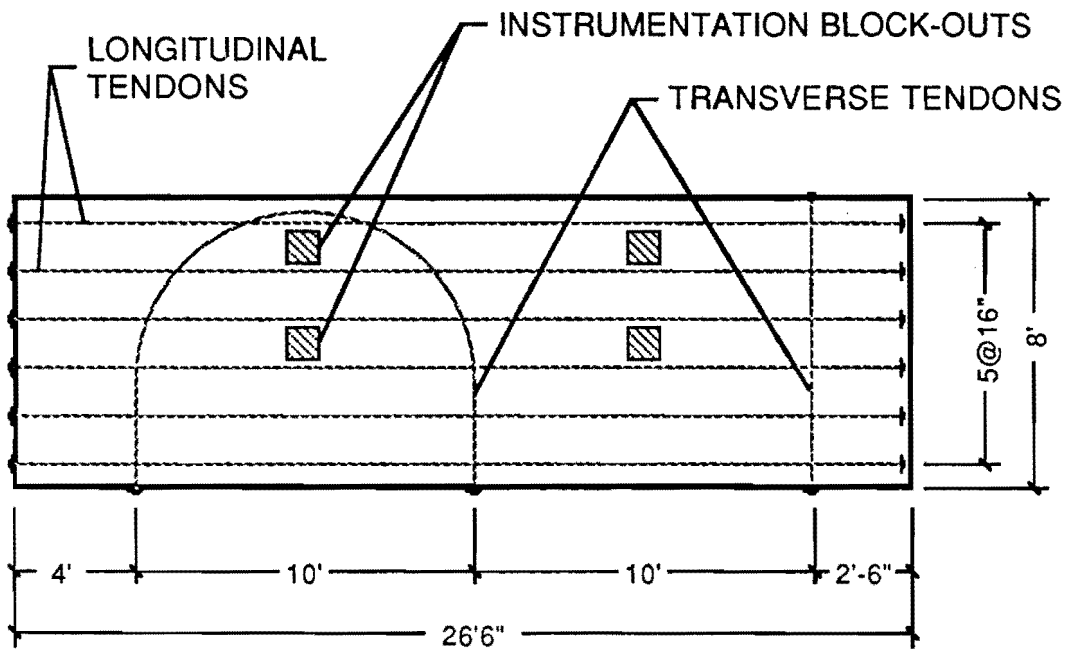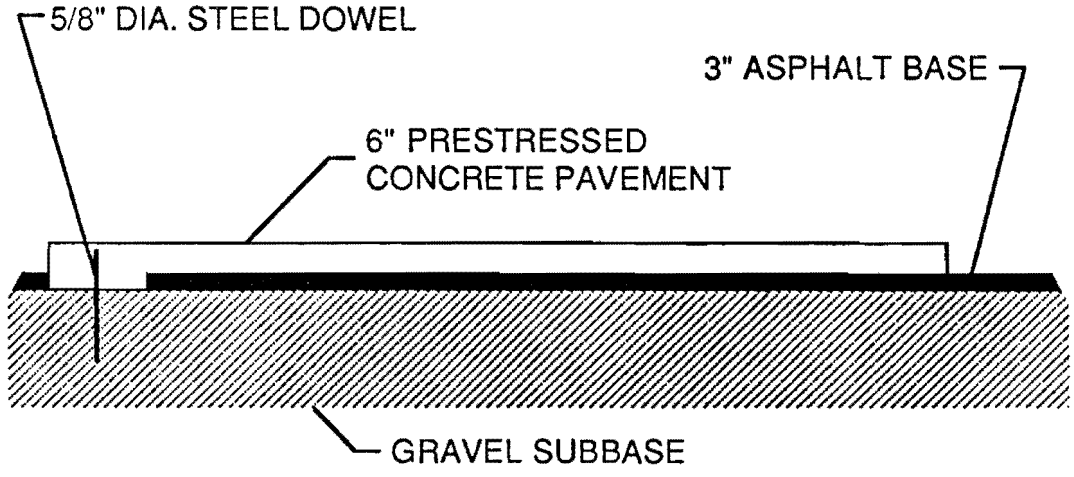
Fig 5.1. Pavement test slab.

The results of the experimentation on the test slab indicate the following conclusions:

(1)   Thermocouples are effective in recording both ambient and concrete temperatures and can be considered accurate to 1°F or better.

(2)   Displacement transducers are very effective in recording horizontal slab movement. The transducers are capable of resolving slab movements accurately to the nearest 0.001 inch.

(3)   Embedded and surface strain gages, positioned longitudinally, are generally effective in recording changes in concrete strain due to longitudinal post-tensioning. One embedment strain gage, however, gave errant results which cannot fully be explained. In most cases, the strain gages could accurately resolve strain changes of 5 microstrain.

(4)   Embedded strain gages positioned transversely were not effective or consistent in recording the changes in concrete strain due to transverse post-tensioning. This is probably because the change in strain due to the transverse post-tensioning is small in comparison to the resolution capabilities of the gages.

Field Implementation

Following the instrumentation objectives given above, the instrumentation for the Texas prestressed pavement is divided into two categories: short-term instrumentation and long-term instrumentation.

The short-term instrumentation for the Texas prestressed pavement consists of (1) continuously recorded electronic instrumentation, (2) mechanical instrumentation to back-up the continuously recording measurements, and (3) intermittently recorded measurements. During construction in the fall of 1985, short-term instrumentation was implemented on two of the prestressed pavement slabs. Since the slabs are staked at mid-length, behavior of the two halves of a slab is symmetric, and only one half of the pavement slab needs to be monitored. One 240–foot–long slab and one 440–foot–long slab were instrumented. The same instrumentation was used for the 240–foot slab and the 440–foot slab.

A listing of the continuously recorded electronic instrumentation used in the two instrumented slabs is shown in Table 5.1. This instrumentation consists of thermocouples for measuring temperature, strain gages for measuring concrete strain, and displacement

TABLE 5.1. CONTINUOUSLY RECORDED ELECTRONIC INSTRUMENTATION

Measurement	Number of Locations Each Slab	Apparatus
Ambient temperature	1	Thermocouple
Slab temperature at 3 depths	2	Thermocouple
Middepth concrete strain	6	Embedment Gage
1/2-inch–deep concrete strain	3	Embedment Gage
5-1/2 inch–deep concrete strain	3	Embedment Gage
Horizontal slab movement	6	Displ. Transducer
Vertical slab movement	2	Displ. Transducer

transducers for measuring horizontal and vertical slab movements. The instrumentation locations for the 220-foot slab (slab 7) are shown in Figs 5.2, 5.3, and 5.4

The data from this instrumentation were continuously recorded over several daily temperature cycles. The automatically timed recording of several channels of data input necessitated the use of a data acquisition system. On this project, a Hewlett-Packard 3497 data acquisition system was used, controlled by a Hewlett-Packard 150 desk-top computer.

Measurements of ambient temperature, slab movement, and concrete strain were also recorded mechanically. Ambient temperature readings were checked intermittently using a thermometer. Horizontal movement was checked at the slab ends by periodically measuring the width across the transverse joint, using a scale and reference marks on either side of the joint. Using a Demac gage, concrete strain was measured periodically at three locations on the slab surface. For both slabs, Demac strain was measured in the locations of surface strain gages.

Intermittently recorded measurements include the measurement of tendon elongations, concrete compressive strength, and concrete modulus of elasticity and an inspection of slab cracking. Tendon elongations during initial and final post-tensioning were measured to the nearest 1/8 inch using tape marks and a ruler. Tendon elongations were recorded on all tendons on all slabs. Concrete compressive strength at very early ages was measured using a compression testing machine at the job-site. For each pavement slab, six cylinders were tested at ages of 8 to 12 hours. Concrete modulus of elasticity at very early ages was measured on six cylinders. Inspection of slab cracking was carried out regularly on all pavement slabs.

The long-term measurement consists of (1) a program to periodically measure joint opening width of the transverse joints, (2) a program to periodically measure the load transfer capabilities of the transverse joints, (3) measurement of the deflection characteristics of the pavement, and (4) measurement of the riding quality of the pavement.

BEHAVIOR

This section includes a presentation of some representative data collected from the field instrumentation. Also included is a brief discussion of some of the important results of the measurements. For a more detailed report on the measured behavior of the Texas prestressed concrete pavement, the reader is referred to Research Report 401-4 (Ref 6).

Fig 5.2. Location of thermocouples for slab 7 (Ref 6).
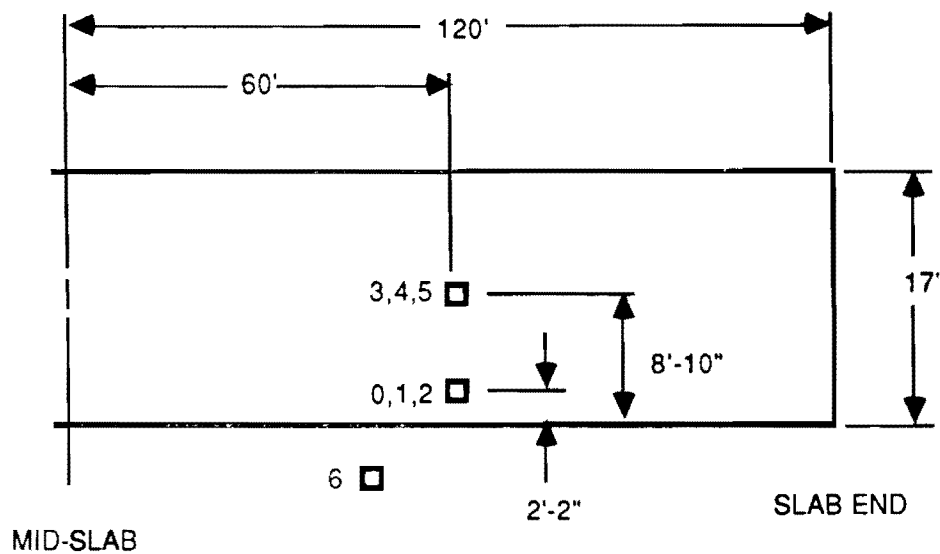
INPUT CHANNEL	THERMOCOUPLE LOCATION
0	5 1/2 IN. DEEP
1	3 IN. DEEP
2	1/2 IN. DEEP
3	5 1/2 IN. DEEP
4	3 IN. DEEP
5	1/2 IN. DEEP
6	AMBIENT
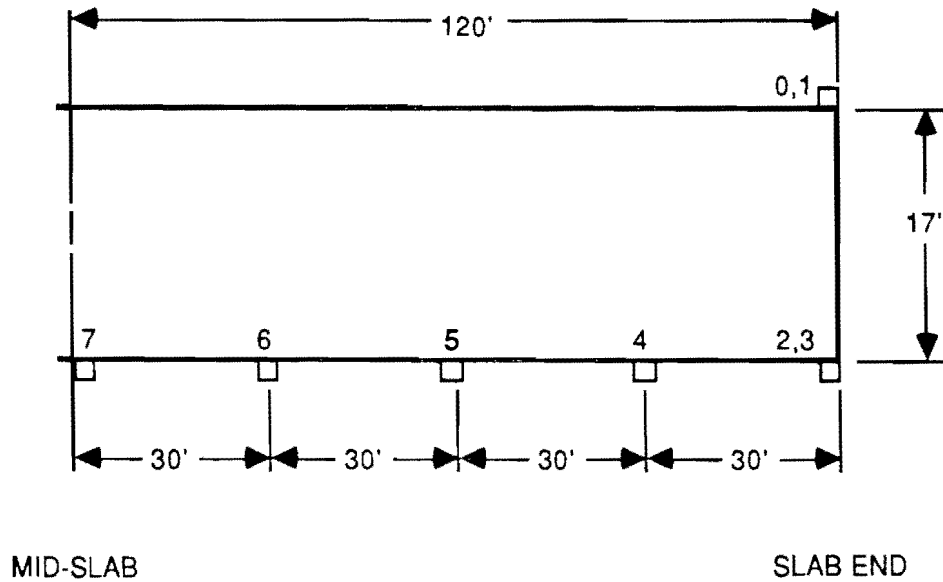
INPUT CHANNEL	TRANSDUCER ORIENTATION
0	VERTICAL
1	HORIZONTAL
2	VERTICAL
3	HORIZONTAL
4	HORIZONTAL
5	HORIZONTAL
6	HORIZONTAL
7	HORIZONTAL

Fig 5.3. Location of displacement transducers for slab 7 (Ref 6).
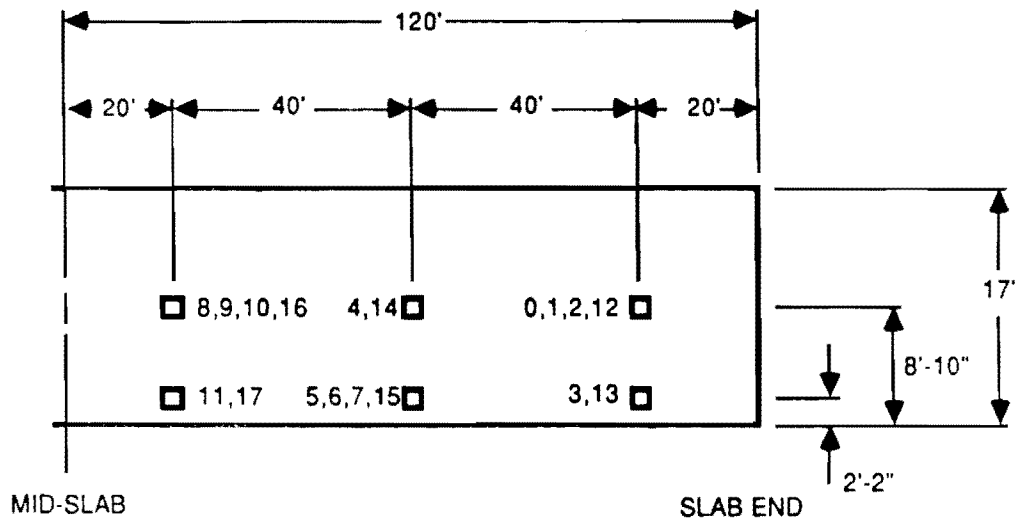
INPUT CHANNEL	STRAIN GAGE LOCATION
0	5 1/2 IN. DEEP
1	3 IN. DEEP
2	1/2 IN. DEEP
3	3 IN. DEEP
4	3 IN. DEEP
5	5 1/2 IN. DEEP
6	3 IN. DEEP
7	1/2 IN. DEEP
8	5 1/2 IN. DEEP
9	3 IN. DEEP
10	1/2 IN. DEEP
11	3 IN. DEEP
12	SURFACE
13	SURFACE
14	SURFACE
15	SURFACE
16	SURFACE
17	SURFACE

Fig 5.4. Location of strain gages for slab 7 (Ref 6).

Data Collected

The data collected from the instrumentation of the Texas prestressed concrete pavement include the following:

(1) Continuously recorded ambient and concrete temperature data which correspond closely to back-up readings taken by thermometer and agree with expected temperature variations according to slab depth.

(2) Horizontal slab movement data which effectively show the contraction of the pavement slab due to post-tensioning and show the cyclic movement of the pavement slab due to daily temperature cycles.

(3) Concrete strain data which effectively show the contraction of the pavement slab due to post-tensioning. The data are less consistent, however, in showing cyclic changes in strain due to daily temperature changes.

(4) Slab curling data which show the vertical displacement of the slab corners due to daily temperature cycles. The data show that, as should be expected, the maximum upward curling of the slabs corresponds to the time when the maximum negative temperature gradient in the slab is acting.

(5) Data on tendon elongations, which are discussed in another report (Ref 14).

(6) Data on concrete compressive strength at very early ages and at 28 days.

(7) Data on concrete modulus of elasticity.

(8) Observations of slab cracking.

Figure 5.5 shows the electronically recorded temperatures for slab 7 over a 17–hour time period from 19:36 on September 26, 1985 to 12:50 on September 27, 1985. These data are for thermocouple channels 0, 4, 5, and 6. The electronically recorded ambient temperatures were checked against thermometer readings taken in the field. The readings were found to correspond closely. It should be noted that Fig 5.5 shows concrete temperatures within 5 hours after concrete placement, so that the heat of hydration due to the concrete curing causes a greater difference between concrete temperatures and ambient temperatures.
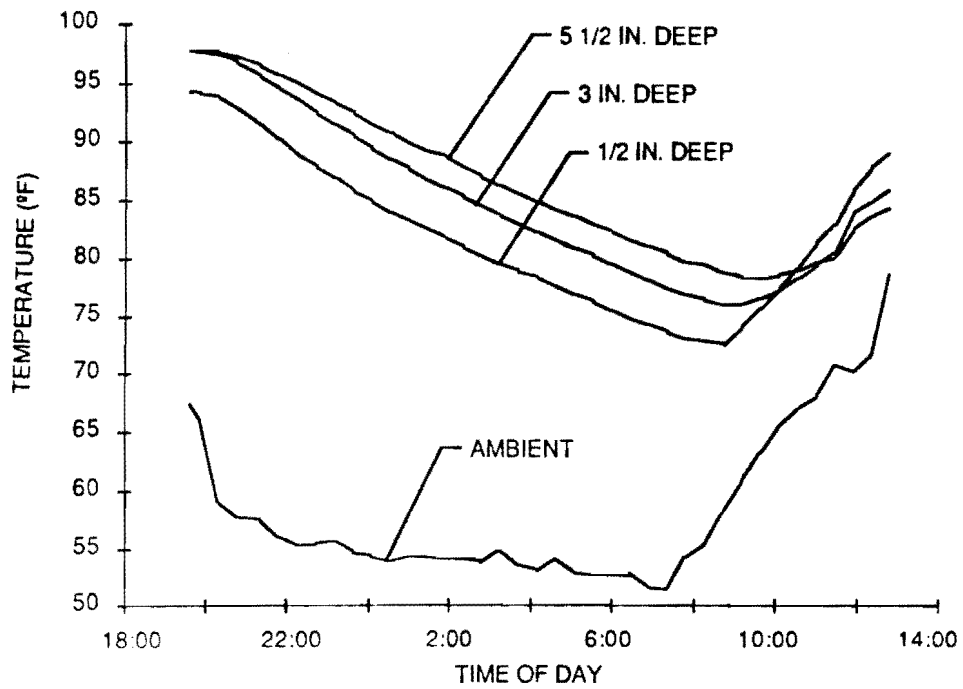
Fig 5.5. Ambient and concrete temperatures for slab 7, September 27, 1985, channels 0, 4, 5, and 6 (concrete placement time 14:00 hours) (Ref 6).
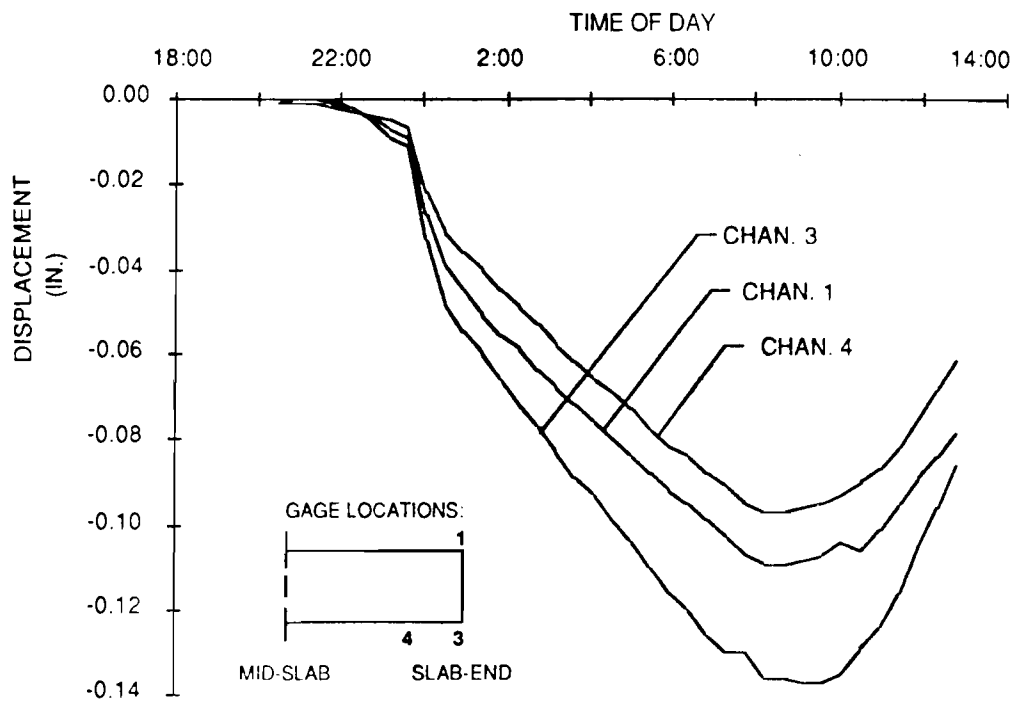
RR401-F8/05

Fig 5.6. Horizontal slab displacement of slab 7, September 27, 1985 (Ref 6).

Figure 5.6 shows the recorded values of horizontal slab displacement for slab 7, recorded continuously over a 17–hour period. The rapid change in displacement seen in Fig 5.6 around 23:50 corresponds to the initial post-tensioning operation. Displacement transducer channels 1, 3, and 4 correspond to the slab locations indicated on the figure itself. Mechanical measurements of joint opening width covering the same time periods as the electronic data show good correspondence with the displacement readings.

The output of three of the embedment strain gages for slab 7, recorded continuously over a 17–hour period, is shown in Fig 5.7 The strain gage locations are as indicated on the figure. The effect of the initial post-tensioning for slab 7 is evident in Fig 5.7 by the drop in concrete strain, by about 25 microstrain, of all of the channels at times corresponding to the post-tensioning time, 23:45 to 00:08.

Results of Measurements

This section presents a discussion of some of the results of the field measurements. These discussions include an examination of horizontal slab movement and concrete strain due to post-tensioning, discussions of concrete strength and modulus of elasticity results, and the observation of slab cracking.

Movement and Strain Due to Post-Tensioning. Taking into account both friction along the post-tensioning tendon and base friction (assumed to be constant) concrete strain due to post-tensioning can be calculated according to the equation

$$\varepsilon(x) = 1/E_c \left[-P_s/A_c \, e^{-Kx} + \mu\gamma \, (L_o/2 - x) \right], \tag{5.1}$$

where

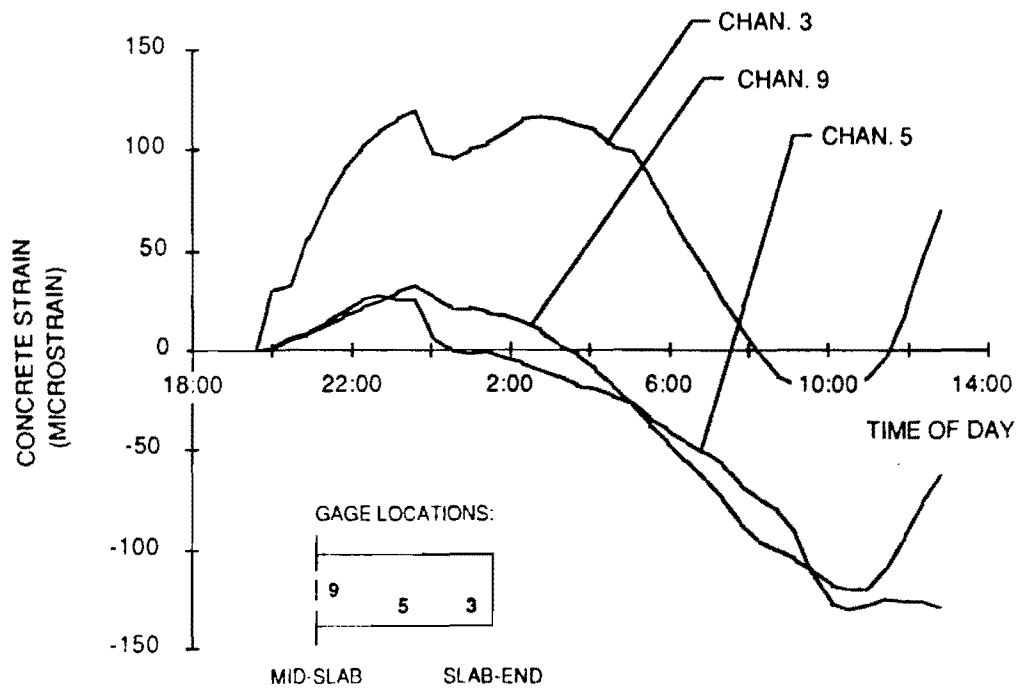|		
$\varepsilon(x)$	=	concrete strain at x (negative for contraction);
x	=	distance away from the stressing location;
E_c	=	concrete modulus of elasticity;
A_c	=	concrete cross-sectional area for each tendon;
P_s	=	applied post-tensioning force per tendon, at the stressing location;
K	=	wobble coefficient for the friction loss in the tendons;
μ	=	coefficient of base friction;

Fig 5.7. Concrete strain for slab 7, September 27, 1985 (Ref 6).

γ =   concrete unit weight; and

L_o =   slab length.

An expression for horizontal slab movement at any point x can be found by integrating the expression of concrete strain, Eq 5.1. The expression can be written

$$z(x) = 1/E_c \left[P_s/A_c \, K \, (1 - e^{-Kx}) - \mu\gamma/2 \, (L_o x - x^2) \right], \qquad (5.2)$$

where

$z(x)$ = horizontal slab movement at x (negative for contraction).

The measured values of slab movement and concrete strain were compared to those predicted by the above equations. A statistical analysis of slab movement and concrete strain data corresponding to the post-tensioning of the pavement slabs was used to back-calculate the coefficient of base friction and concrete modulus of elasticity for the pavement.

The coefficient of base friction was found to be 0.51 according to the initial post-tensioning of slab 7, and 0.45 according to the final post-tensioning of slab 14.   Although these values are much lower than the conservative design value of 0.96, they are considered an accurate indication of the actual coefficient of base friction.

The concrete modulus of elasticity for the initial post-tensioning of slab 7 was found to be 2,900,000 psi. The age of the concrete at the time of this post-tensioning was about 13 hours. For the final post-tensioning of slab 14, the concrete modulus of elasticity was found to be 3,700,000 psi. The age of the concrete at the time of this final post-tensioning was about 60 hours. These values are in line with the results of the concrete modulus of elasticity tests performed on concrete cylinder specimens.

Very Early Concrete Strengths. The results of 61 compressive cylinder tests showed that very early concrete strengths for the project did not depend solely on age and curing temperature. The dosage of set retarder in the concrete appears to have been a factor. It had been suggested that, in future prestressed concrete pavement projects where very early initial post-tensioning is applied, maturity curves could be used to estimate concrete strength at very early ages. Based on the evidence of the compressive cylinder strength results, it can be concluded that the maturity curve approach would not have been the best approach to use on

the Texas prestressed pavement. It is possible however that concrete strength at very early ages could be effectively determined with an insitu method of testing, such as using a rebound hammer. This would eliminate the need for a compression testing machine at the job site and would save labor in casting and testing cylinder specimens.

Concrete Modulus of Elasticity. The results of concrete modulus of elasticity tests performed on compressive cylinder specimens were compared to those from using the ACI formula in which concrete modulus of elasticity is written as a function of compressive strength: $E_c = 57000 \sqrt{f'c}$. For concrete strengths around 600 psi, the measured values of concrete modulus of elasticity correspond closely to those calculated by the ACI formula, but, for concrete strengths of 1500 to 3300 psi, the measured values exceed the calculated values by as much as 68 percent. Since it has been noted that concrete at very early ages gains stiffness faster than it gains strength, the discrepancy is probably due to the fact that all of the data are for concrete at early ages. It is recommended that, in the analysis and design of prestressed concrete pavements, the determination of concrete modulus of elasticity should be based on the most accurate data available.

Slab Cracking. A transverse crack which formed in slab 5 gave positive evidence of the importance of very early initial post-tensioning. Slab 5 was the only one of the pavement slabs in which initial post-tensioning was not applied during the day of concrete placement. Not coincidentally, slab 5 was the only pavement slab to develop a transverse crack. Although the crack closed after the application of prestress, even a small amount of initial prestress applied during the day of casting would have prevented the crack from ever forming.

CHAPTER 6. EFFECT OF PRESTRESS ON FATIGUE LIFE OF CONCRETE

An important consideration in the design of prestressed concrete pavements is the amount of pre-compressive force to be applied on the pavements. Since the compressive strength is high compared to its flexural strength, there is a wide range of precompression levels from which to choose.

This is especially evident if we consider prestressed pavements on a world-wide scale. The highest pre-compressive stress applied was found to be 1,138 psi, in a pavement constructed in 1958 in Anif-Saltzburg, Austria. The lowest was 42 psi, in a highway constructed in 1976 in the city of Tempe, Arizona.

A survey of the prestressed concrete pavements built in the United States in the last 15 years is shown in Table 6.1. The average pavement thickness was found to be 6 inches, with slab length varying from 300 feet to 760 feet long. The prestressed level applied ranged from 200 psi to 331 psi.

Currently the amount of prestress to be applied is governed by two main considerations:

(1)   The thickness of the pavement. Since prestressed pavements are usually thinner than reinforced concrete pavements, higher stresses are developed at the base.

(2)   The slab length. The longer slab length used in prestressed pavements produces higher frictional resistance during low temperature cycles, resulting in higher tensile stresses in concrete.

However, the amount of pre-compressive stress applied must at least be sufficient to compensate for the increase in flexural/tensile stresses.

A survey of the prestressed concrete pavements built in the United States in the last 15 years shows an average pavement thickness of 6 inches with prestress level applied ranging from 42 psi to 331 psi (7 percent to 50 percent of flexural strength of plain concrete).

TABLE 6.1. PRESTRESSED CONCRETE DEMONSTRATION PROJECT IN THE UNITED STATES

Date	Location	Pavement Dimensions			Prestress (psi)	
		Length (feet)	Width (feet)	Thickness (feet)	Longitudinal	Transverse
1971	Milford, Delaware	300	14	6	238	None
1971	Dulles International Airport, Virginia	400 500 600 760 500 400	24	6	200	None
1973	Harrisburg, Pennsylvania	600	24	6	331	None
1973	Kutztown, Pennsylvania	500	24	6	331	None
1977	City of Tempe, Arizona	400	24	6	215	None
1978	Brookhaven, Mississippi	400	24	6	229	None

FATIGUE DESIGN ASPECT OF PRESTRESSED PAVEMENT

Current fatigue design consideration for prestressed concrete pavement considered only the flexural/tensile stress aspect. That is, the net flexural/tensile stress at the base of the middle of the slab is determined using the equation:

$$f_n = f_r + f_p - f_t - f_f - f_1 \tag{6.1}$$

where

f_n = net flexural stress at mid-slab,

f_r = flexural strength of concrete,

f_p = compressive stress due to prestress,

f_t = stresses due to temperature and moisture gradient,

f_f = restraint stress due to subbase friction, and

f_1 = stresses due to wheel load.

Based on the ratio of f_n/f_r, the fatigue life of the pavement can be determined based on equations developed through the AASHTO field survey of reinforced concrete pavements or through experimental work done on fatigue of plain concrete. These are the underlying assumptions made in the current fatigue design of prestressed concrete pavements.

(1)   Presressing does not help in any way to delay microcrack propagation in concrete. Therefore fatigue design is usually based on the fatigue life of plain concrete, or is determined equations developed from AASHTO road tests on unreinforced or reinforced concrete pavements.

(2)   The resultant stress at the bottom surface of the prestressed concrete pavement can be found by the superpostion of stresses. Therefore, the difference between the static nature of prestress and the dynamic nature of the vehicular stresses is not accounted for.

(3)   Bottom cracking will result in rapid deterioration of the structural stiffness of the pavement, leading to large increases in deflection and serviceability failure. Therefore, elasto-plastic behavior and the effect of prestress in helping to

maintain the structural integrity of the prestressed pavement after bottom cracking are not considered in the design.

In order to determine the validity of these assumptions, the results from fatigue tests of 28 prestressed beams conducted by the Portland Cement Association (Ref 15) were evaluated and analyzed. In order to verify the data from the PCA test and to further investigate the effect of prestress on the fatigue life of concrete, a similar investigation was carried out at The University of Texas at Austin. Due to the limited time available, a full scale study was not feasible and only a preliminary investigation was carried out.

DATA FROM PCA TEST

As part of an effort to determine the effect of prestress on concrete fatigue, twenty-eight 6 x 6 x 30-inch concrete beams with a 1/2-inch-diameter, 7-wire prestressing tendon centrally located were cast for fatigue testing. Plain concrete companion specimens were also cast from each batch for static testing to determine the flexural strength (modulus of rupture) using 1/3 point loading.

Three prestress levels were selected: 50, 100, and 150 psi. The prestressed beams were simply supported with an 18-inch span, and were subjected to third point cyclic loading. Failure was defined as the first crack.

Table 6.2. presents the fatigue test results from the Portland Cement Association. In order to determine the effect of prestress on the fatigue life of concrete, regression analyses were carried out to determine a best-fit line for the various presress levels. In the PCA tests, the run-out point for stopping the test was not set at any specific number of cycles. For example, testing was terminated for two specimens at 2,200,000 cycles, two specimens at 2,950,000 cycles, and one specimen at 4,320,000 cycles. Yet, one specimen was tested through 5,190,000 cycles before it failed.

In order to make sense of the data, three separate least square regression analyses were run on the data points. One procedure and reasons for each analysis are as follows.

TABLE 6.2. FATIGUE TEST RESULTS FROM PORTLAND CEMENT ASSOCIATION

Modulus of Rupture, (psi)	Prestress Level, (psi)	Repeated Load Stress/ Beam Cracking Stength, (percent)	Concrete Stress/ Modulus of Rupture (percent)	Number of Cycles to Failure
646	100	70	65	4,320,000*
653	100	80	76	39,800
590	100	70	65	1,140,000
590	100	80	76	13,300
571	100	90	88	2,300
571	100	90	88	870
695	100	75	71	113,000
692	100	75	71	19,800
550	150	70	62	2,200,000*
550	150	70	62	2,190,000*
625	150	80	75	6,340
567	150	75	68	876,000
661	150	80	75	67,900
672	150	90	88	1,650
672	150	90	88	5,050
717	150	75	70	16,800
717	150	75	70	56,200
609	50	70	68	5,190,000
636	50	80	78	4,230
636	50	80	78	1,050
675	50	90	89	170
675	50	90	89	180
590	50	70	67	2,950,000*
590	50	70	67	2,950,000*
610	50	75	73	17,100
610	50	75	73	57,100
668	50	75	73	42,800
668	50	75	73	337,000

*No failure occurred, test was terminated.

Regression Analysis 1 (RA1)

Procedure. All the data points were used. Specimens that did not fail were assumed to have 5,000,000 cycles of loading at failure.

Reason. 5,000,000 cycles was selected because all the specimens for which testing was terminated were subjected to stress levels of less than 0.68. A specimen tested at stress level of 0.68 failed at 5,190,000 cycles.

Regression Analysis 2 (RA2)

Procedure. All the data points except those for specimens that did not fail were analyzed.

Reason. Since the actual number of cycles at failure was unknown, unfailed samples were left out of the analysis.

Regression Analysis 3 (RA3)

Procedure. All the data points used in RA1 except those for specimens that were tested at a stress ratio (fn/fr) greater than 0.85 were used in the analysis.

Reason. It has been found on fatigue testing of plain concrete specimens that, as the stress level gets higher (greater than 0.85), the relationship between the stress level and the log number of cycles becomes nonlinear. Using these data points would make the slope much steeper.

The results from the three regression analyses are presented in Figs 6.1 to 6.3.

DATA FROM THE UNIVERSITY OF TEXAS TEST PROGRAM

In view of the short time available, a full-scale testing program was found to be not feasible. Instead, a preliminary investigation was initiated:

(1)   to verify the results of the PCA investigation,

(2)   to increase the data base on the effect of prestress on the fatigue life of concrete,

(3)   to investigate the structural integrity of the presressed beam after the first crack.

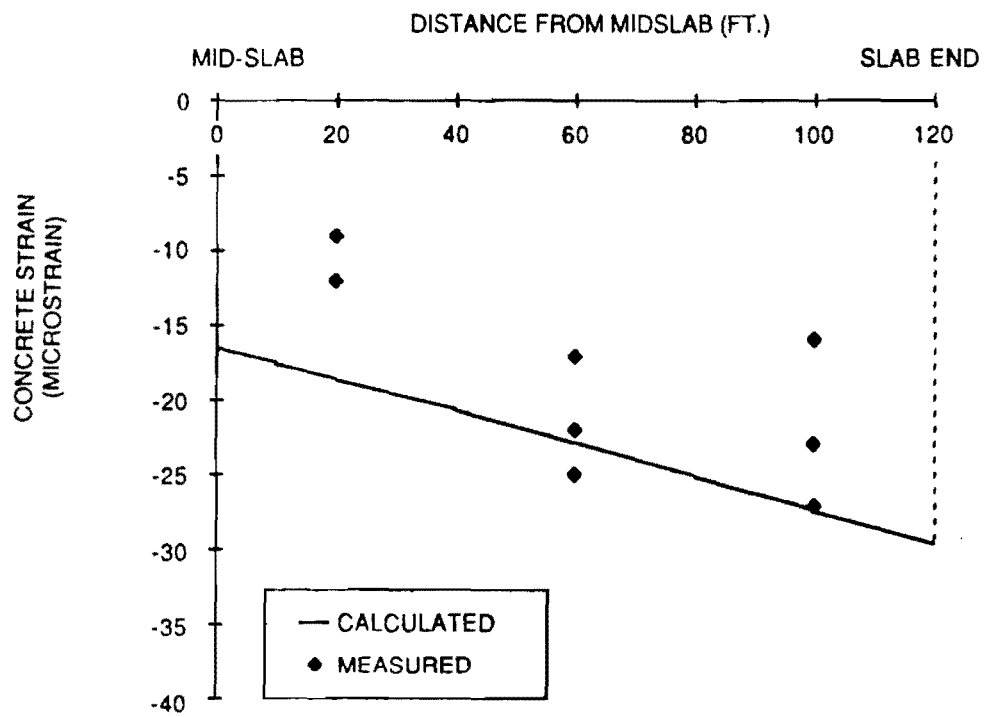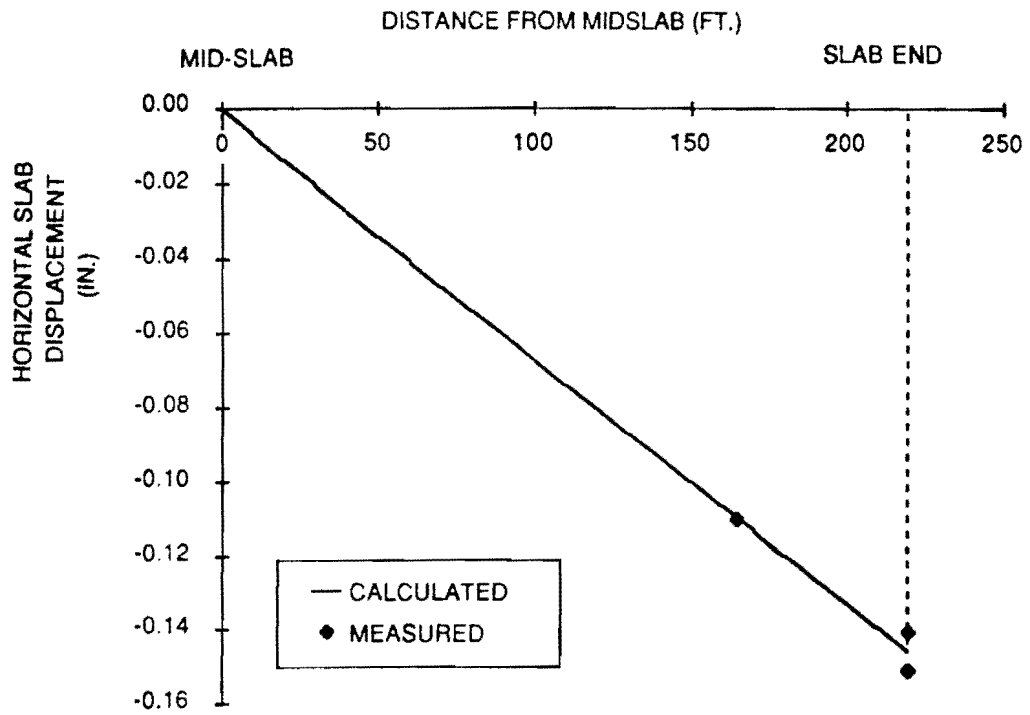Fig 6.1.   Effect of different levels of prestress on fatigue life of concrete based on Regression Analysis 1 (RA1).

Fig 6.2.   Effect of different levels of prestress on fatigue life of concrete based on Regression Analysis 2 (RA2).
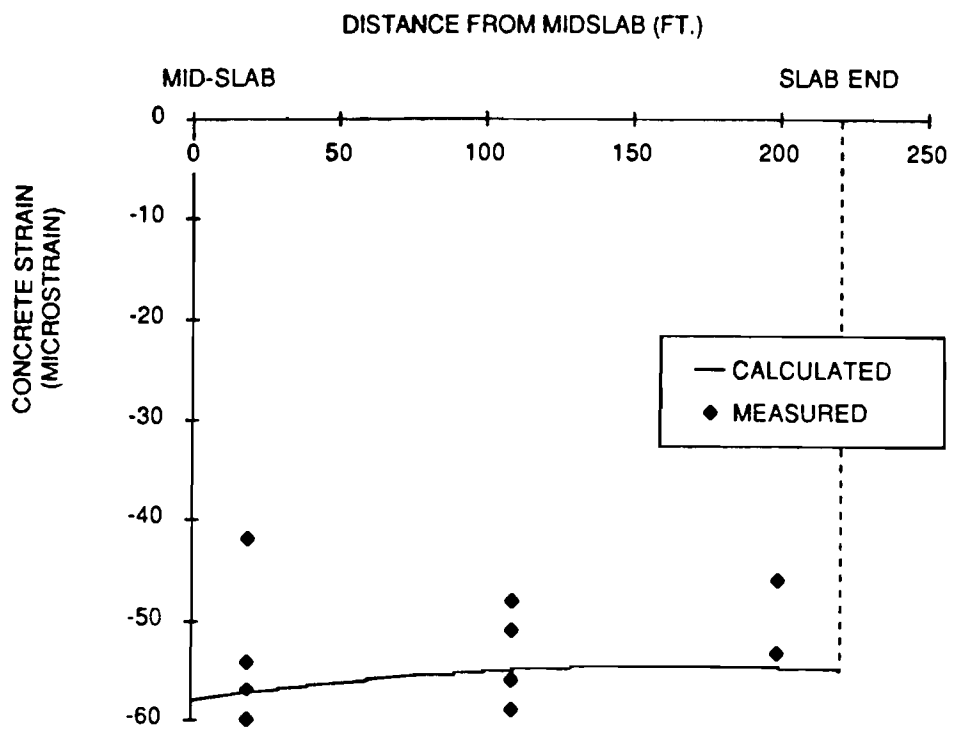
DISTANCE FROM MIDSLAB (FT.)

Fig 6.3.   Effect of different levels of prestress on the fatigue life of concrete based on Regression Analysis 3 (RA3).

RR401-8F/06

For this study, twelve 6 x 6 x 42-inch concrete beams with a 1/2-inch-diameter, 7-wire strand centrally positioned were constructed for repeated loading. Twenty-four 6 x 6 x 21-inch plain concrete comparison specimens and eight cylinders were also cast from the same batch of concrete for static testing to determine the flexural and compressive strength, respectively.

The prestress levels selected ranged from 0 to 300 psi. The three stress ratios (f_n/f_r) the specimen were subjected to were 0.60, 0.70, and 0.85. The specimens were supported on a 36-inch span and loaded at the third points.

Table 6.3 presents the fatigue test results based on the modului of rupture determined by the companion beams as well as test results using the modulus of rupture from the broken "halves" of the failed specimen. The regression analysis carried out on the results of specimens stressed at 100 psi and 300 psi is presented in Fig 6.4. The mid-span deflections of specimens tested at stress ratio levels of 0.6 and 0.7 are presented in Figs 6.5 and 6.6.

CONCLUSIONS

The following summary should not be considered as the final conclusions as the analysis was carried out on a small sample size, only 40 specimens: 28 specimens from the PCA test program and 12 specimens from The University of Texas at Austin.

Despite the shortcomings, some salient facts seem to emerge as a result of this investigation:

(1) Prestressing helps to delay the propagation of microcracks in concrete. The higher the level of prestress, the more profound is the effect in delaying the propagation of the microcracks. However, it does not seem that a direct proportional increase is obtained by a similar increase in prestress level.

(2) The absolute value of the slopes of the equations representing the relationship between stress levels and the logarithm of number of cycles at failure will increase (be steeper) with an increase in the amount of prestress applied.

(3) No fatigue limits exist for prestressed concrete beams subjected to 50 to 300 psi of prestress.

TABLE 6.3. SUMMARY OF FATIGUE TEST RESULTS

Prestress Level (psi)	Companion Beam		Broken Halves		Number of Cycles to Failure
	Modulus of Rupture	Concrete Stress/ Modulus of Rupture	Modulus of Rupture	Concrete Stress/ Modulus of Rupture	
0	583	0.85	677	0.73	13,130
50	650	0.85	743+	0.74	73,880
100	595	0.85	700+	0.72	12,400
150	613	0.85	613+	0.85	131,060
150	652	0.70	642	0.71	190,700
150	653	0.70	672	0.68	41,570
150	651	0.60	618+	0.63	91,710
150	663	0.60	675	0.59	200,670
300	644	0.70	685+	0.66	1,393,000
300	688	0.70	666	0.72	1,079,400
300	682	0.60	650+	0.63	1,753,000
300	654	0.60	638+	0.61	10,000,000*

*No failure occurred, test was terminated.
+Modulus of rupture based on test of one broken half of each failed specimen.

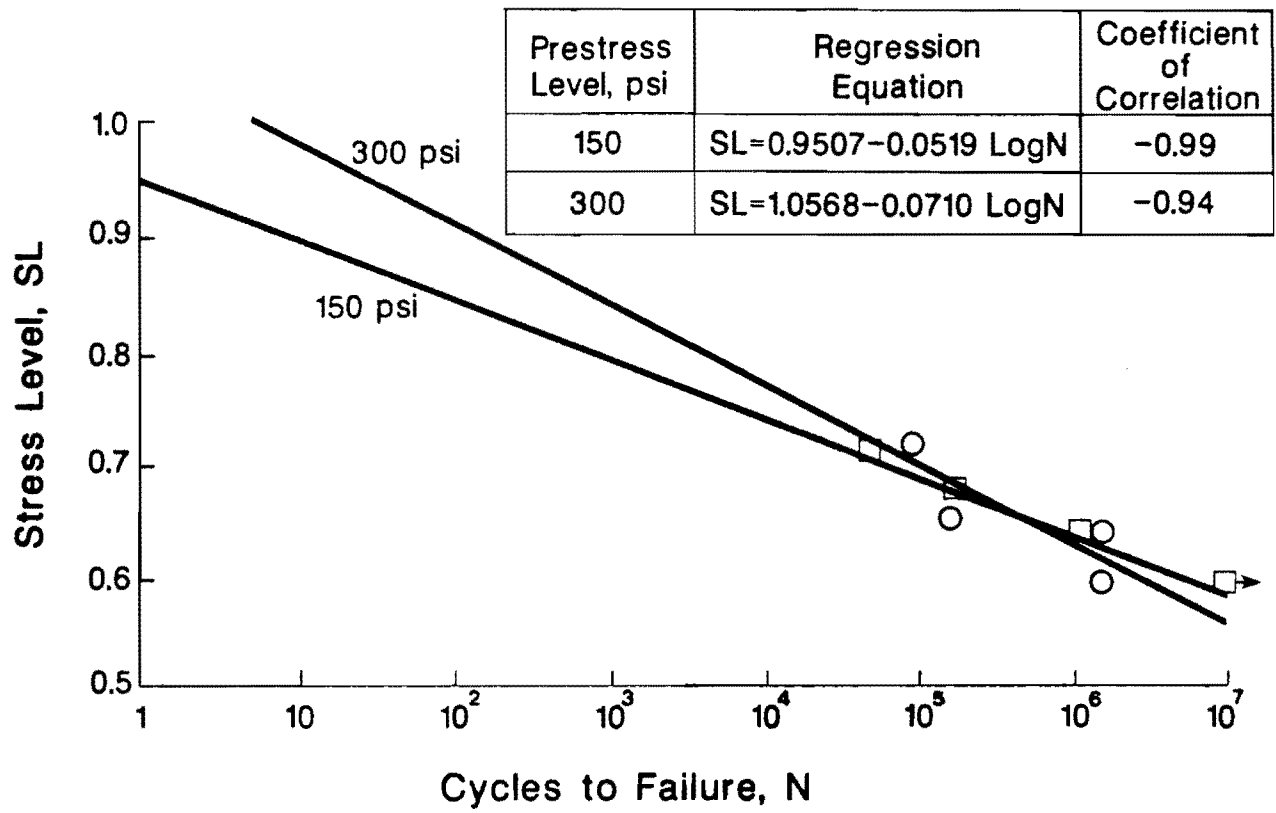| Prestress Level, psi	Regression Equation	Coefficient of Correlation
150	SL=0.9507−0.0519 LogN	−0.99
300	SL=1.0568−0.0710 LogN	−0.94

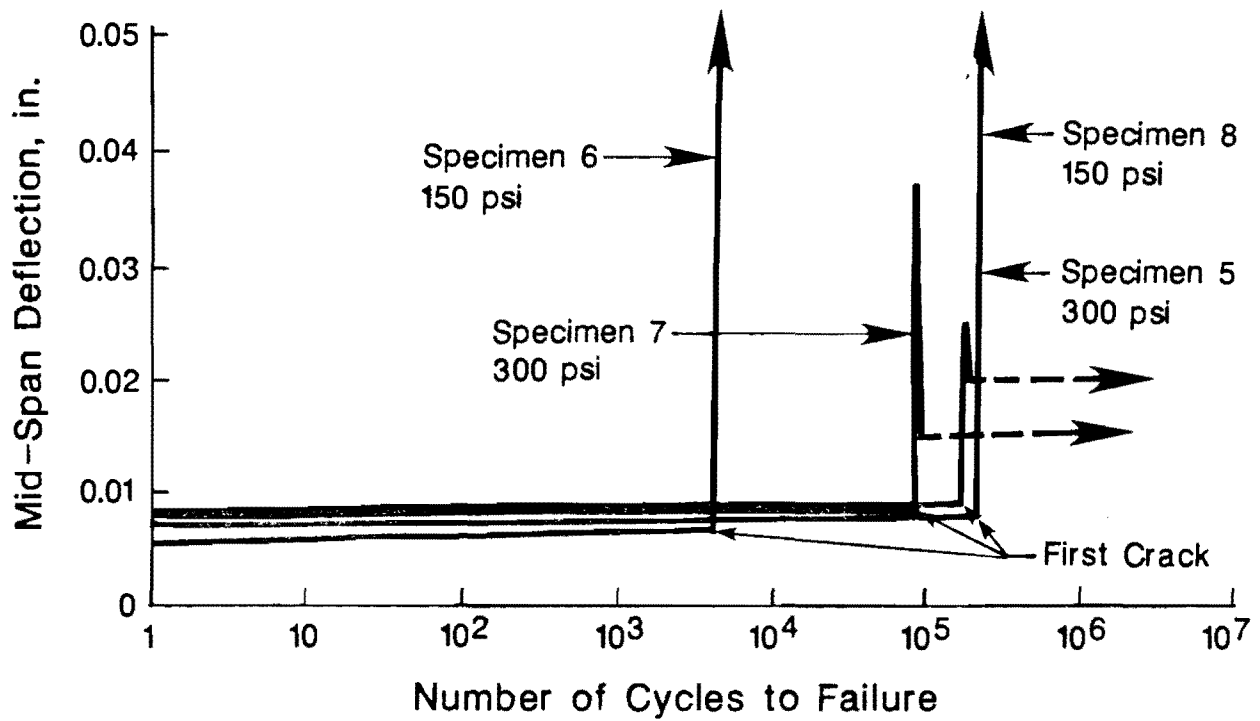Fig 6.4. Regression analysis on fatigue test results from The University of Texas at Austin.
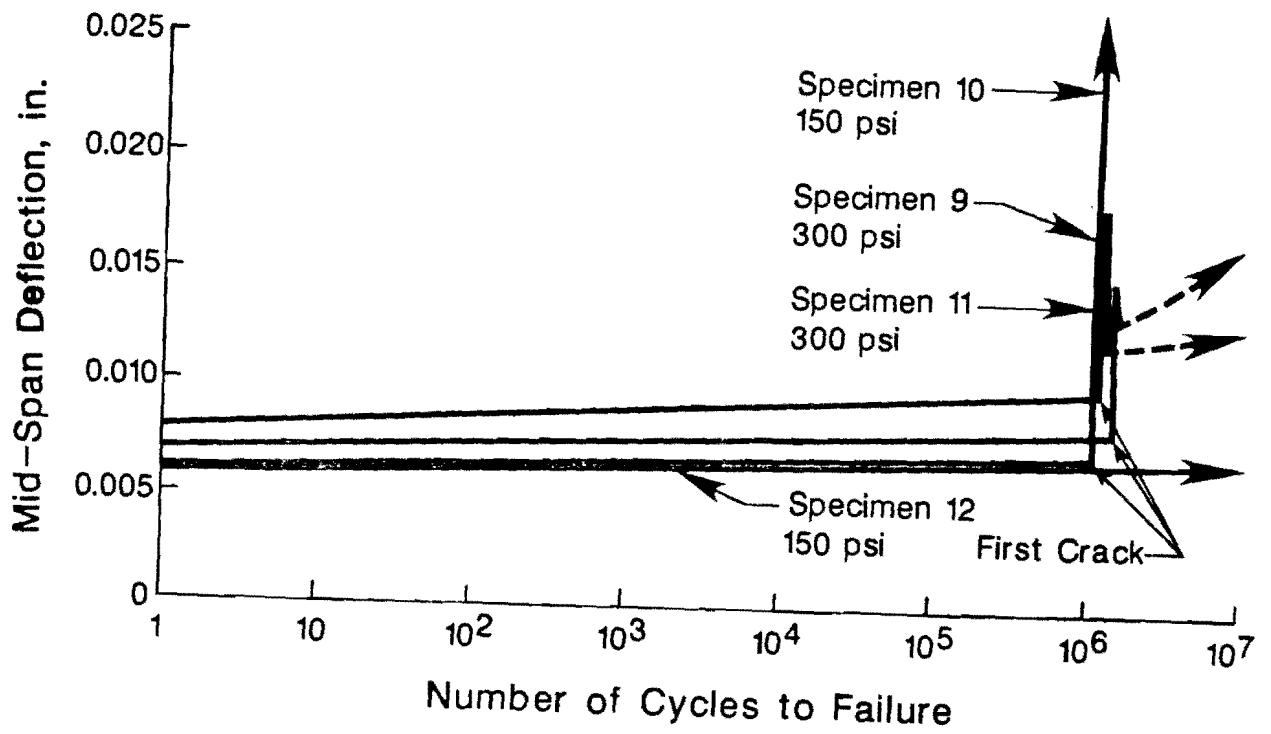
Fig 6.5. Midspan deflection, stress level = 0.7.

Fig 6.6. Midspan deflection, stress level = 0.60.

(4) The fatigue strength at 10 million cycles decreases with an increase in the level of prestress. However, all the prestressed beams have a higher fatigue strength than plain concrete. Therefore current fatigue design based on fatigue life of plain concrete is conservative for prestressed pavements subjected to a prestress level of 300 psi or less. Based on the results of this investigation, the fatigue strength at 10 million cycles for the 50, 100, 150, and 300 psi specimens are 0.652, 0.583, 0.595 (or 0.587), and 0.560, respectively. While The University of Texas study had a very limited number of samples, making the results less statistically significant, the same trend of decrease in fatigue strength at 10 million cycles with increase in the level of prestress was observed.

(5) The assumption of superposition of stresses is not be valid because the fatigue life of prestressed concrete is dependent on the interaction of the static nature of prestress and the dynamic nature of the loading stresses. While prestressing provides a constant benefit throughout the life of the concrete, detrimental effects due to dynamic stresses accumulate linearly as the number of cycles of loading increases. In general, when comparing the fatigue lives with two different prestress levels, the specimens with a higher prestress level will have a higher fatigue life if the specimens are subjected to a stress level higher than the stress level at which the two equations intercept. On the other hand, specimens with a lower prestress level will have a higher fatigue life if they are subjected to a stress level lower than the stress level at which the two equations intercept.

(6) The structural integrity of the specimens is highly dependent on the amount of prestress. Specimens subjected to a higher prestress level were able to maintain better elasto-plastic behavior after the first cracking.

CHAPTER 7. ANALYSIS OF MOVEMENTS, STRESSES, ETC.

In the course of designing the PCP slabs for the McLennan County overlay, a comprehensive study of the nature of frictional resistance was carried out by the authors. An understanding of this phenomenon is essential for developing mathematical models to simulate the behavior of long PCP slabs. The objective of this chapter is to present the salient features of this study phase (Ref 17).

First, the importance of frictional resistance in the design of long slabs of PCP is demonstrated. Then, the behavior of the slabs in terms of temperature and moisture change movements as affected by the subbase friction is described. This description summarizes important results obtained from past studies on the subject. As a starting point for the discussion herein, the basic principles of friction are reviewed. Relevant features of the frictional resistance as observed during field and laboratory testing are subsequently described. A discussion is then presented of the nature of the frictional resistance under rigid pavements to explain the observed behavior of actual PCP slabs. Finally, several implications from behavior prediction based on modeling the subbase friction forces as inelastic forces are addressed.

IMPORTANCE OF THE SUBBASE FRICTIONAL RESISTANCE IN THE DESIGN OF PCP SLABS

Environmental variables cause stresses and time dependent variations of the net prestress level longitudinally and vertically in long PCP slabs. Environmental factors producing stresses are

(1) temperature and moisture stresses due to resistance of horizontal movements by the subbase friction,

(2) restrained curling produced by temperature differentials from top to bottom of the slabs, and

(3) restrained warping produced by moisture differentials from top to bottom.

The importance of studying the frictional resistance for the design of PCP slabs is centered on two aspects:

(1) Before application of prestress forces, the tensile stresses produced in the slabs due to temperature drops may cause premature cracking of the pavement, especially during the first night if the slabs are placed at the peak daily temperatures. Predictions of the friction restraint stresses during the first hours after concrete placement are required in this case, along with knowledge of the strength gain properties of concrete at very early ages. The prediction of these stresses permits assessment of the applied prestress forces at the earliest possible time following placement, to minimize the risks of developing premature cracking in the slab and, also, to avoid applying excessive forces which may cause failure of the concrete near the anchor zone.

(2) Predictions of friction restraint stresses, primarily as a result of the daily temperature change movements, represent an essential part of the design of thickness and longitudinal prestress level. Slab thickness and longitudinal prestress are designed so that the concrete flexural strength is not exceeded by the stresses due to (a) frictional resistance, (b) restrained curling and warping, and (c) wheel loads.

If thickness and prestress level are determined so that the fatigue strength of the concrete is not exceeded by the tensile stress due to frictional resistance, restrained curling and warping, and the static application of the wheel load producing the maximum tensile stress in the PCP, then a premature fatigue failure of the pavement is unlikely and the elastic behavior of the concrete is assured. This design criterion is usually referred to as elastic design of PCP slabs (Ref 17). The damage to the pavement is more significant if wheel loads are applied when the temperature decreases. In this case, the subbase frictional resistance induces tensile stresses in the slab when the PCP tends to contract (Ref 18). With both design criteria, the prediction of the friction restraint stresses is, therefore, essential.

EFFECT OF THE FRICTIONAL RESISTANCE ON THE MOVEMENTS OF PCP SLABS

Length changes of PCP slabs occur due to post-tensioning and they are restrained or unrestrained by the subbase friction depending on the construction.. Long prestressed and

conventionally reinforced pavements have been explored in this respect in recent years, and excellent data on movements have been obtained. In a 1312-foot PCP in Germany (Ref 19), it was observed that the central portion of the pavement was fully restrained by the friction from the movements due to the daily temperature changes, as illustrated in Fig 7.1. Cashell and Benham (Ref 20) report daily temperature change movements restrained by the friction in a 1310-foot continuously reinforced pavement (CRCP) but not movement from seasonal temperature changes, as shown in Fig 7.2. The daily movements of the CRCP were smaller than those of the PCP slabs due to the internal relief provided by the cracks of the CRCP. The large end movements in the CRCP due to seasonal influences corresponded closely to contraction or expansion without frictional resistance.

In accordance with the outlined behavior, the slab movements can be classified with respect to the frictional resistance as follows:

(1)   <u>Movements partially restrained by the friction.</u> This category includes the movements produced by daily temperature changes.

(2)   <u>Movements unrestrained by the friction.</u> These movements include concrete swelling, shrinkage, and creep.

(3)   <u>Elastic shortening which is diminished by the friction when the prestress force is applied, but which affects the full slab length shortly after post-tensioning</u> (Ref 21).   This movement is, therefore, a temporarily restrained movement.

REVIEW OF BASIC PRINCIPLES FOR FRICTION FORCES

In classical mechanics, the friction force is defined as the tangential force that develops when two surfaces which are in contact tend to move, one with respect to the other. The nature of the friction force is not completely known; however, it is assumed to be produced by two factors: (1) molecular attraction and the nature of the surfaces in contact and (2) the irregularities between the surfaces in contact. In a block model, as shown in Fig 7.3, if a horizontal force is applied to the block, the friction force that develops before the block experiences any movement is called static friction force. The friction coefficient corresponding to the maximum static friction force is named static coefficient of friction. The friction force that develops after the maximum static friction force, F_m, is
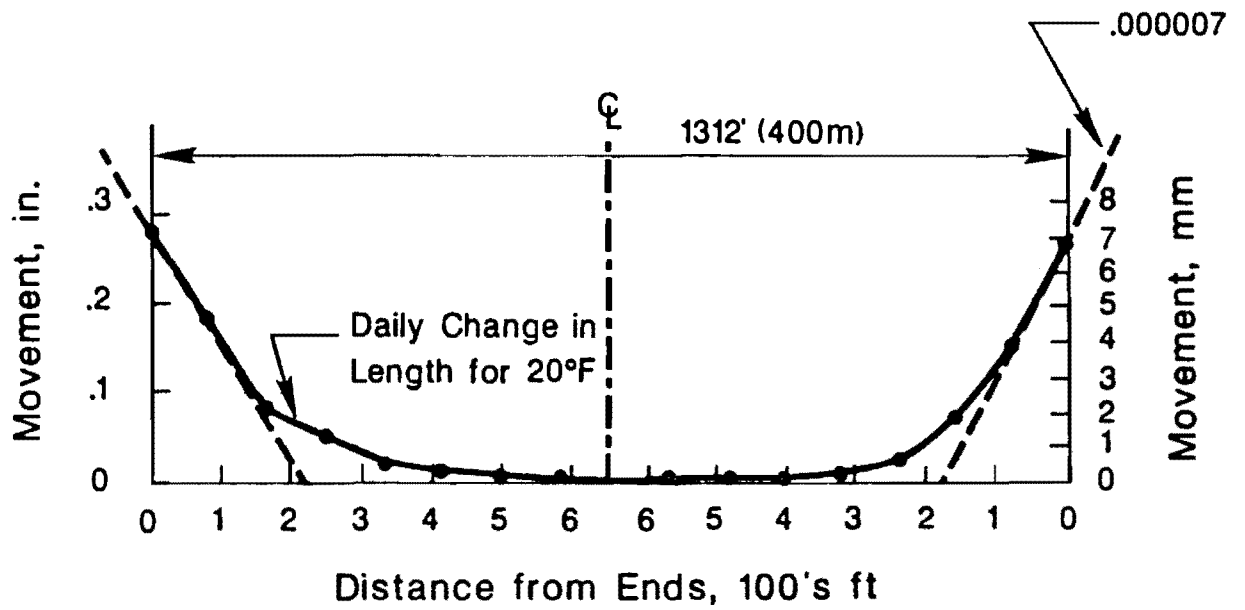
Fig 7.1.   Restrained temperature expansion in a 1312-foot prestressed slab in Vernheim, Germany, for a 20°F temperature increase from 5:45 AM to 5:25 PM (Ref 19).
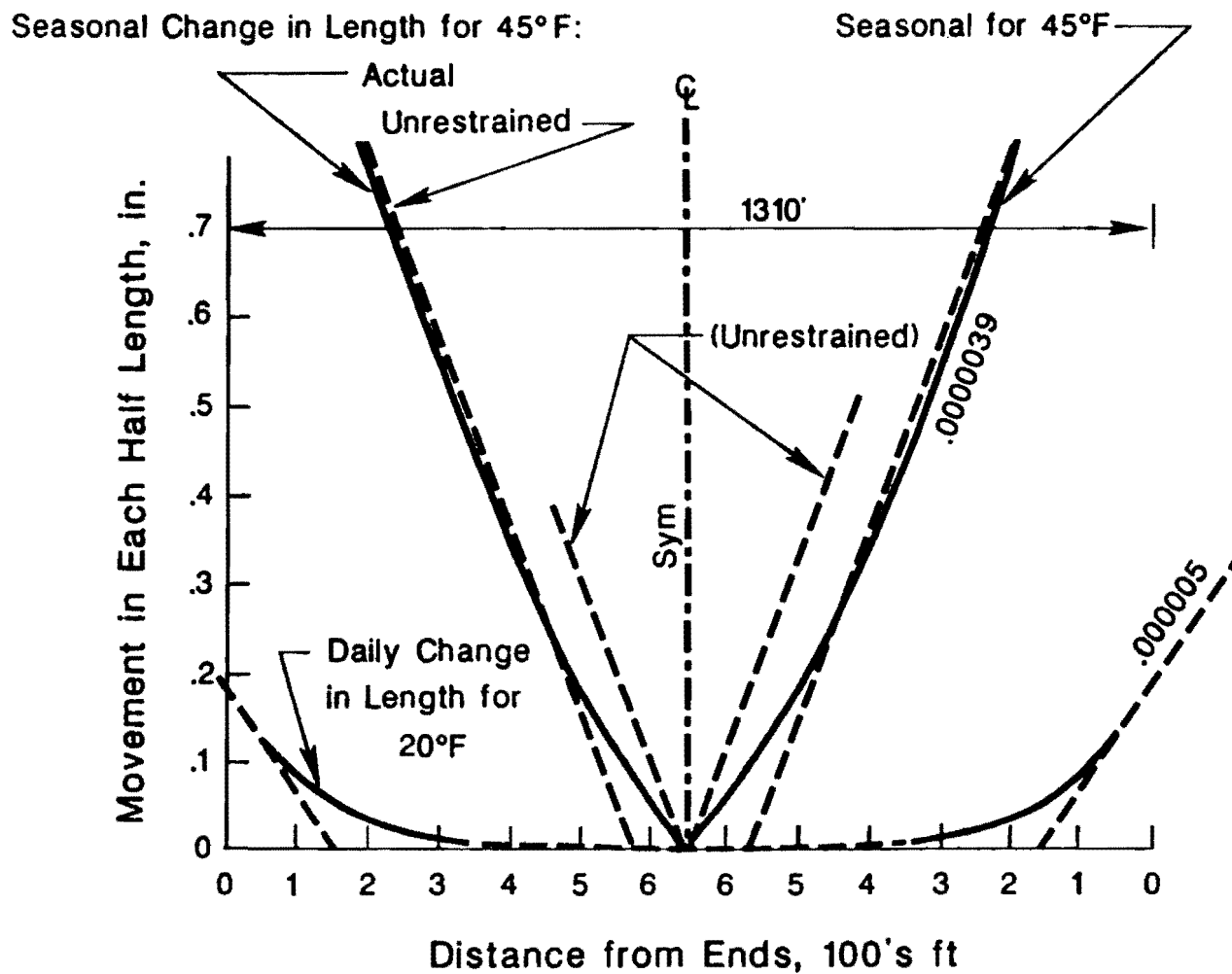
Fig 7.2.   Restrained daily expansion and unrestrained seasonal movement for 1310–foot–long CRCP (Ref 20).
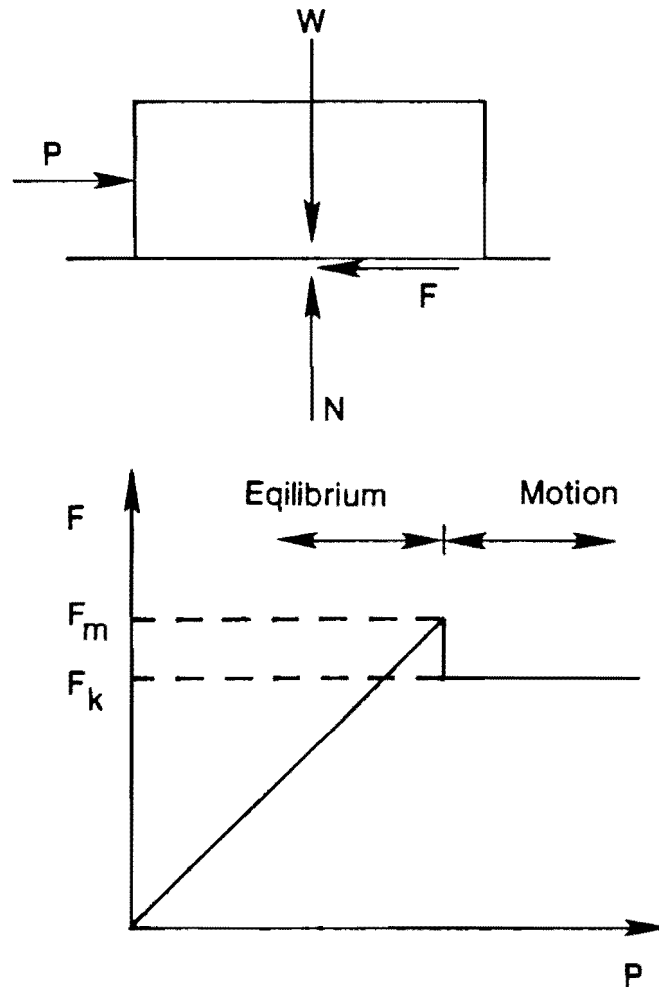
Fig 7.3. Classical friction model.

exceeded and the block slides is named the kinetic friction coefficient. It is interesting that, if the block is pushed until sliding occurs in both directions, the movements of the block are governed by perfect hysteretic friction force versus displacement curves, as shown in Fig 7.4.

The friction coefficient that corresponds to the kinetic friction force is called the kinetic friction coefficient, and it is lower than the static friction coefficient. The relevant properties of these coefficients are that (1) both coefficients are independent of the normal force, (2) both coefficients depend on the nature of the surfaces in contact and the exact condition of the surfaces, and (3) both coefficients are independent of the area of the surfaces in contact.

FEATURES OF THE SLAB-SUBBASE FRICTIONAL RESISTANCE OBSERVED DURING FIELD TESTS

Studies have been conducted since 1924 to investigate the nature of the frictional resistance under rigid pavements. Some of the features observed during field tests are presented below.

Goldbeck

Studies conducted in 1924 by the U.S. Bureau of Public Roads (Ref 22) gave the first relevant features on the nature of the frictional resistance offered by different materials to horizontal movements of concrete pavement slabs. The following important conclusions may be drawn from these studies:

(1)   If a pushing force is exerted on a pavement slab cast over a certain subbase material, the irregularities between the surfaces in contact act as resistance to slab movements. This resistance results in the development at shear stresses at the surface of the subbase material and which tends to elastically deform it when the slab tends to move. More roughness in the subbase results in more resistance for the slab, with a consequent increase of the amount of subbase
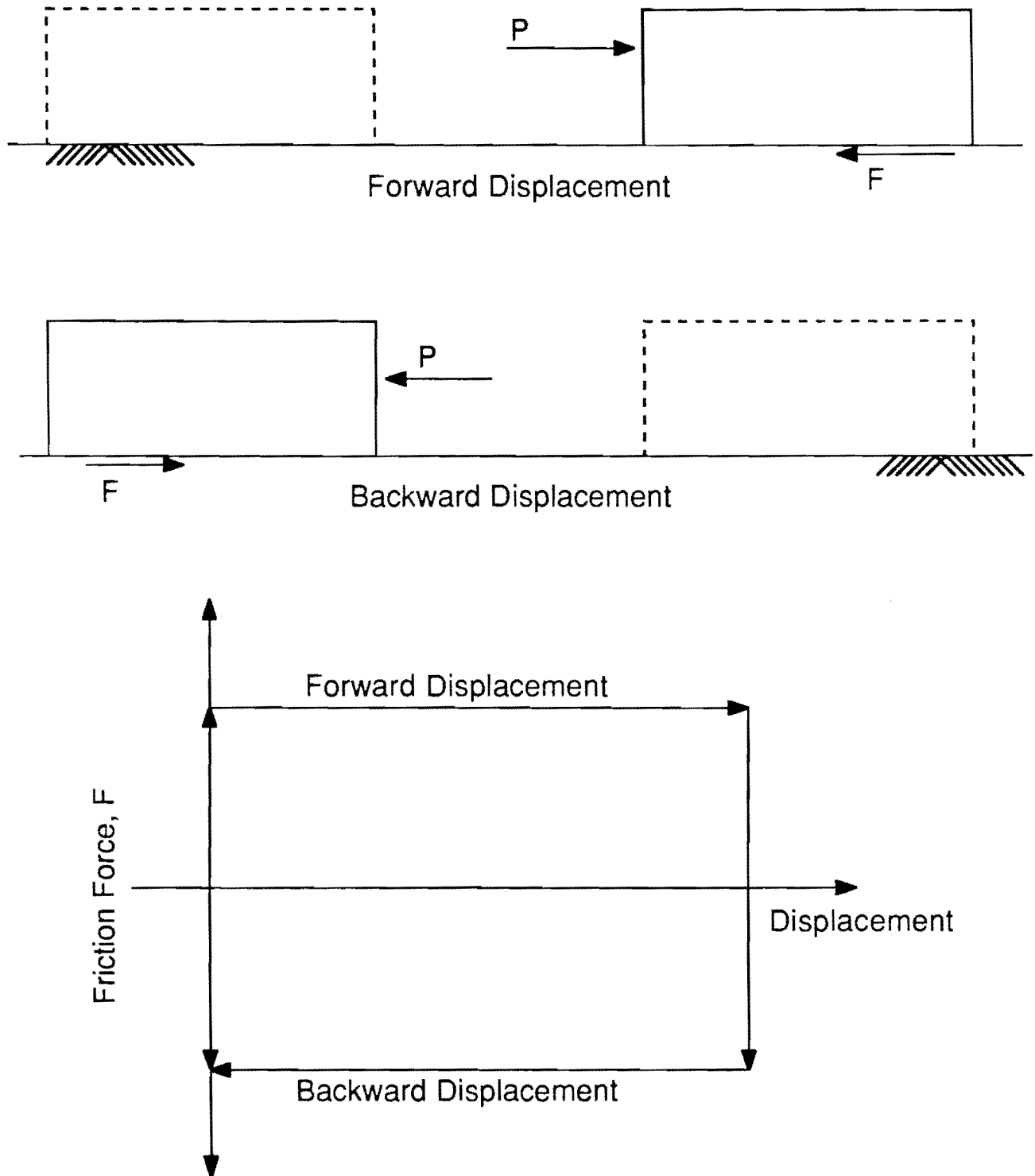
Fig 7.4.   Perfect hysteretic friction force versus displacement curve for a block under consecutive cycles of movement.

material pushed by the slab and, therefore, a subsequent increase of the frictional resistance.

(2) The frictional resistance may be greatly reduced in concrete pavements if more slippage of the slab is allowed by the elimination of ridges and depressions in the subbase or if a sand layer is introduced between the subbase and the pavement.

(3) A secondary observation of interest to this research is that the frictional resistance is considerably lower when subbase materials are tested under saturated conditions. This is due to the fact that the water acts as a lubricant which permits the slabs to slip easier and the moisture affects the consistency of most subbase materials.

After the studies conducted by Goldbeck were reported, a thick layer of sand was introduced under highway pavement slabs. However, in prestressed concrete pavements, the slabs are relatively thin and tend to experience large deformations at edges and joints of the pavement under wheel loads. These deformations may cause voids beneath the pavement due to pumping, which may eventually lead to other serious problems. This led highway engineers to study other types of friction relieving materials.

Timms

Relevant results pertaining to the behavior of friction are reported by Timms (Ref 23). His study, conducted for the U. S. Bureau of Public Roads in 1963, consisted of pushing concrete slabs cast on different types of materials. The following conclusions are important.

(1) The friction coefficient is greater when the slabs are pushed initially and decreases for the average of subsequent movements. Figure 7.5 shows this condition for the materials tested.

(2) On release of the thrusting force, a slab slightly tends to return its original position. This slight return is a semi-elastic recovery of the subbase material being tested. This particular feature is also reported by Friberg in tests with 100-foot-long slabs (Ref 24).
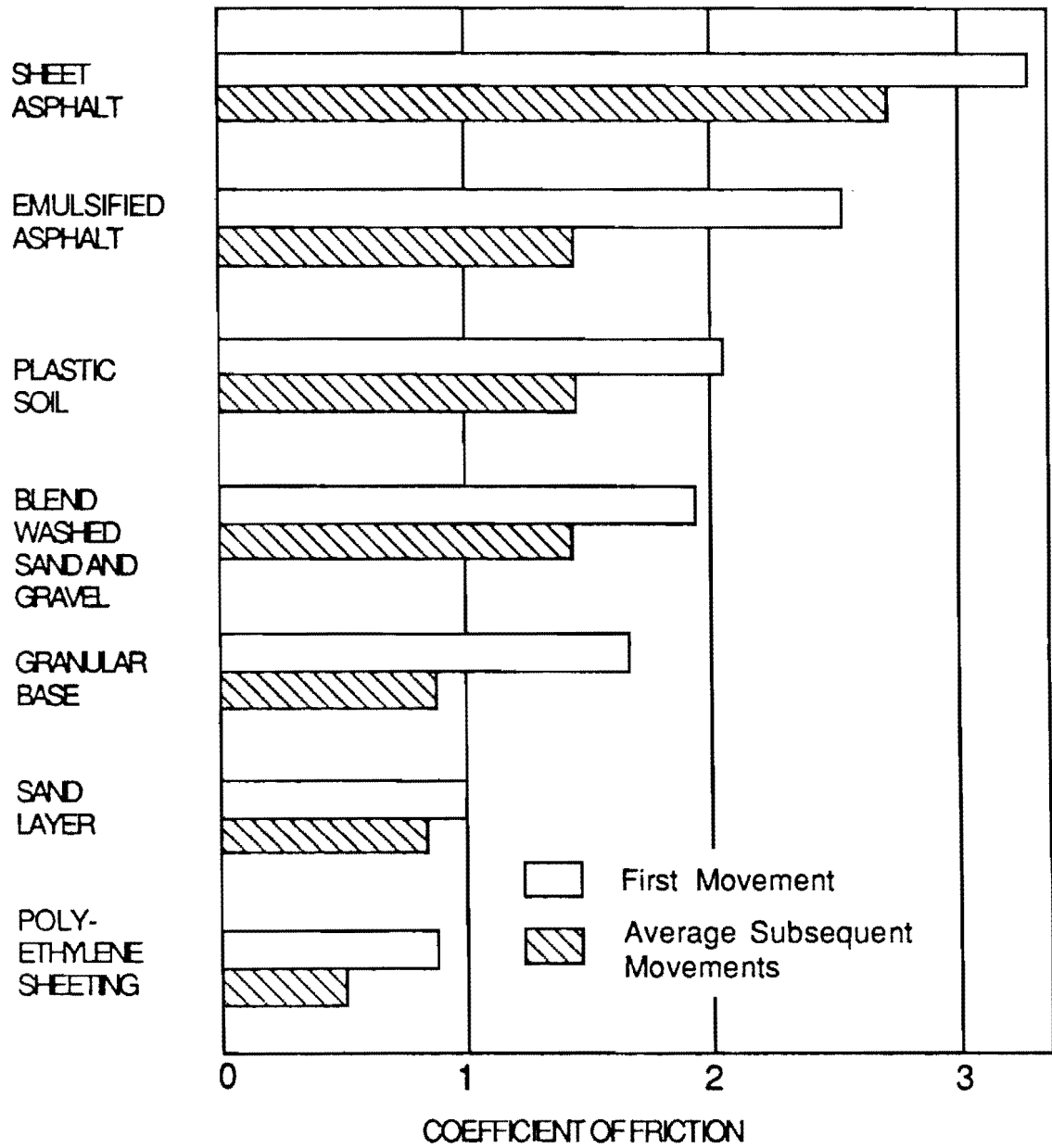
RR401-8F/07

Fig 7.5. Summary of friction coefficients obtained by Timms (Ref 23).

(3)   From Fig 7.5, it is evident that the lowest friction coefficients are obtained
        with double layers of polyethylene films, followed by sand subbases, granular
        subbases, plastic clays, and emulsified and asphalt sheet layers.

Other Field Tests

The results from other field tests that evaluate the properties of particular materials
are reported in the literature. Two of these tests are reported herein.

Saudi Arabia Tests. The design of the apron zone of the King Fahd International Airport
(KFIA) in Dhahran, Saudi Arabia, was conducted by Austin Research Engineers (Ref 18). The
severe climatological conditions in Dhahran, where large daily temperature changes are
characteristic, required that the merits of different subbase types be carefully assessed to
avoid premature cracking of the pavement. Concrete cylinders 22.5 inches in diameter and
16 inches deep were cast and pushed over the following materials:

(1)   an aggregate subbase coated with a medium curing asphalt cutback (MC-70),

(2)   a fine grade bituminous subbase course, and

(3)   one-sheet of visqueen over a bituminous subbase course.

The testing procedure is described in Ref 25. The results from these tests are
graphically depicted in Fig 7.6.

Field Tests at Gainesville, Texas. A series of field tests were conducted by The
University of Texas at Austin, as part of a program for designing the PCP overlay in McLennan
County (Ref 26). In these tests, 6-inch-thick concrete slabs were cast and tested over the
following materials:

(1)   an asphalt subbase,

(2)   a 6-mil polyethylene sheeting on an asphalt subbase, and

(3)   a double layer of 6-mil polyethylene sheeting on an asphalt subbase.

The testing procedure is described in great detail in Refs 27 and 28. The results are in
complete agreement with the results obtained in Saudi Arabia, and thus are independent of the
difference in geographical locations of the testing sites. The results from both tests are,
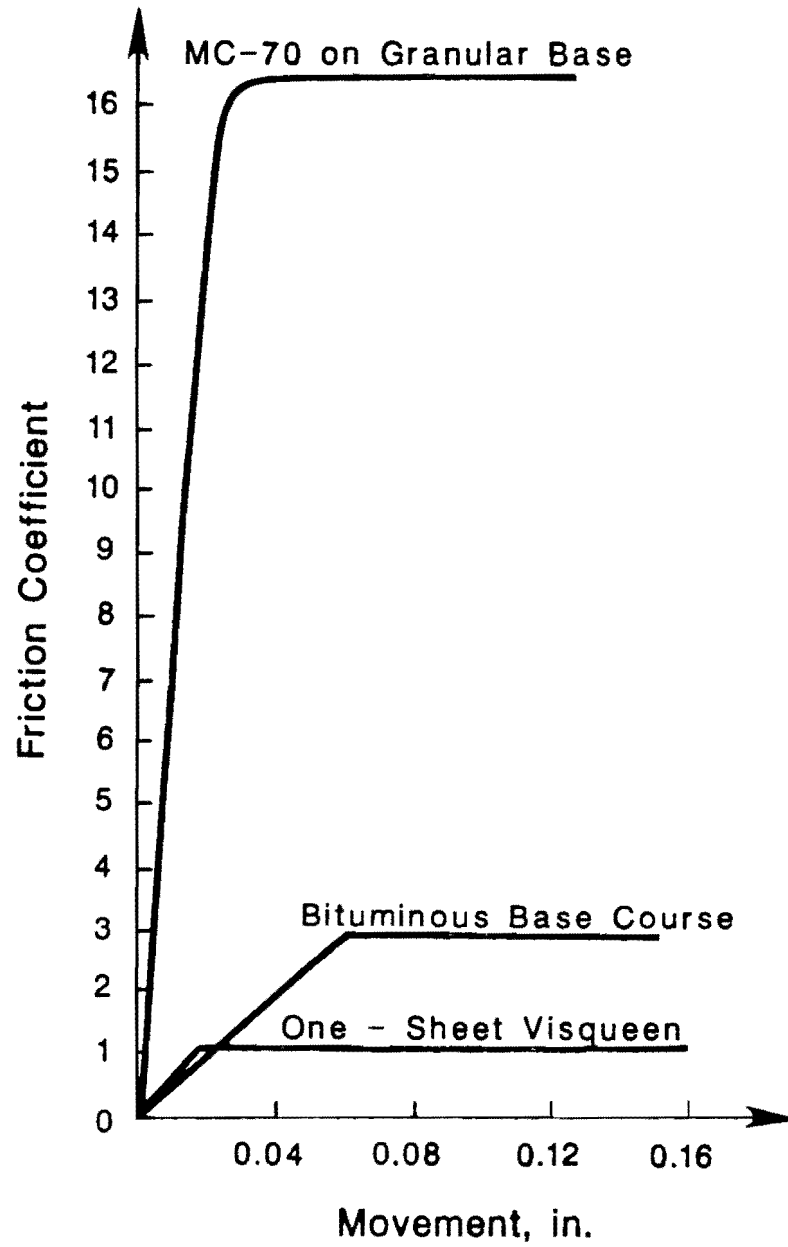
Fig 7.6. Friction coefficient versus movement for materials tested in Saudi Arabia (Ref 25).

likewise, in full agreement with the results reported by Timms for similar materials. Figure 7.7 presents the friction coefficient versus displacement curves for the three conditions analyzed in Gainesville. In Chapter 2 a more detailed presentation of results from friction tests and evaluation is presented.

HYSTERETIC BEHAVIOR

In 1963, Stott (Ref 29), of the Road Research Laboratories of Great Britain, presented the results of a comprehensive laboratory investigation. Stott cycled slabs placed on various materials back and forth. The amplitude of the cycles of movement and the rate of application of the force were varied in the experiment. The materials tested included sand layers, aggregate layers, polyethylene sheetings, and asphalt cements having different nominal penetration values. These tests provided excellent information on the behavior of the friction under rigid pavement slabs. Figure 7.8 shows the typical friction force versus movement curve obtained for most materials tested by Stott. These are the important features of this curve.

(1)   First, the force exhibits a rise until it reaches an initial peak. The friction force that develops along this part of the curve is similar to the classical static friction force. The peak observed in the curve is equivalent to the static friction force from which the static friction coefficient is defined. In this zone of the curve, most materials show a quasi-elastic behavior. If the force that produces the movement is gradually released, the slab tends to return to its original position as the friction force drops to zero.

(2)   The friction force that develops after the initial peak is similar to the kinetic friction force of the block model in Fig 7.3. Like the kinetic friction force, this force remains practically constant after sliding if further displacement of the slab occurs. The displacements that occur after sliding are non-recoverable when the pushing force is removed.

(3)   The backward movement R observed in Fig 7.8 when the pushing force is removed is a quasi-elastic recovery of the material underneath.
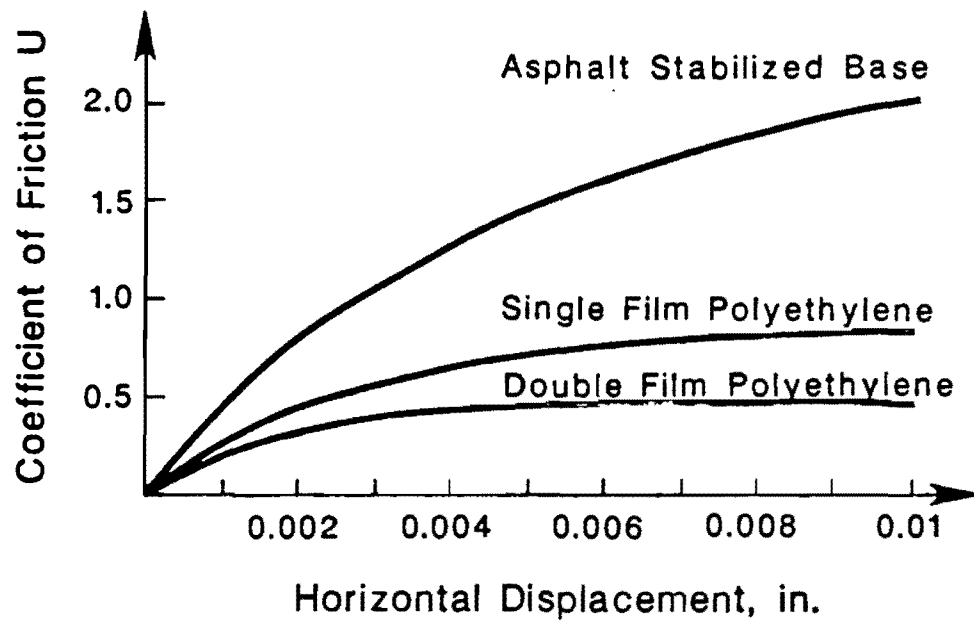
Fig 7.7.   Friction coefficient versus displacement for materials tested for the design of the McLennan County overlay (Refs 27 and 28).
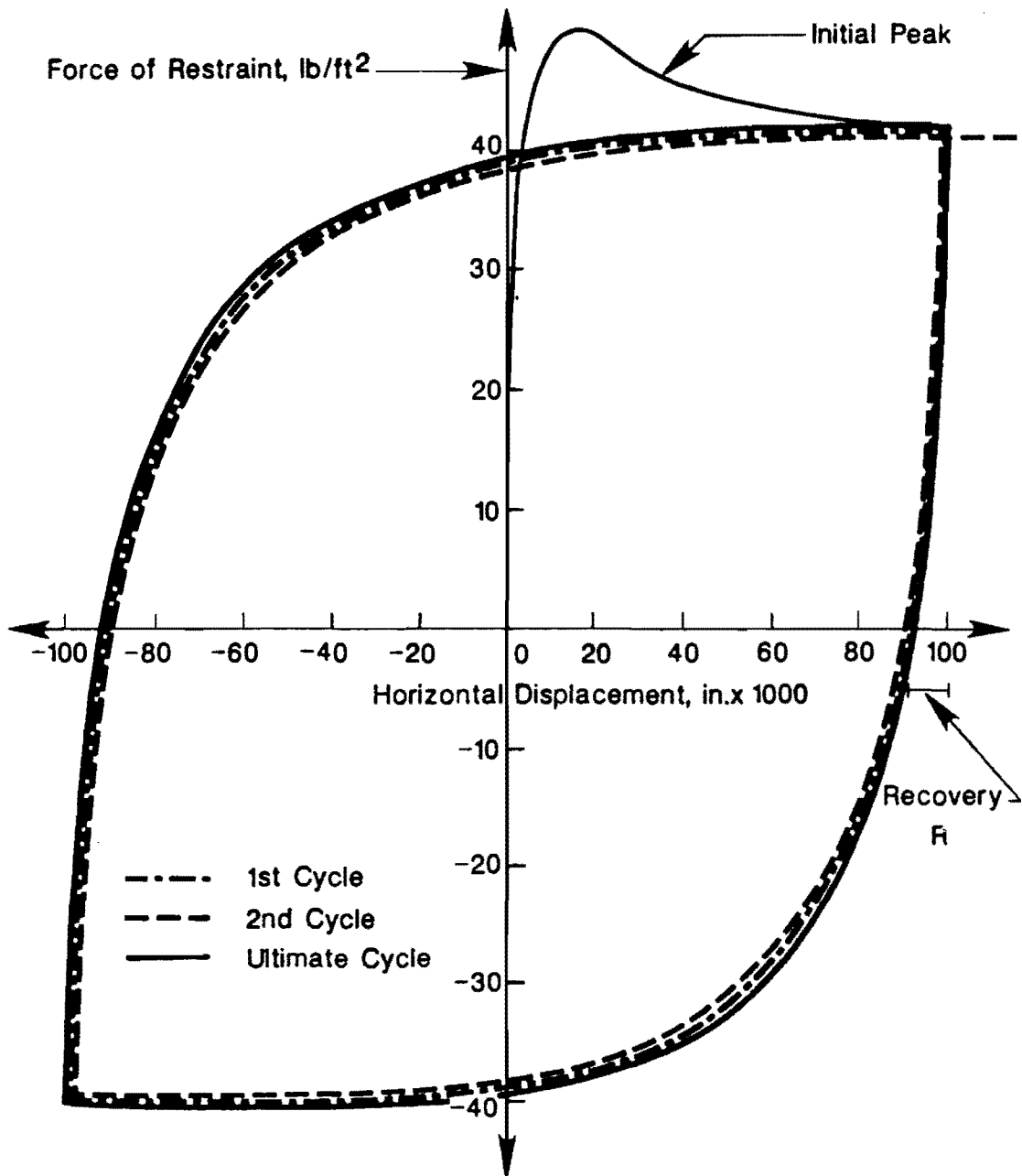
Fig 7.8.   Typical force of resistance versus displacement curve that develops under rigid pavement slabs (Ref 29).

(4) The consecutive application of cycles of displacement produces hysteretic curves. During these cycles, the initial peak is not observed again and, rigorously, it is not possible to establish a boundary between static and kinetic friction forces. However, the resistance force resembles the static friction force (with quasi-elastic properties) in the zone where the curve is more vertical and looks like the kinetic friction force where the curve becomes flatter. In this zone of the curve, the slab is sliding and the movements are non-recoverable after removal of the external force.

(5) During the first few cycles of displacement, the maximum force of resistance that develops in each cycle decreases slightly, but, at the end, it reaches a steady condition. This friction force versus movement curve is probably the one that may be encountered in practice under rigid pavement slabs.

(6) An observation irrelevant to this study though important from the standpoint of materials behavior is that asphalt cement sticks to the bottom face of the slabs and the resistance force that develops is due to viscous shear through the depth of the material. For this reason, it is independent of slab weight and dependent on grade, thickness, temperature of the bituminous layer, and rate of movement of the slab.

NATURE OF THE FRICTIONAL RESISTANCE UNDER RIGID PAVEMENTS

The review of concepts and tests presented above clearly indicates that the relationship between friction forces and horizontal displacements developing beneath long pavement slabs is substantially inelastic.

The resistance force verus movement curve for most subbase materials placed under road slabs is defined by two factors: (1) the elastic properties of the material beneath the slab and (2) the condition of the sliding plane and the nature of the surfaces in contact at the interface. The first defines the slope of the curve before sliding, and the second the maximum of kinetic friction force obtained after the slab slides. Figure 7.9 shows the zones of the curve for each factor.

The interaction of the factors mentioned above is illustrated conceptually in Fig 7.10. If the material beneath the slab is infinitely rigid and does not experience deformations due to
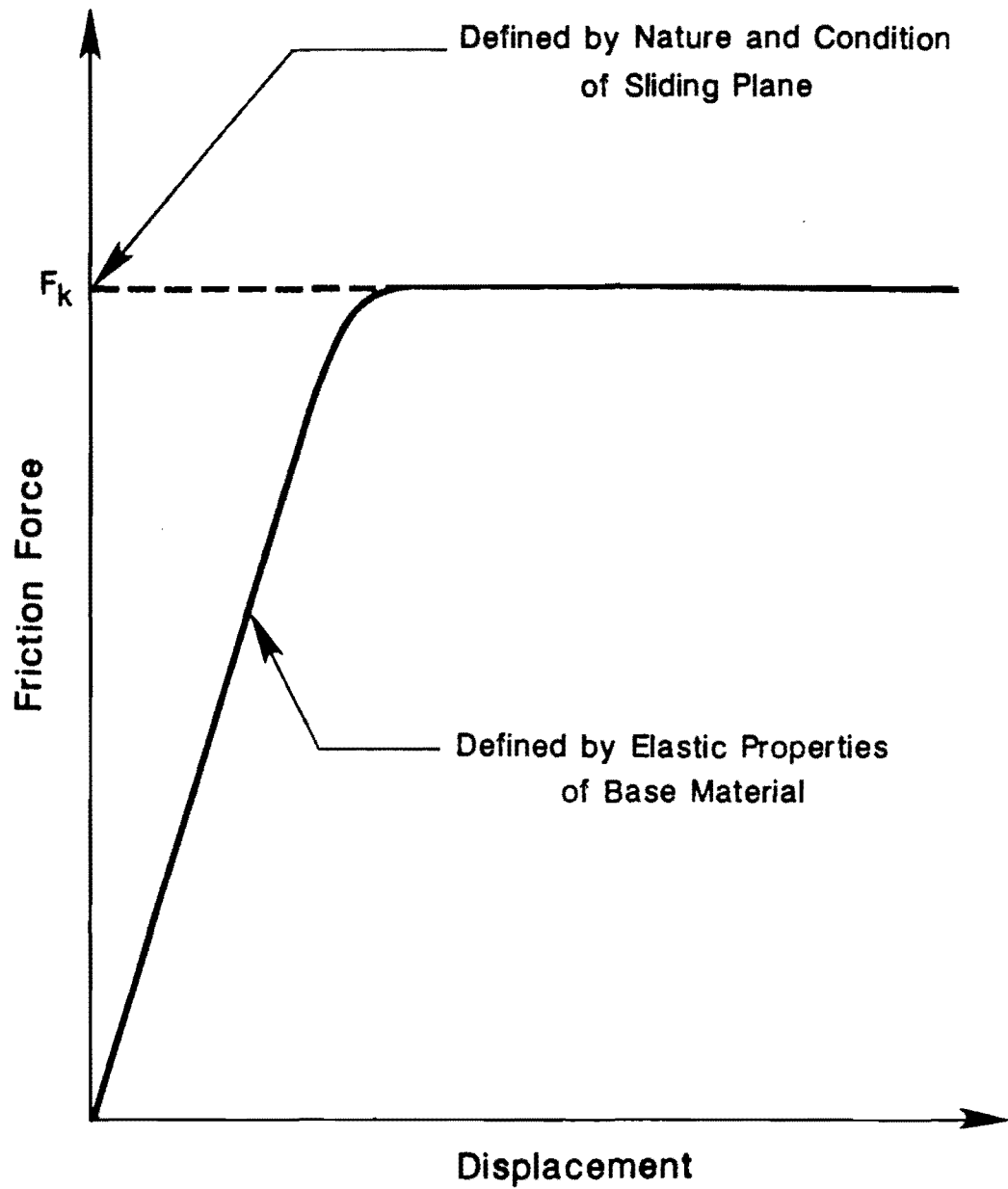
Fig 7.9. Factors affecting the shape of the force versus displacement curve.
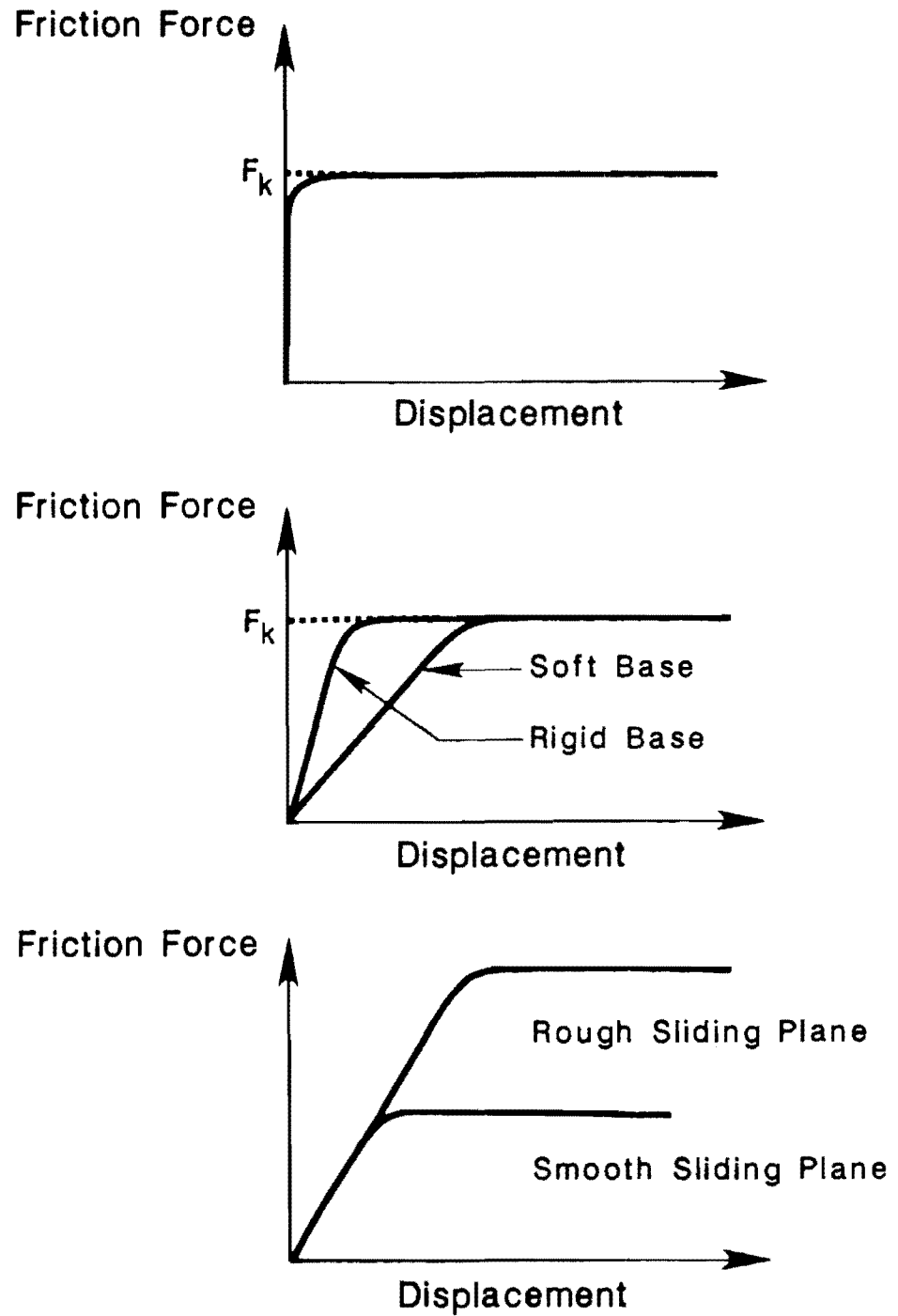
Fig 7.10.   Effect of stiffness of base material and texture of sliding plane on the friction force versus displacement curve.

friction related shear at the interface, the force versus movement curve may look as illustrated in Fig 7.10(a). This case may correspond to the ideal case of the block in Figs 7.3 and 7.4, in which the initial peak has not been drawn, since it disappears after a few cycles of displacement. Figure 7.10(b), in turn, shows the curves for two materials having different elastic properties (shear stiffnesses). The sliding plane for the case depicted in Fig 7.10(b) is assumed to have characteristics similar to the one in Fig 7.10(a). The kinetic friction forces F_k are the same in both cases, but the point of sliding is different. Finally, Fig 7.10(c) shows the effect of having two different sliding plane textures for the same subbase material. This is the case of the rough sliding plane with a granular subbase with and without a sand layer on top of the subbase. This may also be the case of slabs cast on bituminous materials with and without layers of polyethylene provided at the interface.

Modeling of Friction Forces

The purpose of the previous discussion is to indicate that the friction forces may be considered elastic if sliding does not occur along the slab length. This is the case for plain concrete and conventionally reinforced concrete pavements, which are typically shorter than 40 feet. These slabs develop maximum movements below 0.02 inch under a normal daily cycle, and the frictional resistance that builds up is defined by the quasi-elastic properties of the subbase material.

Implications in Behavior Prediction of Assuming Elastic Friction Forces

An elastic system of friction forces, following a force versus movement curve as shown in Fig 7.11, is assumed by McCullough et al (Ref 30) and Rivero–Vallejo et al (Ref 31) in developing procedures for the design of continuously reinforced concrete pavements (CRCP) and jointed reinforced concrete pavements (JRCP). However, the need is recognized in both efforts for simulating the real effects to improve the reliability of the prediction methods. In Fig 7.11, friction forces and displacements are drawn as having equal signs. This convention was adopted to obtain uniformity with similar graphs in this chapter. The reader should keep in mind, however, that displacements and friction forces are vectors having opposite directions, as the friction forces always oppose the direction in which the pavement displacements take place.
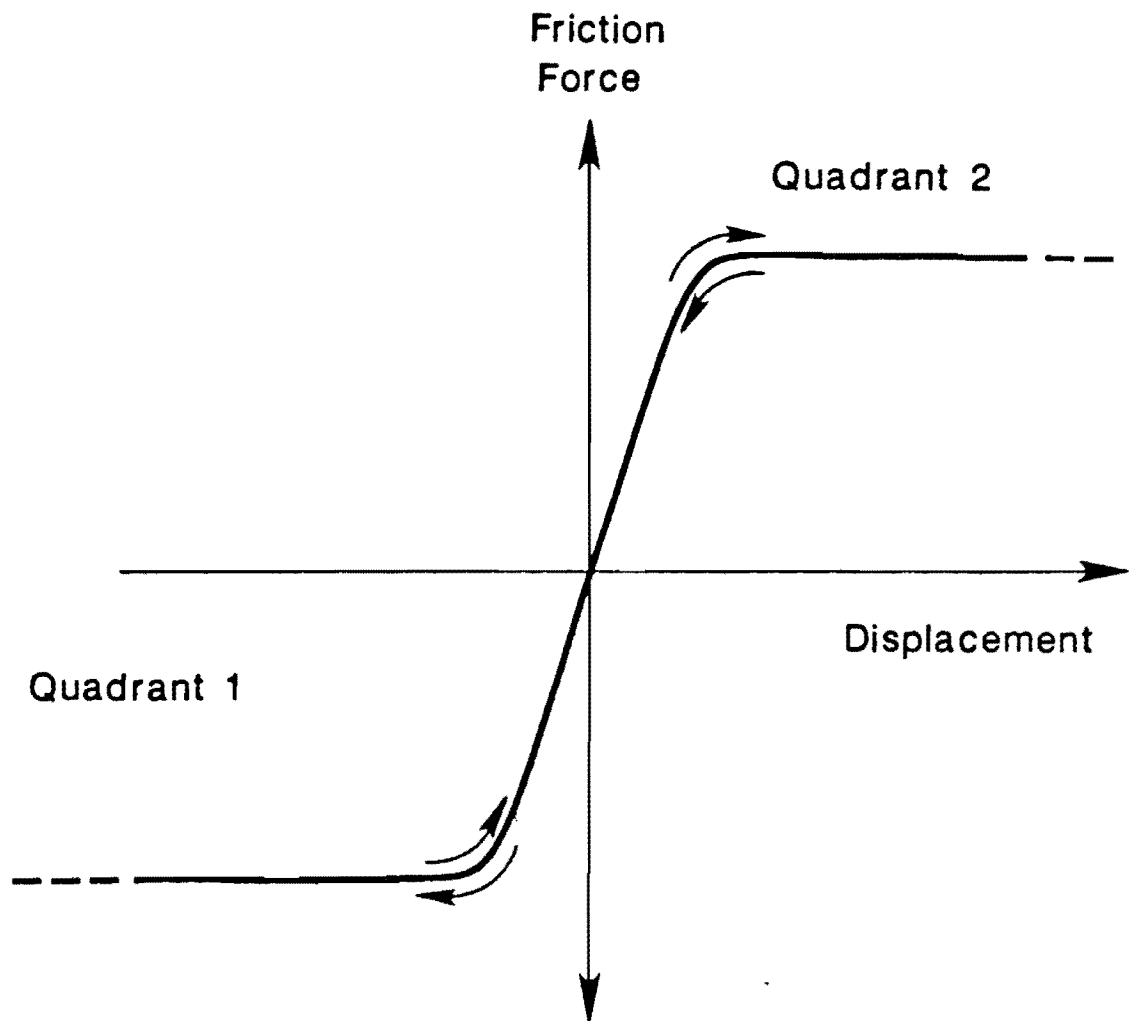
RR401-8F/07

Fig 7.11. Elastic friction force versus displacement curve.

Some relevant implications in behavior prediction of assuming elastic friction forces are given here.

(1)   The slab will develop compressive stresses when the temperature exceeds an initial reference temperature, usually referred to as the slab setting temperature (Ref 17). At this reference temperature, all the slab points are considered as having zero movements and their behavior can be located at the origin in Fig 7.11. Friction forces and stresses are zero for this initial condition. When the points of the half slab shown in Fig 7.12(a) are displaced to the right of their initial position, they are assumed as behaving in Quadrant 2 in Fig 7.11, thus developing compressive stresses as shown in Fig 7.12(b). This is the case for higher temperatures than the reference temperature. Accordingly, a slab cast at the minimum temperature of the day will develop exclusively compressive stresses during the entire day. Furthermore, a slab cast at the minimum temperature of the year will develop compressive stresses during the year only if shrinkage and other sources of slab contraction are ignored.

(2)   Figure 7.13 shows an extension of implication (1) for a series of consecutive temperature cycles. For times t_1, t_2, t_3, t_4, and t_5, with equal temperature T_1 above the reference temperature T_0, the slabs will develop compressive stresses of the same magnitude irrespective of whether the slab is contracting or expanding. Likewise, equal stresses are obtained for other temperatures representing equal temperature changes with respect to the reference temperature.

(3)   Shrinkage and other sources of long term longitudinal movement do not occur without frictional resistance, but accumulate on a daily rate basis, resulting eventually in the build up of maximum friction forces and concrete restraint stresses. This mechanism is illustrated in Fig 7.14. If the slab starts contracting from the maximum temperature of the day, Point A in Fig 7.14 moves from its initial position, Z_{A0}, to position Z_{A1} after the maximum contraction of the day. The part of the movement Z_{A1} due to the daily temperature drop is Z_{AT1}, whereas the rest of the movement is produced by shrinkage and other sources of long-term contraction. If the temperature

(a) Half-slab initial position at reference temperature.

Concrete
Stress

Distance from Midslab

(b) Friction forces and concrete stresses whenever the half-slab
points are displaced to the right of their initial position.
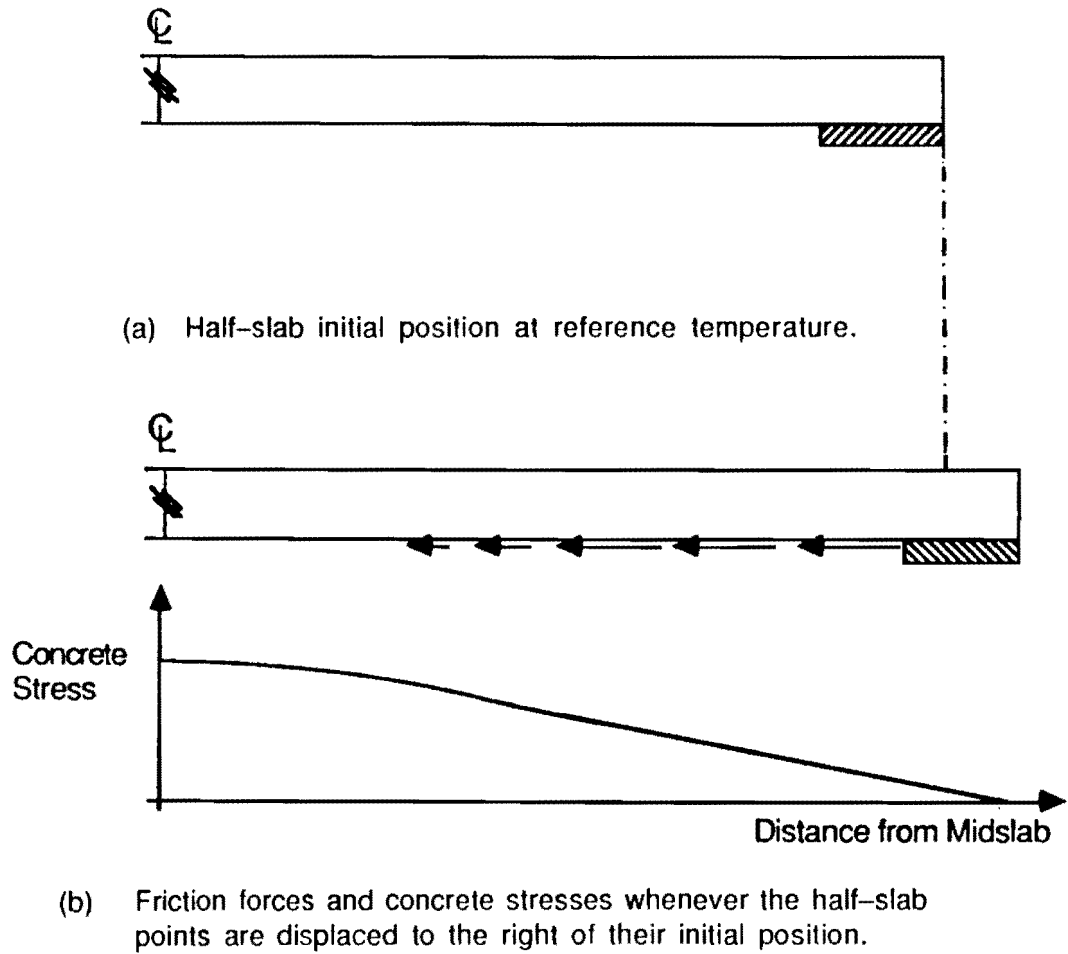
Fig 7.12. Development of compressive stresses when the half-slab points are displaced
to the right of their initial position. System of elastic friction forces.
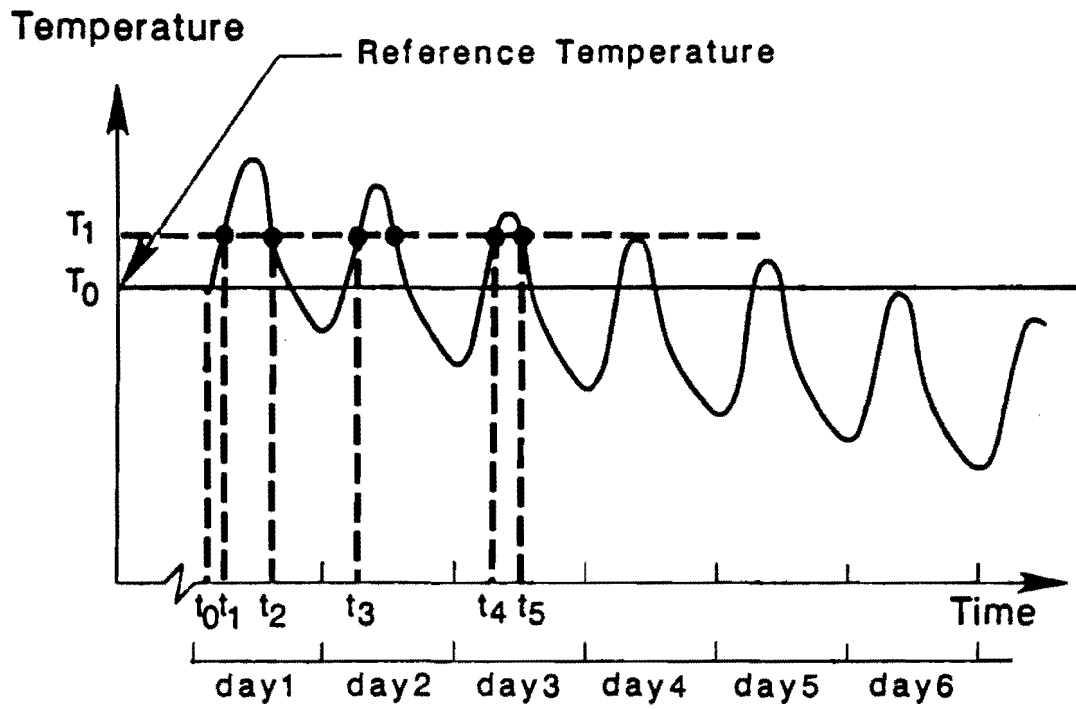
Fig 7.13. At times t_1, t_2, t_3, t_4, and t_5, when the same temperature T_1 is reached, the same slab compressive stresses will be obtained if elastic friction forces are assumed.
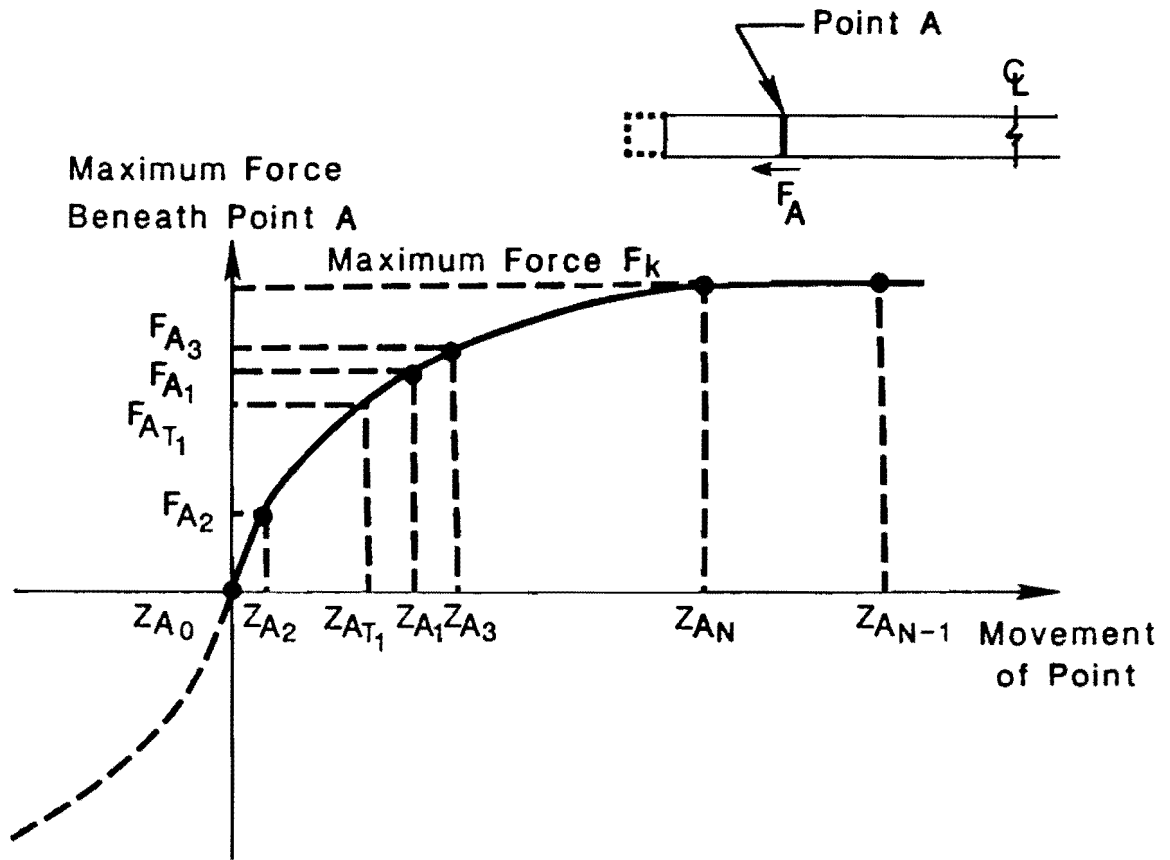
Fig 7.14.   Eventual build-up of maximum friction forces under assumption of elastic system of friction forces.

increases to the maximum again, point A moves to position Z_{A2} following the same path along the curve. The point does not return to its initial position, Z_{A0}, because a small portion of long-term movement has occurred. If long-term movements did not take place, point A would move between positions Z_{A0} and Z_{AT1} indefinitely for subsequent daily temperature cycles. However, the accumulation of shrinkage, creep, and the elastic shortening induced in PCP slabs when the prestress is applied insure that, a few days after the start of this process, the oscilation of point A will shift to occur between positions Z_{An-1} and Z_{An} for daily temperature change movements. The daily slab expansion will not suffice to remove point A from the sliding zone of the curve. Movements within this zone do not result in changes of magnitude or direction of the friction force, F_A, under the point. This concept has been exemplified for a single slab point; however, a similar behavior would be observed for the rest of the slab points. In this context, a direct implication of assuming elastic friction forces under the PCP is that, a few days after slab placement, maximum friction forces opposing the long-term contraction plus elastic shortening of the slab would be constantly and indefinitely predicted under all the slab points. Once this condition is reached, the effect of the maximum friction forces would be to decrease the precompression due to the prestress in all points of the slab at all subsequent times of prediction. This situation is illustrated in Fig 7.15. To assume that maximum friction forces along the entire slab produce stresses in the PCP which always decrease the precompression due to the prestress is very unrealistic and may lead to very conservative designs.

Implications in Behavior Prediction of Assuming Inelastic Friction Forces

For the case of long PCP slabs, a substantial portion of the slab works in the sliding range for the movements of the daily temperature cycle. The inelasticity of the frictional resistance and the significant sliding of the slab points cause reversals of movements exceeding 0.01 to 0.02 inch that result in reversals of frictional resistance. This is particularly true if friction reducing materials are used beneath the slab.
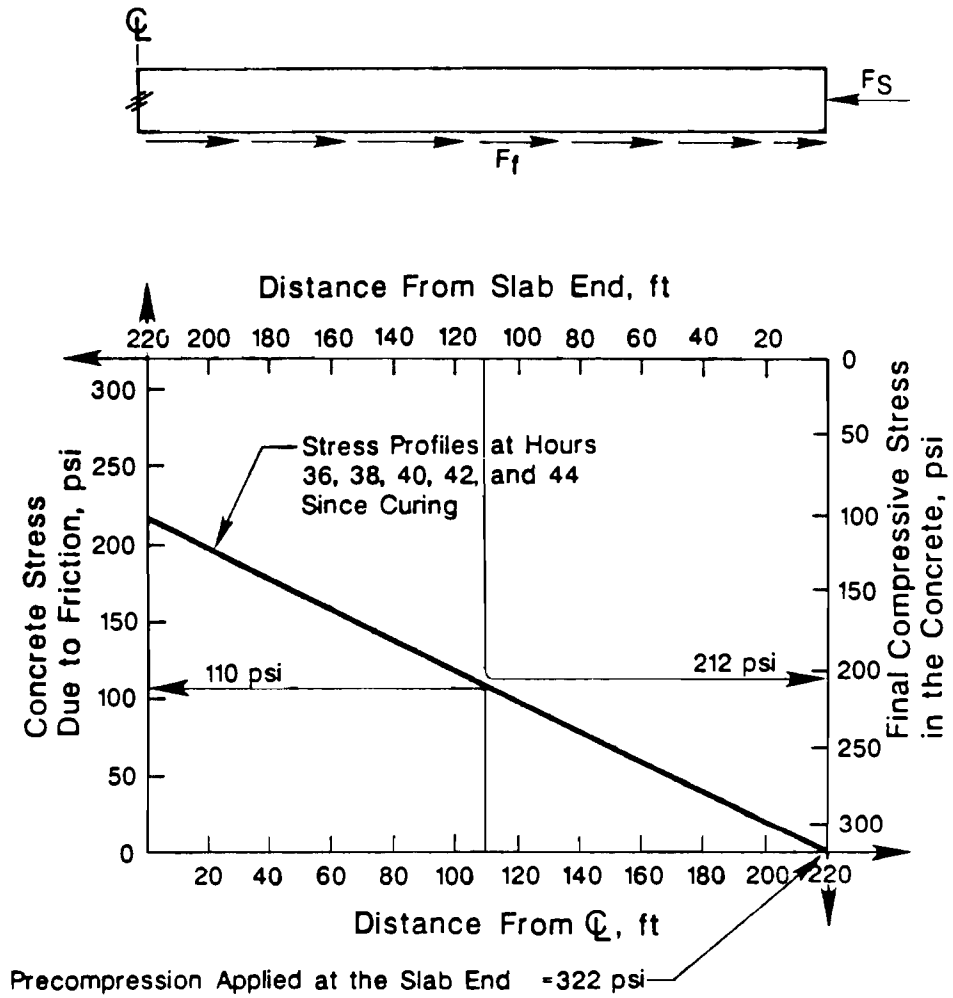
Fig 7.15.   If elastic friction forces are assumed, maximum friction forces decrease the precompression due to the prestress in all slab points at all subsequent times of prediction after post-tensioning.

The following are the implications of assuming an inelastic system of friction forces beneath the pavement:

(1)   A slab cast at the minimum temperature of the day will develop compressive stresses during the part of the temperature cycle when the temperature increases above the set temperature. A few hours after the peak temperature, the reversal of frictional resistance causes the build up of tensile stresses in the slab.

(2)   The long-term longitudinal movements, occurring at minute daily rates in comparison to the daily contraction and expansion, take place without significant frictional resistance. Therefore, these sources of movement do not cause stresses in the PCP slab. As mentioned earlier, this behavior type was observed by Cashell and Benham (Ref 20) in experiments with a 1310-foot CRCP. This behavior can be explained through the mechanism shown in Fig 7.16. If the slab starts contracting from the maximum temperature of the day, point A in Fig 7.16 will move from its initial position, Z_{A0}, to Z_{A1} for the maximum contraction of the day. The part of the movement Z_{A1} due to the temperature drop is Z_{AT1}. The rest of it is produced by the small portion of long-term movement occurring during the day. This portion of movement does not result in a significant increment of the friction force (from F_{AT1} to F_{A1}). If the temperature rises to the maximum again, point A moves to position Z_{A2}, unloading the force F_{A1} first and then developing the friction force F_{A2} in the opposite direction. Point A does not return to its initial position, Z_{A0}, because a portion of long-term contraction (due to shrinkage, creep, etc) has already occurred. Z_{A2} becomes the new initial position for the movements of the next thermal cycle. For the next cycle, the portion of long-term movement taking place during the day induces a small increment of friction force again, similar to the increase from F_{AT1} to F_{A1} during the previous cycle. However, the effect is not cumulative with the increment of the previous cycle, which had already dissipated when the slab reversed movements after the minimum temperature of the previous cycle. Point A, like the rest of the slab points, will shift following this mechanism without significant build up of friction forces for long-term movements of the slab. A
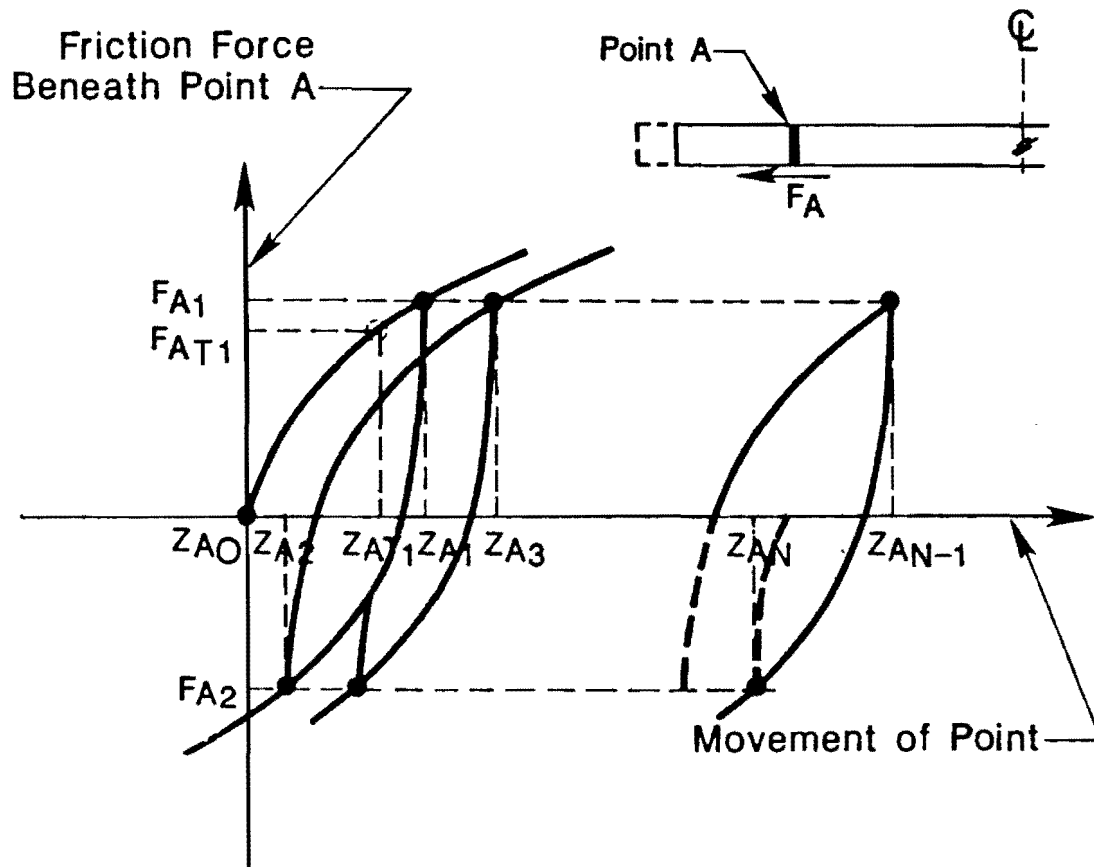
Fig 7.16.   Shifting of point A without frictional resistance for long-term movements if an inelastic system of friction forces is assumed.

direct implication of assuming inelastic friction forces is, then, that the magnitude of the friction forces depends almost exclusively on the magnitude of the daily temperature change. Likewise, the direction of friction forces and related concrete stresses depends on the nature of the temperature change. The stresses generated by the friction decrease the precompression due to the prestress if the slab contracts when the temperature drops. Vice versa, the friction forces increase the precompression due to the prestress if the slab expands with the temperature increments of the daily thermal cycle. This situation is illustrated in Fig 7.17.

104

$$F_X = -\int_X^{L/2} U_X \cdot \gamma \cdot D \cdot dx + F_S$$
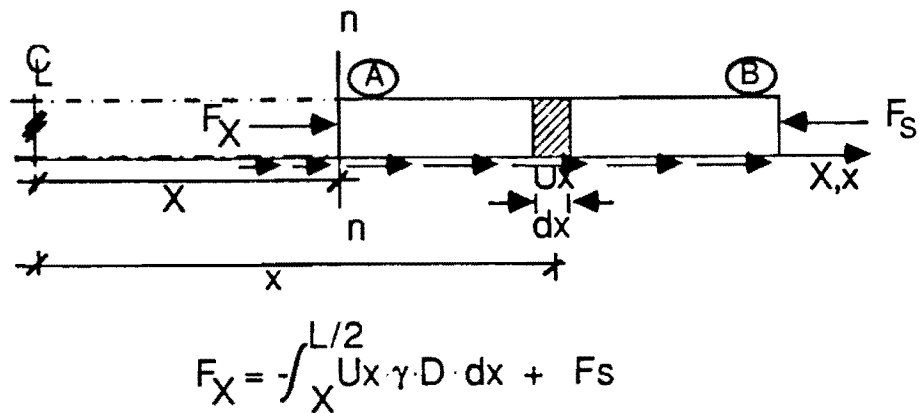
(a) The friction forces reduce the concrete precompression when the slab contracts.

$$F_X = \int_X^{L/2} U_X \cdot \gamma \cdot D \cdot dx + F_S$$
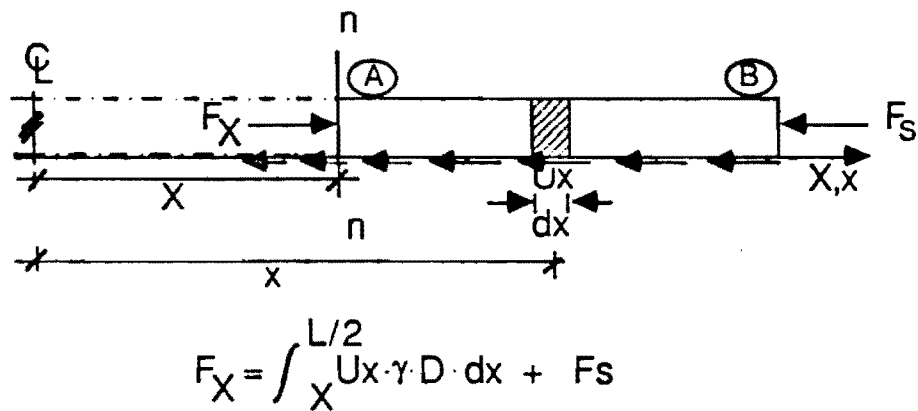
(b) The friction forces increase the concrete precompression when the slab expands.

Fig 7.17.   If the friction forces under the slab are assumed inelastically, the magnitude and direction of the friction forces depend primarily on the slab movements due to daily temperature changes.
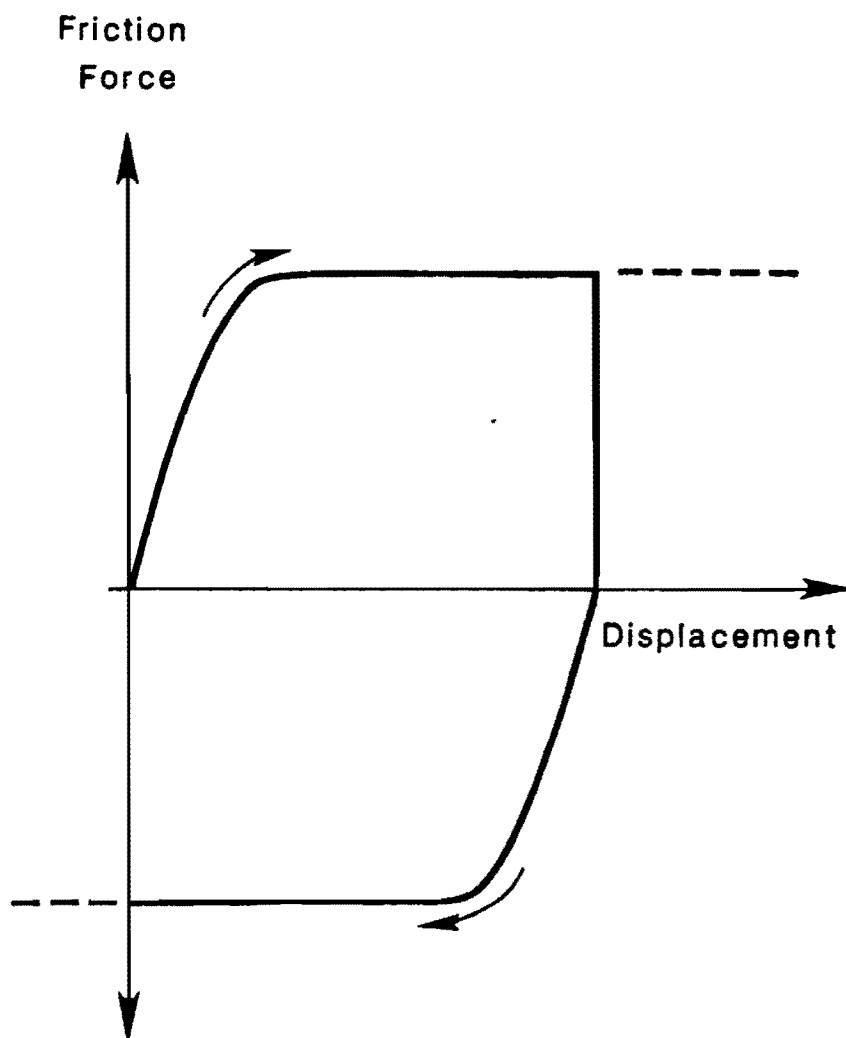
Fig 7.18. Friction force versus displacement curve assumed in this study.

DESCRIPTION OF NEW CONCEPTS

Concept 1: Central Stressing of Slip-Formed Pavement

All of the past FHWA sponsored PCP projects consisted of consecutive slip-formed slabs separated by short openings to permit post-tensioning of the prestressing tendons from the slab ends. Due to the long slab lengths and correspondingly high strand and subgrade frictions, it was necessary to stress each strand from both ends. After the post-tensioning had been applied and the elastic shortening and most of the creep had occurred, the openings were filled with concrete gap slabs.

One of the objectives was to find a method of post-tensioning the strands which would eliminate gap slabs and the problems associated with their use but still permit taking advantage of the slip-form method of pavement construction. The most promising alternative was central stressing. Central stressing is a procedure in which the strands are stressed at internal blockouts or stressing pockets. The blockouts are filled with concrete after the post-tensioning force has been applied.

Another objective was to investigate alternative methods for transversely prestressing pavement. It was felt that transverse prestressing is important to resist the applied wheel loads, prevent longitudinal pavement cracking, and prevent possible separation of separately placed pavement lanes or longitudinal pavement strips.

This concept is illustrated in a plan view of the pavement, in Fig 8.1, and an enlarged plan view of a stressing pocket is shown in Fig 8.2. The advantages and disadvantages of using a looped transverse tendon configuration are discussed in detail in Ref 32. This design was accepted by the Texas State Department of Highways and Public Transportation (SDHPT) for construction of the one-mile demonstration overlay project on U.S. Interstate Highway 35 near Waco, Texas.

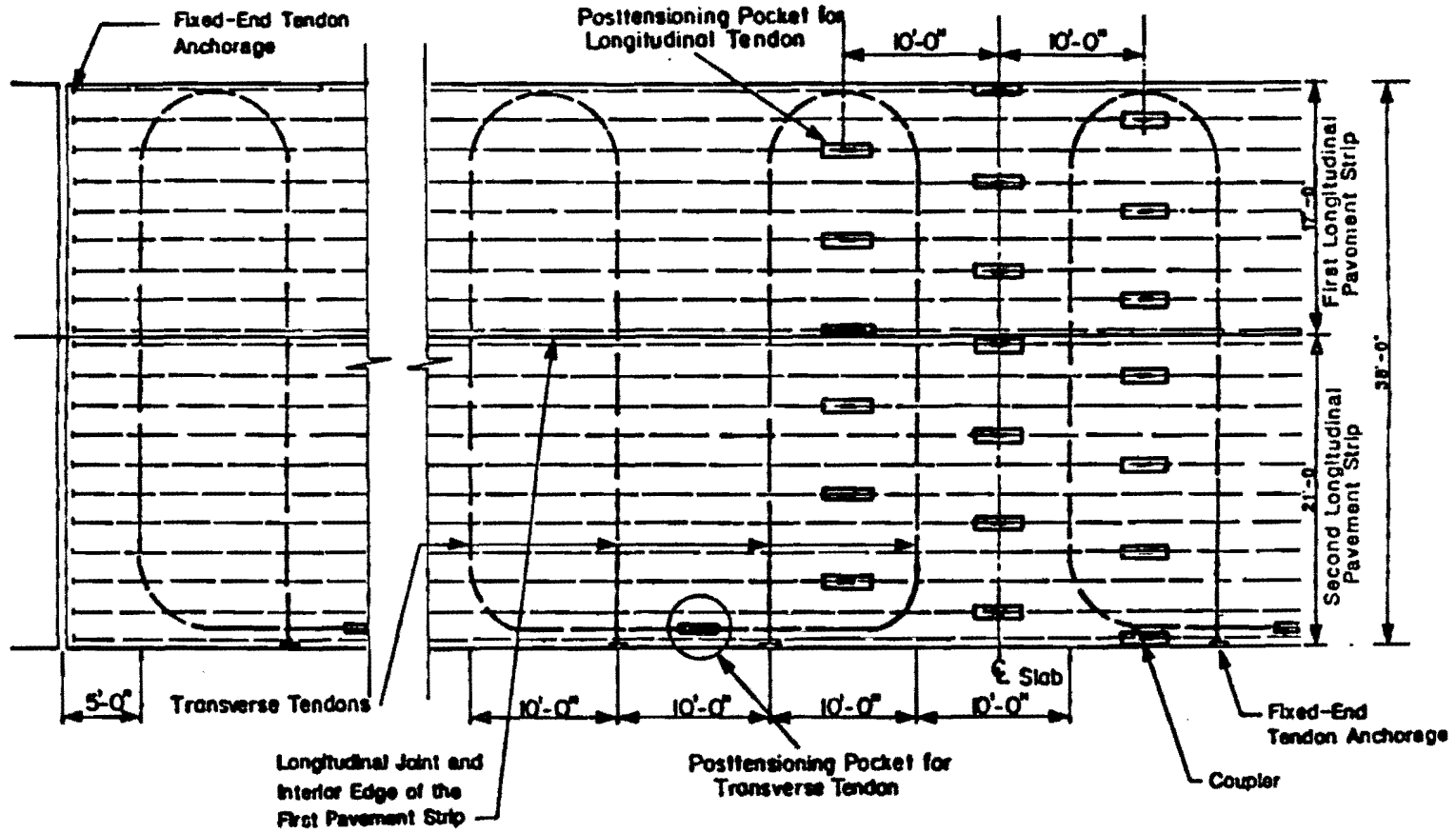Fig 8.1. Plan view of the pavement - central stressing.
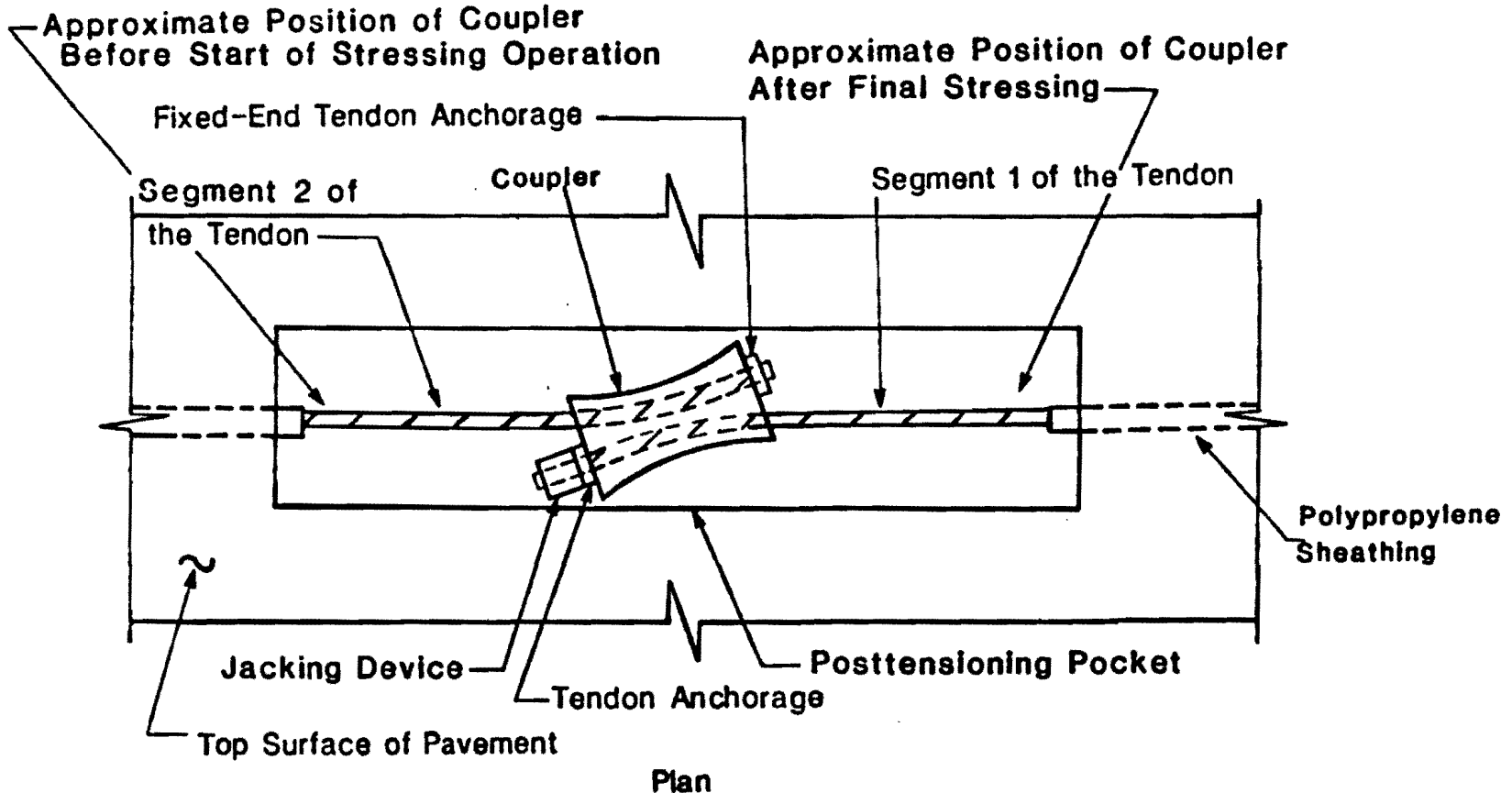
Fig 8.2. Stressing pocket detail.

Concept 2: Precast Joint Panels and Slip-Formed Pavement

As implied by its name, precast concrete joint panels are utilized with this PCP concept. The remainder of the pavement would be slip-formed. Concept 2 is illustrated in Figs 8.3 and 8.4.

The panels would most likely be cast off the job site in a precast plant or in a construction yard near the job site and would then be transported to the site and set in place.

The precast panels would be provided in pairs, one on each side of every transverse joint. The same type of transverse joint assembly as in concept 1 would also be used with this PCP concept. Each pair of joint panels would contain an entire transverse joint assembly, including the steel extrusion into which the neoprene seal is inserted, associated headed studs or deformed bar anchors, base angle (if required) to support the steel extrusion, dowels, and dowel expansion sleeves.

Each panel would contain the pockets for stressing the longitudinal pavement tendons and a single rigid transverse duct which would be used for post-tensioning the precast joint panels together in the first and second pavement strips.

Each individual panel would be prestressed on the casting bed in the precast plant, to a level that would be sufficient to prevent it from cracking due either to lifting and handling prior to placement, or to traffic loads after the panel is in its final position in the pavement.

Concept 3: Precast Joint Panels, Central Stressing Panels, and Slip-Formed Pavement

This PCP concept utilizes precast concrete joint panels as described in concept 2 (see Figs 8.3 and 8.4). In addition, precast concrete central stressing panels are also used. These panels would be located at the midlength of each pavement segment and would contain stressing pockets in which longitudinal tendons would be jacked (see Figs 8.5 and 8.6). They would also contain a rigid transverse duct which would be used to post–tention two adjacent stressing panels together. These panels would also permit the use of couplers for stressing the longitudinal tendons.

Formed Recess for Transverse
Posttensioning Tendon
Anchorage, Typical

C
L
Transverse Joint Assembly

4'-0"   4'-0"

Exterior Edge of Pavement Strip

I" Dia. Galvanized Steel
Sleeve for Longitudinal
Tendons Typical

Width of Longitudinal Strip of PCP

3/8" Dia. Pretensioning
Strands

Longitudinal Tendon
Stressing Pocket,
Typical,
See Figure 5.13

I" Dia. Galvanized Steel
Conduits for Transverse
Tendons

Interior Edge of
Pavement Strip

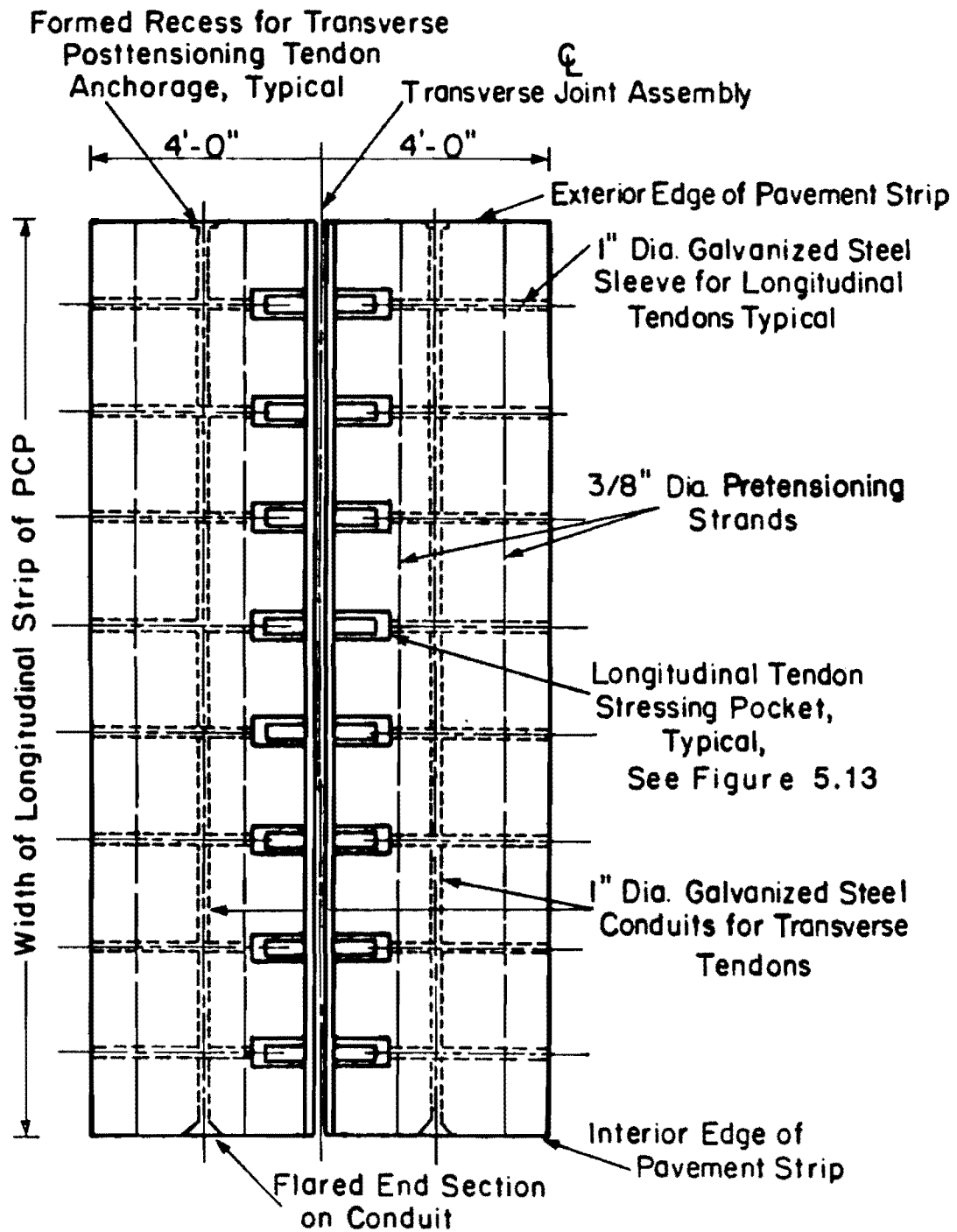Flared End Section
on Conduit

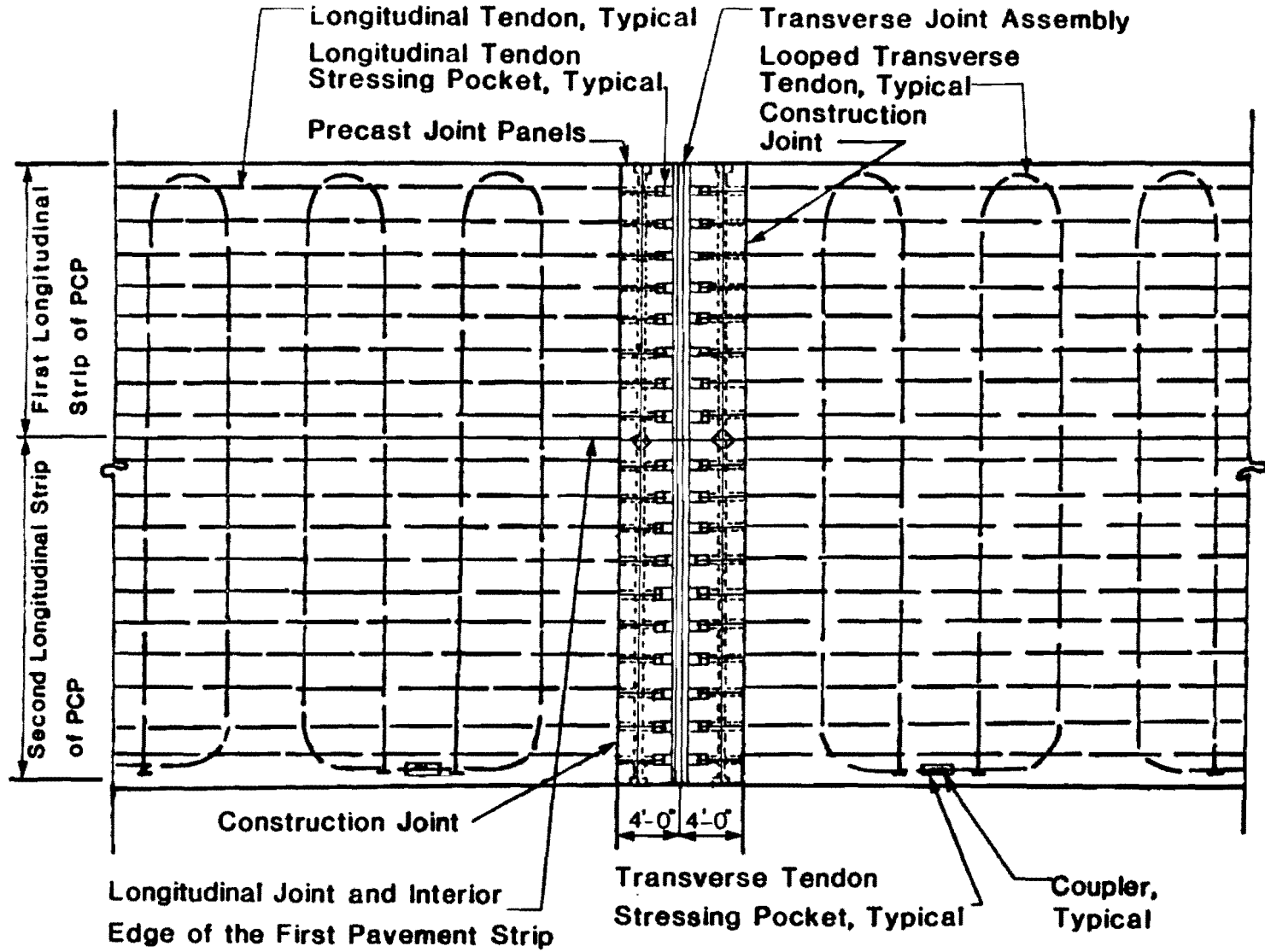PLAN

Fig 8.3. Precast joint panels.

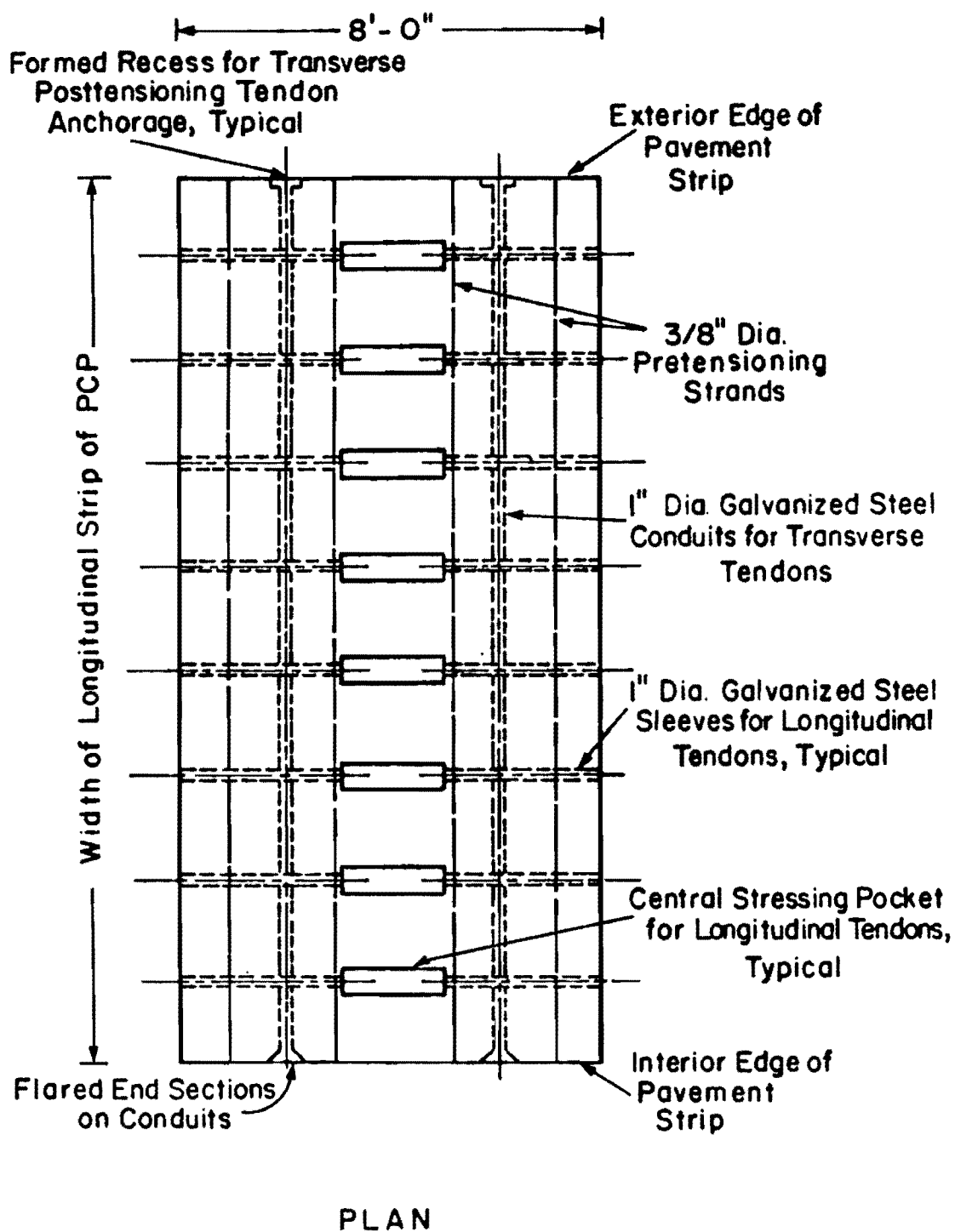Fig 8.4. Precast joint panels and slip-formed pavement.
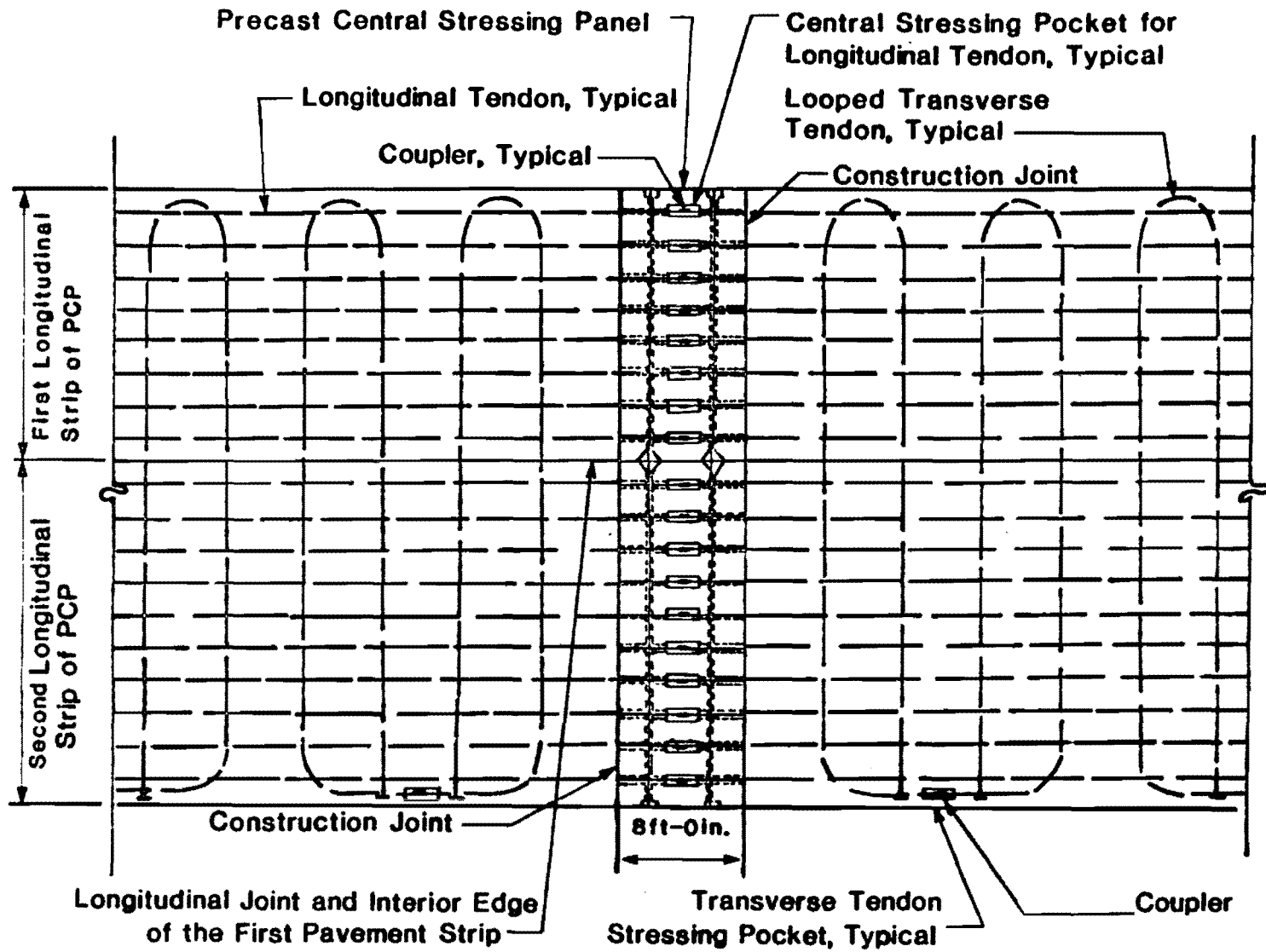
PLAN

Fig 8.5. Central stressing panel.

Fig 8.6. Precast joint panels, central stressing panels, and slip–formed pavement.

All the panels would be cast off the job site and would then be transported to the job site, where they would be set in place with a truck crane. The remainder of the pavement would be slip-formed.

Concept 4: Composite Prestressed Concrete Pavement Type I (CPCPI)

Precast concrete joint panels similar to those used with PCP concepts 2 and 3 would also be used with this PCP concept (see Fig 8.3). These joint panels were described in concept 2. Central stressing panels similar to those used in PCP concept 3 could be used with this concept if central stressing is desired (see Fig 8.5).

In addition, still another type of precast panel is involved with this PCP concept. It will be referred to in this section as a base panel and is illustrated in Figs 8.7 and 8.8. Like the panels used with the previous concepts, these panels would be cast off the job site. They would be prestressed on the casting beds to compensate for both handling and some in-place stresses. In addition, each base panel would contain a hollow transverse conduit.

All of the various types of precast panels would be transported to the job site, where they would be set in place with a truck crane. The concrete wearing course would be slip-formed with this concept.

Concept 5: Composite Prestressed Concrete Pavement Type II (CRCPII)

Precast concrete joint panels similar to those used in PCP Concepts 2, 3, and 4 would be used for CPCPII. These joint panels were described in detail. Also, central stressing panels similar to those used in PCP Concept 3 could be used with this concept if use of the technique of central stressing is desired (see Fig 8.5).

Base panels, having the following similarities to the ones used for CPCPI, would be used for CPCPII: (a) they would be cast off the job site; (b) they would be prestressed on the casting bed to compensate for both handling and some in-place stresses; (c) they would have a rough top surface finish; and (d) each base panel would contain a hollow transverse conduit. However, the base panels for CPCPII would be different from the ones used for CPCPI in three respects (see Figs 8.9 and 8.10). First, the base panels for CPCPII would be thicker than those for CPCPI. Second, grooves would be provided in the top surface of the panels which would allow the longitudinal tendons to be located at, or slightly below, the centroidal axis of

Exterior Edge of Pavement
Strip

8'-O"

Note:

Top Surface of Panels
Shall Receive a
Broom Finish.

Formed Recess for Transverse
Posttensioning Tendon
Anchorage

Width of Longitudinal Strip of PCP

A   A

1" Dia. Galvanized Steel
Conduit for Transverse
Tendon

3/8" Dia. Pretensioning
Strands

Interior Edge of
Pavement
Strip

Flared End Section
on Conduit

PLAN

SECTION A-A

Fig 8.7. CPCPl base panel.

Precast Joint Panels, Typical
Precast Base Panels, Typical
Longitudinal Tendon, Typical
Transverse Joint Assembly
Transverse Tendon, Typical
Construction Joint

First Longitudinal Strip

Second Longitudinal Strip of PCP

8' – 0"   4'– 0" | 4'– 0"   8' – 0"

Joint Between Precast
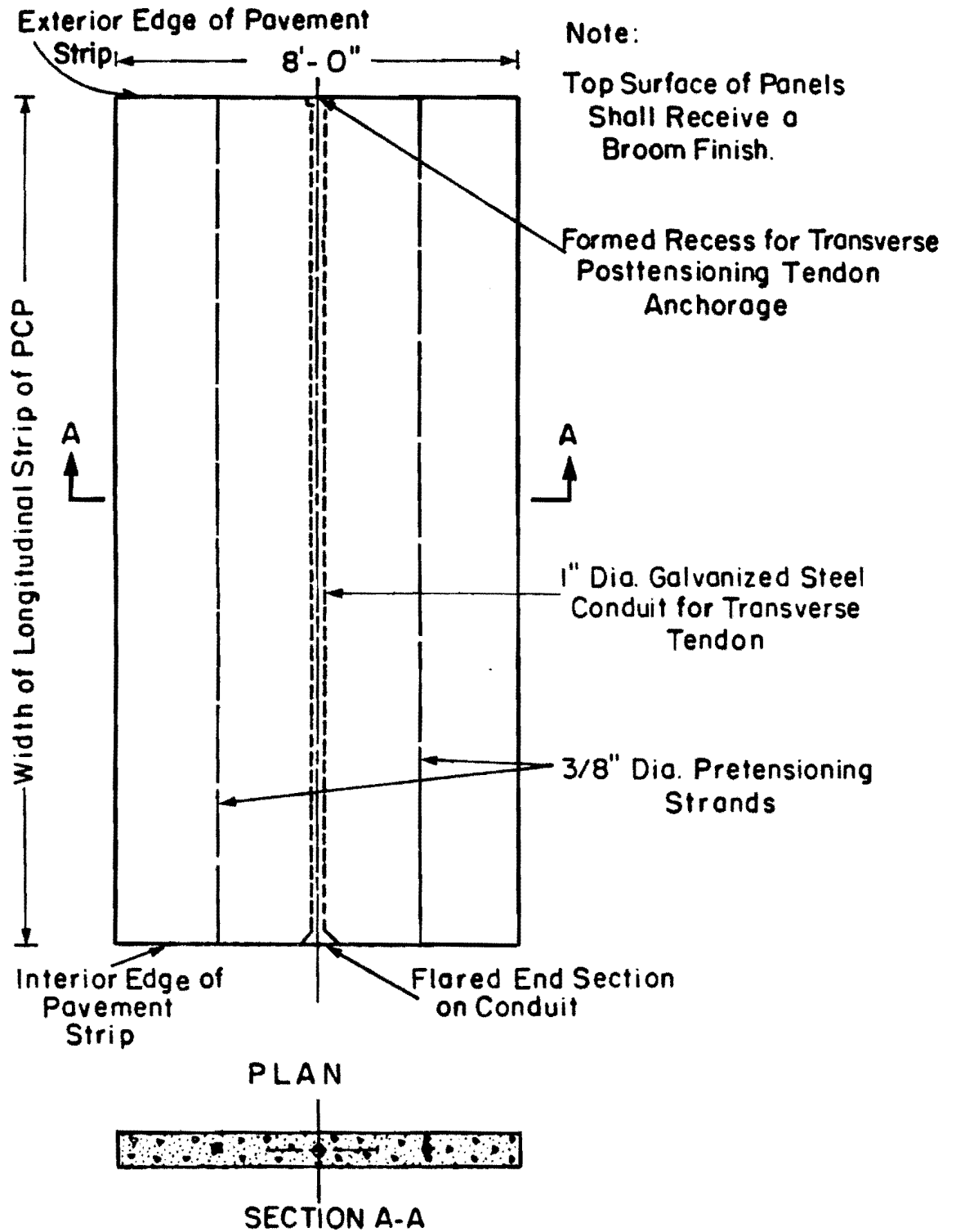Base Panels, Typical

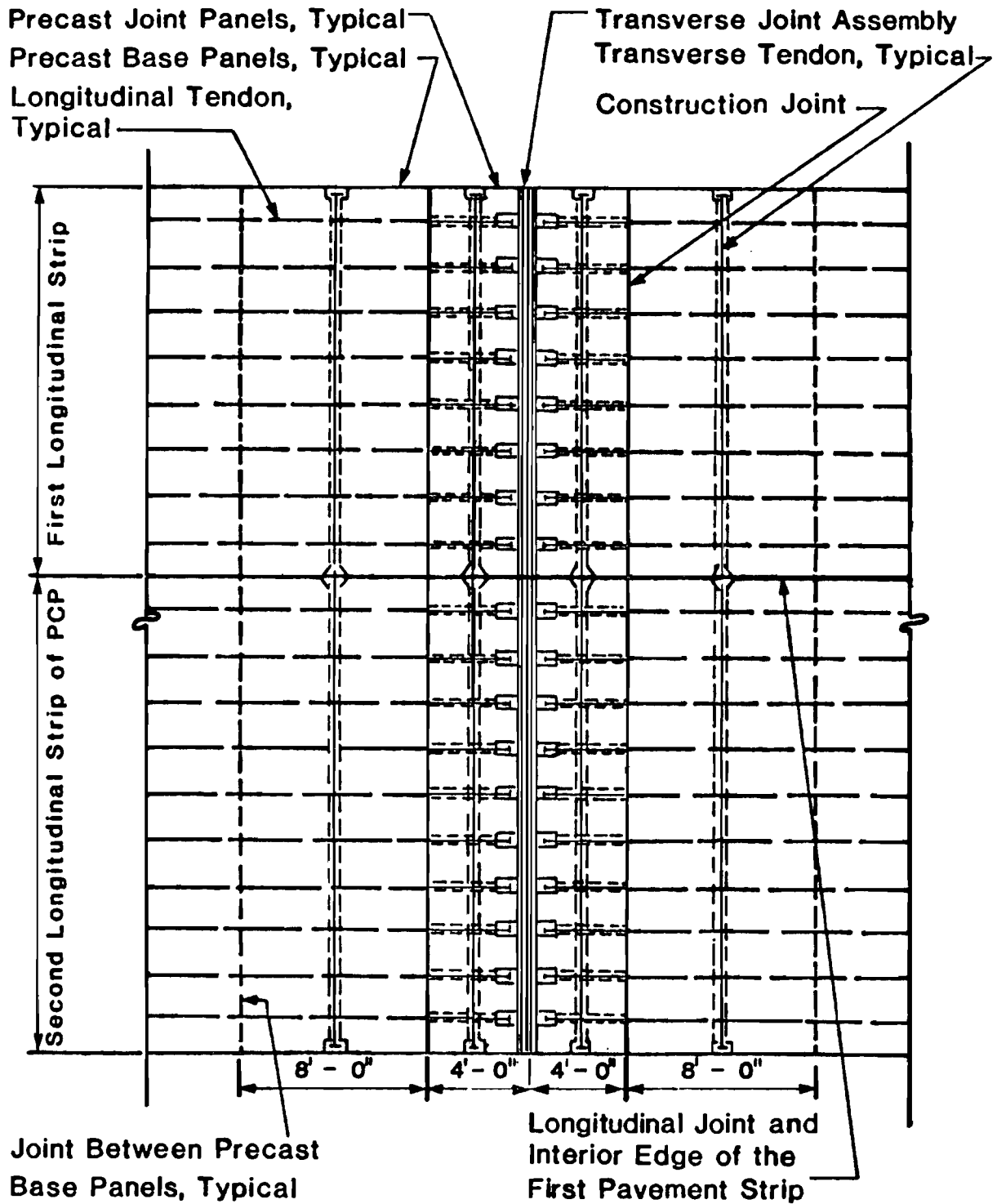Longitudinal Joint and
Interior Edge of the
First Pavement Strip

Fig 8.8. Composite Prestressed Concrete Pavement Type I (CPCPI).
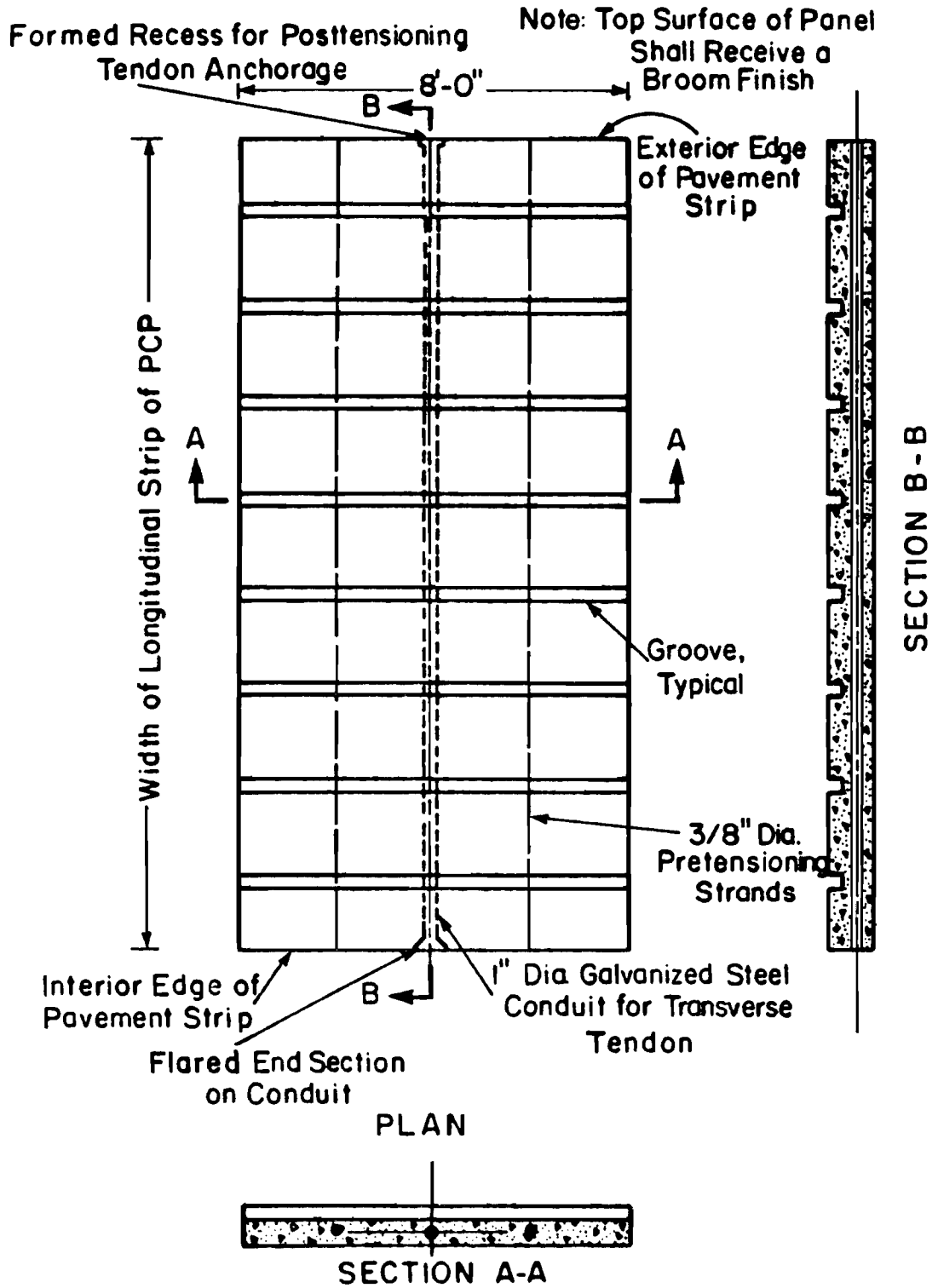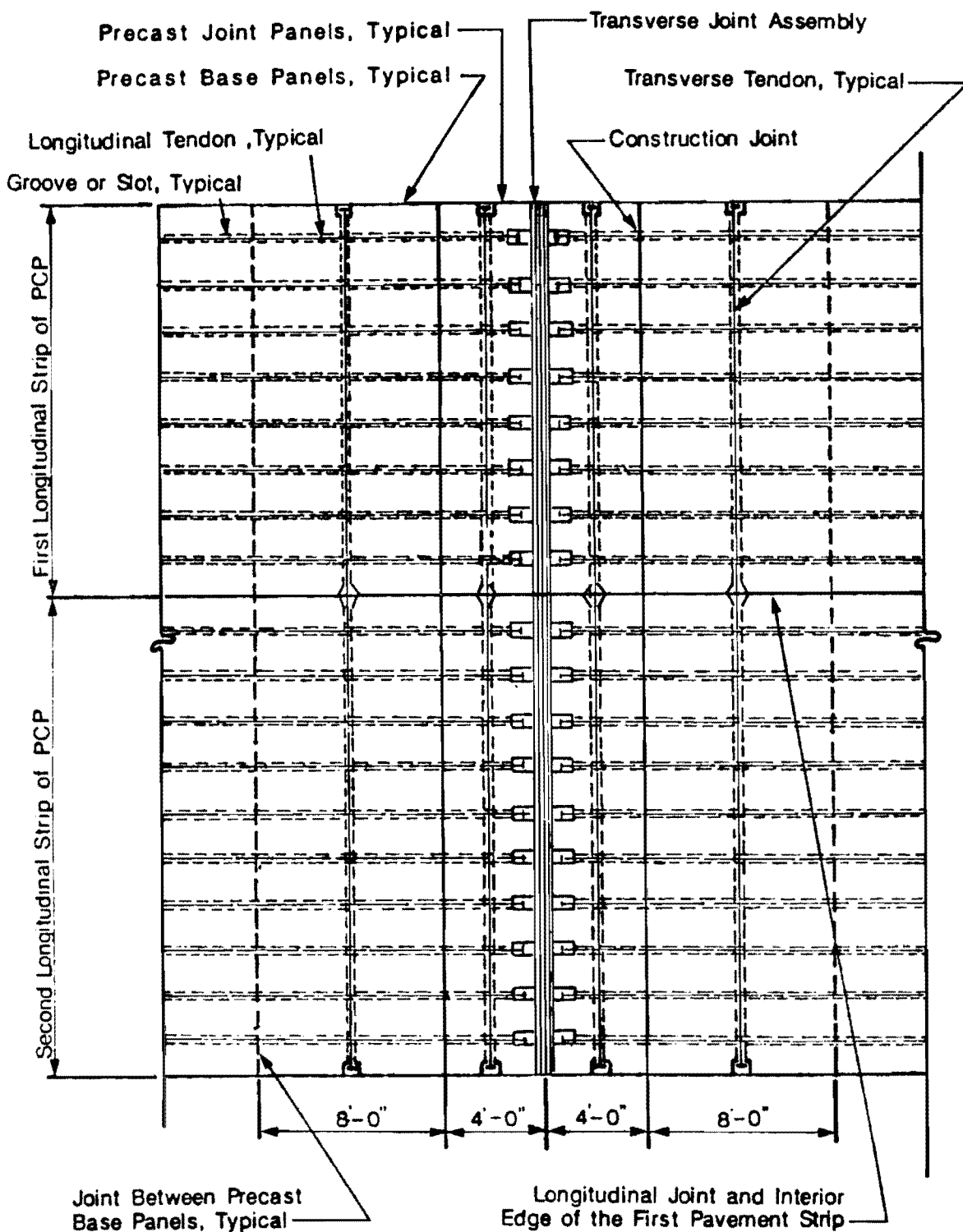
Fig 8.9. CPCPII base panel.

Fig 8.10. Composite Prestressed Concrete Pavement Type II (CPCPII).

the panels.   Third, the edge of the panel would be formed in a manner to permit grouting of the joints between adjacent panels after they are set in place at the job site.

All of the various types of precast panels would be transported to the job site, where they would be set in place with a truck crane.   The concrete wearing course would be slip-formed with this concept.

Concept 6: Segmentally Precast Prestressed Concrete Pavement (SPPCP)

Precast concrete joint panels similar to those used in PCP Concepts 2 through 5 would also be used with this concept (see Fig 8.3).   In addition, central stressing panels similar to those used in PCP Concept 3 could be used with this concept if use of the technique of central stressing is desired (see Fig 8.5).

A panel type, referred to in this section as a "full-depth pavement panel" (for reasons that will become obvious in the following discussion), would be used with this PCP concept. This panel is illustrated in Figs 8.11 and 8.12.   Like all the panels used with the previous concepts, these panels would also be cast off the job site.   They would be prestressed on the casting beds to compensate for both handling and some in-place stresses.   In addition, each full-depth panel would contain hollow longitudinal conduits and a single hollow transverse conduit.

All of the various types of precast panels would be transported to the job site, where they would be set in place with a truck crane.

Concept 7: Continuous Composite Concrete Pavement (CCCP)

CCCP is very different from any of the concepts discussed thus far, and, in reality, is more similar to the concept of continuously reinforced concrete pavement, as will become apparent in the following discussion.

No joint panels would be used with CCCP because no transverse joints would be required, except where construction joints are required when the paving operation is interrupted or where expansion joints are required, such as at bridges.   Only precast concrete base panels (as shown in Figs 8.13 and 8.14) would be used in CCCP construction.   These panels would be cast off the job site similar to panels used in the previously discussed concepts.   They would be prestressed in both directions on the casting bed to compensate for all handling and in-place stresses.   In addition, the panels would contain grooves or slots which
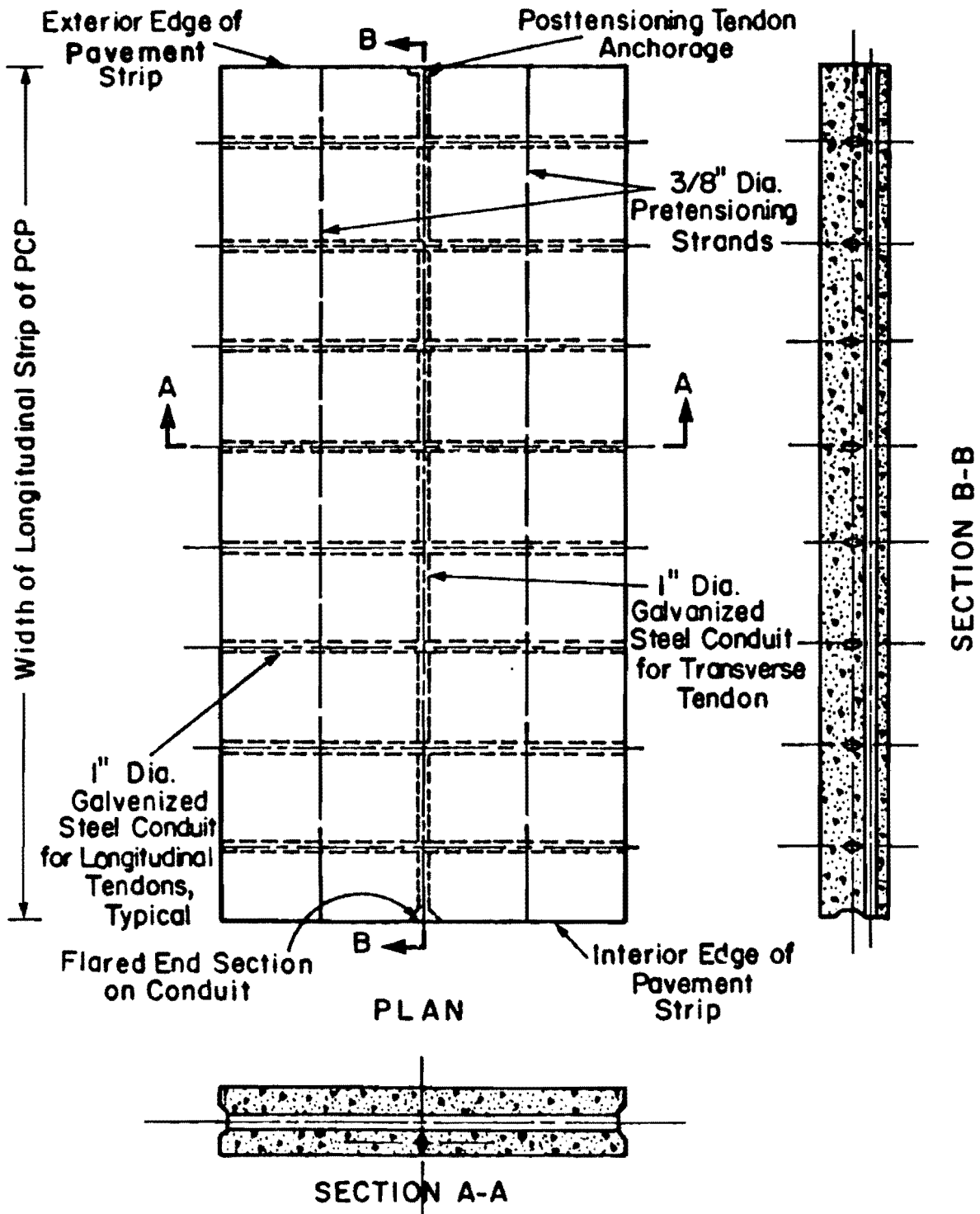
Fig 8.11. Full-depth pavement panel.
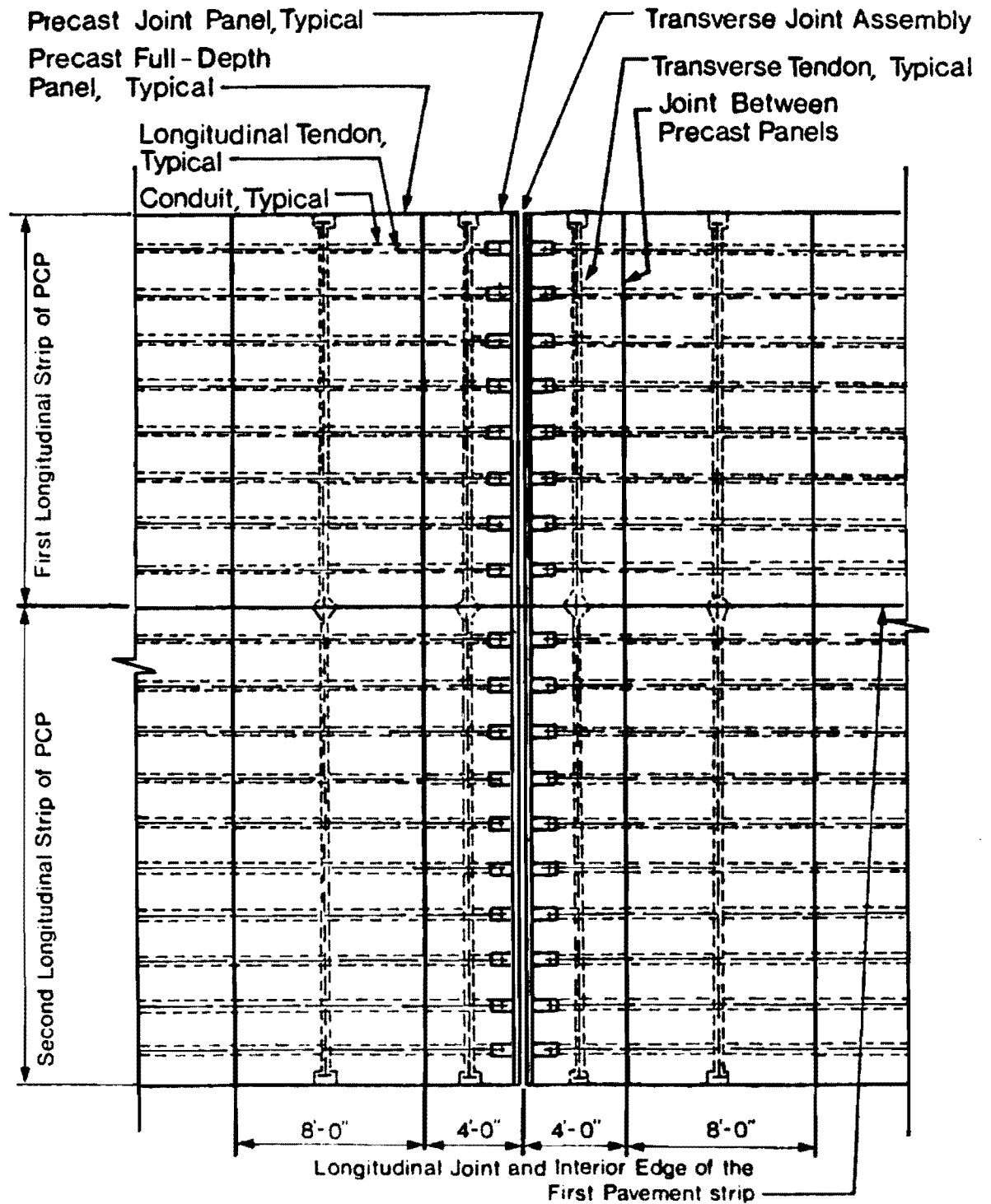
Fig 8.12. Segmentally Precast Prestressed Concrete Pavement (SPPCP).
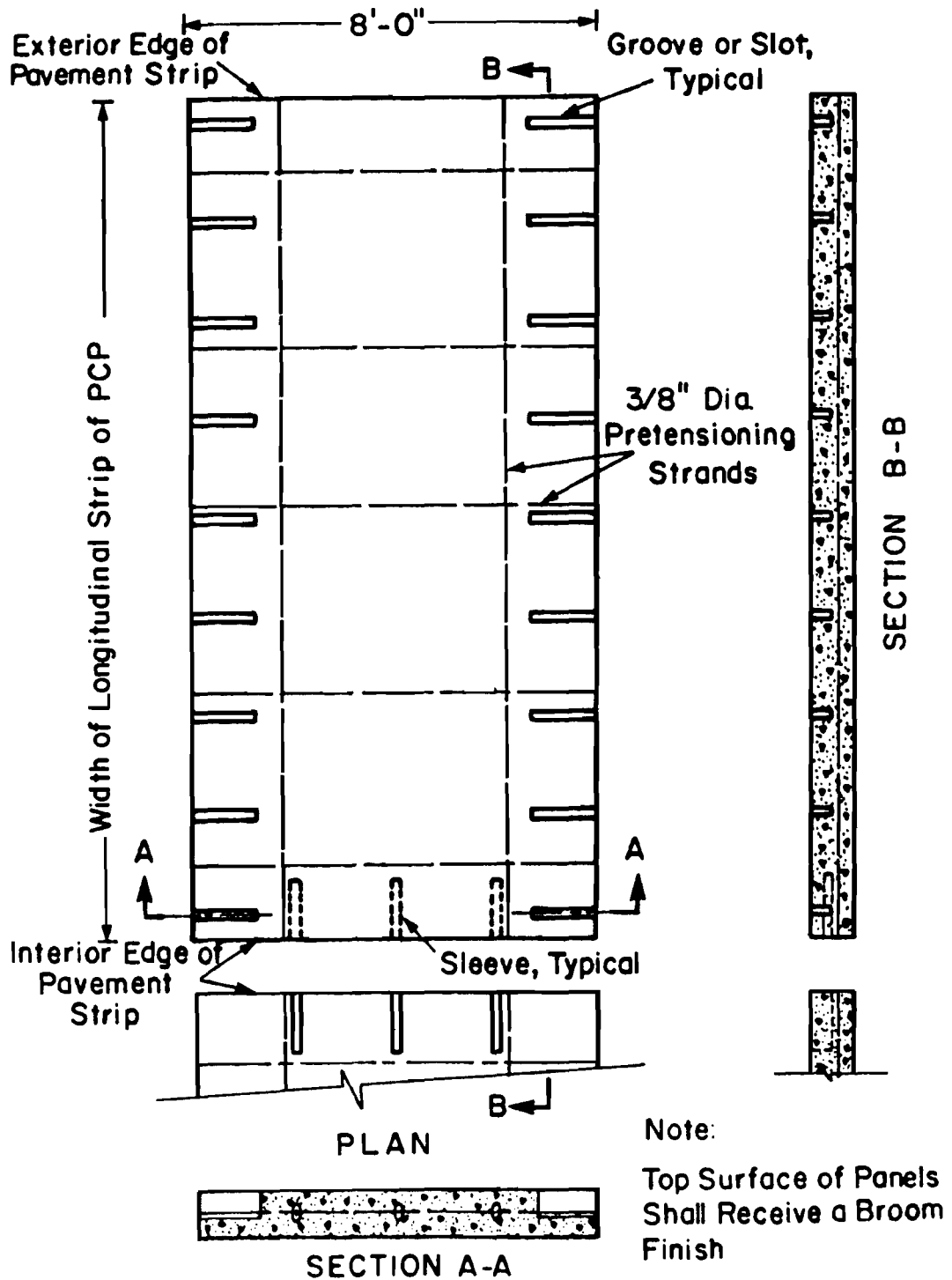
Fig 8.13. CCCP base panel.

124
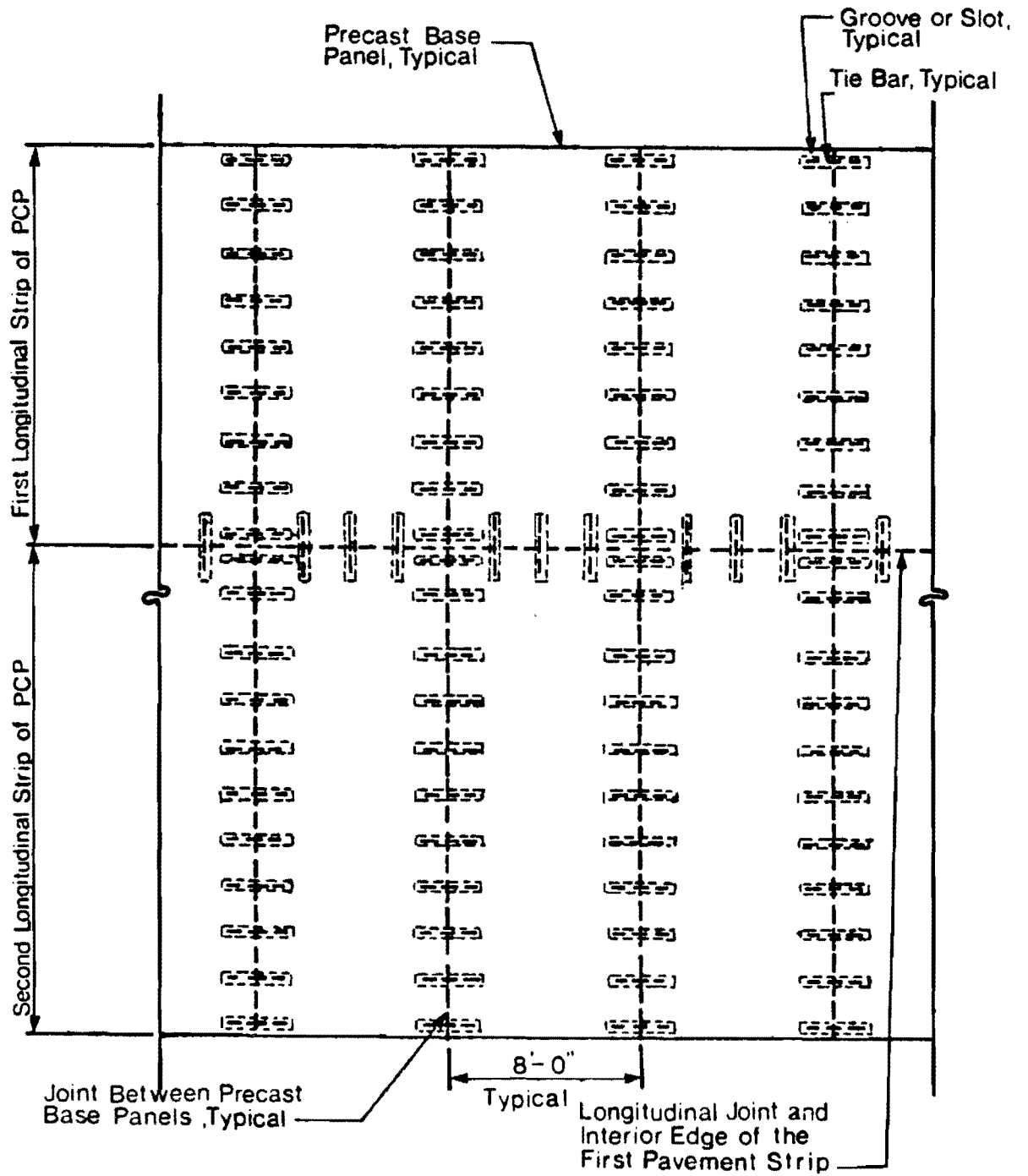
Fig 8.14. Continuous Composite Concrete Pavement (CCCP).

would be perpendicular to the panel edges. These grooves would accommodate tie bars between adjacent panels.

The precast concrete panels would be transported to the job site to be set in place with a truck crane. The concrete wearing course would be slip-formed in place after placement of the precast panels.

COMPARISON OF CONCEPT CHARACTERISTICS

Table 8.1 summarizes the relative ability of each of these new concepts to address the problems encountered on previous projects and to effectively utilize the potentials of PCP, together with possible new problems created with each concept. The comparison is made with regard to the following aspects:

(1) bonded versus unbonded tendons,

(2) transverse prestressing and looped tendons,

(3) friction reducing mediums,

(4) gap slabs versus central stressing,

(5) prestress force transference,

(6) tendon placement,

(7) transverse joints,

(8) multiple longitudinal strip construction,

(9) concrete compaction,

(10) protection of tendon anchorages,

(11) adverse construction conditions,

(12) alternate uses,

(13) alternate materials and methods, and

(14) unfamiliarity.

TABLE 8.1. COMPARISON OF PCP CONCEPT CHARACTERISTICS

CHARACTERISTIC	PCP CONCEPT NUMBER						
	1	2	3	4	5	6	7
Precast Concrete Panels							
- Utilization of high quality, mass produced, precast, prestressed concrete panels:							
(a) Significant				X	X	X	X
(b) Less significant		X	X				
(c) None used	X						
- Relative importance of the fact that the precast panels must be transported to the job site:							
(a) Significant				X	X	X	X
(b) Less significant		X	X				
(c) Not a factor	X						
Bonded vs. Unbonded Tendons							
- Suited to the use of unbonded tendons	X	X	X	X	X	X	NA*
- Relative difficulty associated with the use of bonded tendons							
(a) Significant	X	X	X				
(b) Less significant				X			
(c) Least significant					X	X	X

(continued)

RR401-8F/08

TABLE 8.1. (CONTINUED)

CHARACTERISTIC	PCP CONCEPT NUMBER						
	1	2	3	4	5	6	7
- Number of posttensioning operations required for each longitudinal tendon:							NA
(a) One					X	X	
(b) Three	X	X	X	X			
- Less expensive unsheathed posttensioning strands could be used					X	X	
Transverse Prestress							
- Difficulties associated with laying out and holding the transverse tendons in a looped configuration	X	X	X				
- Pavement transversely prestressed before being subjected to construction traffic				X	X	X	X
- Transverse prestress level in adjacent lanes can be varied in accordance with the anticipated traffic volumes				X	X	X	X
- Eliminate all posttensioning operations in the field							X
Friction-Reducing Mediums							
- Relative difficulty associated with handling and placing polyethylene sheeting:							
(a) Significant	X	X	X				
(b) Less significant				X	X	X	
(c) None							X
- Construction operations (i.e., setting tendon chairs, placing tendons, and slipforming pavement) would be conducted in direct contact with polyethylene sheeting	X	X	X				

(continued)

TABLE 8.1. (CONTINUED)

CHARACTERISTIC	PCP CONCEPT NUMBER						
	1	2	3	4	5	6	7
- Polyethylene sheeting would be protected from construction operations				X	X	X	
- Eliminate the need for polyethylene sheeting							X
Gap Slabs vs. Central Stressing							
- Elimination of gap slabs	X	X	X	X	X	X	X
- Number of tendon stressing pockets which must be formed in the field:							
(a) Greatest	X						
(b) Minimal		X	X				
(c) None				X	X	X	X
- Couplers for posttensioning tendons:							
(a) Required	X		X				
(b) Optional				X	X	X	
(c) None used		X					X
- An additional concrete placement operation is required to fill the stressing pockets after completion of final posttensioning operations	X	X	X	X		X	NA
Prestress Force Transference							
- Level of compressive stress which can be applied by posttensioning at early concrete age is dependent on:							NA
(a) Concrete strength	X	X	X	X	X	X	
(b) Tendon anchorage size	X						
(c) Tendon spacing	X						

(continued)

TABLE 8.1. (CONTINUED)

CHARACTERISTIC	PCP CONCEPT NUMBER						
	1	2	3	4	5	6	7
- Application of initial prestress force:							NA
(a) Prestress force transferred from tendons to immature concrete via individual tendon anchorages, thus limiting the amount of prestress that can be applied at early concrete age	X						
(b) Prestress force transferred from tendons to precast joint panels and then to the immature concrete, allowing greater initial prestress force to be applied at early concrete age		X	X	X	X	X	
- Possible long-term problems due to tensile stresses at the end of each pavement section caused by prestressing							
(a) Possible	X						
(b) Significantly decreased likelihood		X	X	X	X	X	
(c) No likelihood							X
Tendon Placement							
- Chairs required to support tendons during slip-forming	X	X	X				
- No chairs required to support tendons during slip-forming				X	X	X	X
Transverse Joints							
- Relative difficulty associated with holding the transverse joint assembly stationary while applying tension to the longitudinal tendons before the pavement concrete is placed:							NA

RR401-8F/08

TABLE 8.1. (CONTINUED)

CHARACTERISTIC	PCP CONCEPT NUMBER						
	1	2	3	4	5	6	7
(a) Significant	X						
(b) Less significant		X	X				
(c) None				X	X	X	X
- Difficulties associated with concrete placement and consolidation in the vicinity of the transverse joint assembly in the field	X						
Multiple Longitudinal Strip Construction							
- Problems associated with transverse tendons protruding from the first pavement strip	X	X	X				
- Concrete formwork required along the interior edge of the first pavement strip	X	X	X				
Concrete Compaction							
- Reduced difficulty in obtaining good compaction of slip-formed concrete because of reduced cast-in-place concrete depth				X	X	NA	X
Protection of Tendon Anchorages							
- Tendon anchorages completely encased and protected in the concrete pavement	X	X	X	X	X	X	X
Adverse Construction Conditions							
- Reduction in required quantity of cast-in-place concrete which reduces vulnerability to adverse construction conditions:							
(a) Significant				X	X	X	X
(b) Less significant		X	X				
(c) None	X						

TABLE 8.1. (CONTINUED)

CHARACTERISTIC	PCP CONCEPT NUMBER						
	1	2	3	4	5	6	7
- Problems associated with stopping construction at intermediate points:							
(a) Significant	X	X	X				
(b) Less significant				X	X	X	X
- Possibility of being able to quickly open the pavement to traffic						X	X
Alternate Uses							
- Possibility of being used for a special purpose, temporary, reusable pavement						X	
- Damaged sections easily repaired							X
Alternate Materials and Methods							
- In addition to strand, high-strength bars can be used for transverse posttensioning				X	X	X	
- Possibility of using high-strength bars for longitudinal posttensioning					X		
- Couplers for posttensioning tendons:							
(a) Required	X		X				
(b) Optional				X	X	X	
(c) None used		X					X
- Possibility of using alternate wearing course materials							X
Unfamiliarity							
- Organizations responsible for selecting							

(continued)

RR401-8F/08

TABLE 8.1. (CONTINUED)

CHARACTERISTIC	PCP CONCEPT NUMBER						
	1	2	3	4	5	6	7
pavement systems are unfamiliar with the concept	X	X	X	X	X	X	X
- Paving contractors unfamiliar with the concept	X	X	X	X	X	X	X

*NA = Not Applicable

CHAPTER 9. SUMMARY, CONCLUSIONS, AND RECOMMENDATIONS

This project has fully explored the use of PCP in a number of areas by numerous engineers. In the following sections the summary, conclusions, and recommendations derived from this study are presented.

SUMMARY

Based on the results of this study, PCP is a viable pavement type that may be used as a new pavement or as a rehabilitation alternative on Texas highways. The general warrants for this pavement type are high traffic volumes, low maintenance, and vertical clearance problem areas. The report presents information and procedures, in accordance with the objectives, related to

(1) pavement thickness, joint spacing, and post-tensioning design for the wheel loads, material properties, and environmental factors for a specific project.

(2) The characterization of performance of an inservice pavement on IH-35 in McLennan County is reported.

(3) evaluation of various post-tensioning techniques.

(4) new concepts that may be used in the design and construction of PCP.

CONCLUSIONS

After each chapter a summary and/or conclusions are presented. Following are the pertinent conclusions:

(1) The double layer of polyethylene gives the lowest friction values, but observations of performance and the mechanism indicated a single layer was the most cost effective method of reducing the friction at the pavement-subbase interface.

(2) The use of stressing pockets has been demonstrated to be an efficient method of post-tensioning that provides the maximum stress level at critical locations and eliminates the need for the use of gap slabs. The pocket sizes must be tailored to the anticipated stressing jacks since many sizes are currently available.

(3) The most efficient tendon looping patterns may be developed using the equations and tables presented in Chapter 4.

(4) The study has shown that initial stressing at an early age (less than 12 hours) will eliminate premature cracking, thereby reducing future problem areas. Equation 4.1 may be used to estimate the permissible early loading based on slab thickness, strand spacing, concrete tensile strength, and anchorage areas.

(5) A design procedure is summarized in Chapter 7 that permits the derivation of the most effective combination of slab thickness, post-tensioning level, and joint spacing for a specific set of design conditions. The pavement may be designed rather than extrapolated from past experience based on Ref 17 from which Chapter 7 is taken.

(6) Field measurements of in-service pavements and test slabs indicate the design models reliably predict concrete stress and joint movement for a range of environmental conditions and age.

(7) Fatigue tests of prestressed laboratory beams indicate that the predicted life from the equations used in fatigue analysis is conservative.

(8) Seven new concepts are presented that may increase the viable alternate uses of PCP. The design procedures presented herein may be used to investigate their viability for specific projects.

RECOMMENDATIONS

Following are key recommendations from this study:

(1) A location should be selected so a larger project may be designed and constructed using the concepts in this report. A large project along with the experience codified herein should lead to a more cost competitive pavement.

(2)   The new concepts presented in Chapter 8 should be explored with a feasibility study to select the most promising and economical approach; then this approach should be implemented in a full scale construction project.

REFERENCES

1. Chia, Way Seng, N. H. Burns, and B. Frank McCullough, "Field Evaluation of Subbase Friction Characteristics," Research Report 401-5, Center for Transportation Research, The University of Texas at Austin, November 1986.

2. American Concrete Institute, Committee 318, Building Code Requirements for Reinforced Concrete (ACI 318-83), Second Printing, September 1984.

3. Post-Tensioning Institute, Post-Tensioning Manual, 1976.

4. O'Brien, J. S., N. H. Burns, and B. F. McCullough, "Very Early Post-Tensioning of Prestressed Concrete Pavement," Research Report 401-1, Center for Transportation Research, The University of Texas at Austin, June 1985.

5. Guyon, Yves, Prestressed Concrete, John Wiley & Sons, Inc., New York, 1953.

6. Maffei, Joseph, B. Frank McCullough, and Ned H. Burns, "Instrumentation and Behavior of Prestressed Concrete Pavements," Research Report 401-4, Center for Transportation Research, The University of Texas at Austin.

7. Brunner, Raymond J., "Prestressed Pavement Demonstration Project," Research Project No. 72-22(2), Pennsylvania Department of Transportation, Bureau of Materials, Testing, and Research, Annual Meeting of the Transportation Research Board, 1975.

8. Friberg, Bengt F., and T. J. Pasko, "Prestressed Concrete Highway Pavement at Dulles International Airport: Research Progress Report to 100 Days," Report No. FHWA-RD-72-29, U. S. Department of Transportation, Federal Highway Administration, August 1973.

9. Albrittion, Gayle E, "Prestressed Concrete Highway Pavement: Construction -- As Built Performance, Brookhaven, Mississippi (Research Supplement)," U. S. Department of Transportation, Federal Highway Administration, Region 15, Demonstration Projects Division, Arlington, Virginia, August 1978.

10. Morris, Gene R., and Hal C. Emery, "The Design and Construction of Arizon'a Prestressed Concrete Pavement," Research Section, Highway Division, Arizona Department of Transportation, Fifteenth Paving Conference, University of New Mexico, Department of Civil Engineering, Albuquerque, New Mexico, January 1978.

11. Friberg, Bengt F., "Investigations of Prestressed Concrete for Pavements," Bulletin No. 332, Highway Research Board, 1962, pp 40-94.

12. Wray, Warren K. (Principle Investigator), "Interim Report: Measurement of Slab-Subgrade Friction on a Full Scale 80 ft. x 150 ft. Slab at Slidell, La.," Department of Civil Engineering, Texas Tech University, October 3, 1984.

13. Texas State Department of Highways and Public Transportation, Standard Specifications for the Construction of Highways, Streets, and Bridges, 1982.

14. Dunn, Brian W., Ned H. Burns, and B. Frank McCullough, "Friction Losses in Unbonded Post-Tensioning Tendons," Research Report 401-6, Center for Transportation Research, The University of Texas at Austin, November 1986.

15. Nussbaum, Peter J., Adrian T. Ciolko, and Shiraz D. Tayabji, Prestressed Pavement Volume 1, Joint Design, U. S. Department of Transportation, Federal Highway Administration, Offices of Research and Development, Report No. FHWA/RD-81/090. Springfield, Virginia: NTIS, June 1983.

16. Chia, Way Seng, Ned H. Burns, and B. Frank McCullough, "Effect of Prestress on Fatigue Life of Concrete," Research Report 401-7, Center for Transportation Research, The University of Texas at Austin, November 1986.

17. Mendoza, A., B.F. McCullough, and Ned H. Burns, "Behavior of Long Prestressed Pavement Slabs and Design Methodology," Research Report 401-6, Center for Transportation Research, The University of Texas at Austin, August 1986.

18. McCullough, B.F., and A. Mendoza, "Report on a Mechanistic Analysis of the PCC Aprons at King Fahd International Airport, Kingdom of Saudi Arabia," Austin Research Engineers, October 1985.

19. Weil, G., "Der Verschiebewiderstand von Betonfahrbahnplatten," Betonstein Jahrbuch, Bauverlag GMBH, Wiesbaden, 1960.

20. Cashell, H.D., and Benham, S.W., "Experiments with Continuous Reinforcement in Concrete Pavements," Proceedings, V.29, Highway Research Board, 1949, pp. 44-80.

21. ACI Committee 325, "Proposed Design of Experimental Prestressed Pavement Slab, and Restrained Temperature Movements in Long Slabs," ACI Journal, Proceedings Vol. 64, No. 4, April 1968, pp. 249-265.

22. Godbeck, A.T., "Friction Tests of Concrete on Various Subbases," Public Roads 5, July 1924.

23. Timms, A.G., "Evaluating Subgrade Friction Reducing Mediums for Rigid Pavements," Highway Research Record 60, Highway Research Board, 1963, pp. 28-38.

24. Friberg, B.F., "Frictional Resistance Under Concrete Pavements and Restraint Stresses in Long Reinforced Slabs," Proceedings, V.33, Highway Research Board, 1954, pp. 167-184.

25. Ware, K.R., "KFIA Friction Test Results, Arabian Bechtel Company Ltd., January 1982," ARE Inc., August 28, 1984.

26. Mendoza, A., B.F. McCullough, and Ned H. Burns, "Design of the Texas Prestressed Concrete Overlays in Cooke and McLennan County and Construction of the McLennan County Project," Research Report 556-1, Center for Transportation Research, The University of Texas at Austin, February 1986.

27. Mendoza, A., and Neil D. Cable, "Field Tests Conducted Near Valley View, Texas, for the Design of the Prestressed Highway Pavement Demonstration Projects in Cooke and McLennan Counties," Technical Memorandum 401-17, Center for Transportation Research, The University of Texas at Austin, September 19, 1984.

28. Mendoza, A., "Repetition of the Friction Tests on the Test Slabs Constructed Near Valley View, Texas, for the Design of Prestressed Highway Project in Cooke County," Technical Memorandum 401-20, Center for Transportation Research, The University of Texas at Austin, November 1984.

29. Stott, J.P., "Tests on Materials for Use as Sliding Layers Under Concrete Road Slabs," Civil Engineering 56, 1961, pp. 663-665.

30. McCullough, B.F., A. Abou-Ayyash, W.R. Hudson, and J.P. Randall, "Design of Continuously Reinforced Concrete Pavements for Highways," NCHRP 1-15, Center for Transportation Research, The University of Texas at Austin, August 1974.

31. Rivero-Vallejo, F., and B.F. McCullough, "Drying Shrinkage and Temperature Drop Stresses in Jointed Reinforced Concrete Pavements," Research Report 177-1, Center for Transportation Research, The University of Texas at Austin, August 1975.

32. Cable, Neil D., N. H. Burns, and B. Frank McCullough, "New Concepts in Prestressed Concrete Pavement," Research Report 401-2, Center for Transportation Research, The University of Texas at Austin, December 1985.